

Novelty Detection using a Mobile Robot: Challenges and Benefits

by

Muhammad Fahmi Miskon

Submitted in fulfillment of
the requirements for the degree of
Doctor of Philosophy

Intelligent Robotic Research Centre
Department of Electrical and Computer Systems Engineering
Monash University

August 2009

Addendum

1. Page iv para 3 line 3: replace “localized” with “localize”
2. Page 1, three lines from the bottom: replace “supervise” with “supervised”.
3. Page 1, line 7 from the bottom, add new sentences after “... from an environment.”: There are approaches [56-58, 114] that consider novelty as experiences that are seen once and will not be considered novel if they are seen again. However, in general, these approaches are not suited to on-line learning. The reason for this is given in [16]. Marsland et al. highlighted the fact that the type of novelty filter that is suitable for on-line training and also for use on an autonomous mobile robot must have a degree of robustness to accidental training (i.e. occasionally seeing features during training that should be identified as novel). This thesis will particularly address the problem of novelty detection for on-line training and for use on an autonomous mobile robot. For this reason, the definition of novelty as given in [16] is more suited to this thesis.
4. Page 1: Add a new paragraph at the end of Section 1.1: It is impossible for a machine learning system to learn all possible object classes whose data the system is likely to encounter. That is why novelty detection is required as the system training is based only on available data. Different novelty detection methods have been discussed extensively in [56-58]. There is no single best model for novelty detection as the success of detection is based on the type of application and data handled. The methods in novelty detection are generally divided into two different approaches; statistical and neural network. Statistical approaches are based on modeling data based on its statistical properties and use this to test whether new information belongs to the same distribution or not. Prior data is needed to model its distribution [56]. Unlike a statistical approach, neural network approaches are based on machine learning of normal data and comparing what it learns with new inputs to find whether they belong to the normal class or not. The neural network approach has the advantage that a very small number of parameters need to be optimized for training networks and no priori assumptions on the properties of data are made [57]. These features suited the requirement of the system developed in this thesis. For that reason a novelty detection system that uses the neural network approach was chosen for this project. The selection and description of the novelty detection method used in this thesis is further discussed in Section 2.5.
5. Page 2: Add line 3 of para 2 in Section 1.2, after “for collision detection [6-8]”: “, in assisting human robot interaction [114]”
6. Page 2 para 3 line 9: Add: “a” different level of competence
7. Page 2 para 3 line 12: replace “wander” with “wandering”, “explore” with “exploring”, and “build” with “building”
8. Page 3: Add a new para at the top of the page: The difference between the works in the novelty detection field that do not consider applications on mobile robots [2-5] and those used on a mobile robot [6-16] is the need to take into account that the normal situation usually varies from place to place. The work described in [7-16] did consider the application of novelty on a moving mobile robot, but it used no map by assuming that there was only one normal condition for the whole environment. In [17], the variety of normal conditions at different places in the environment is considered by storing the information at fixed intervals along the robot’s path. In [6], all normal state information is stored using a grid map, meaning that they are stored at fixed intervals throughout the whole of the robot’s working environment (not only on the robot path). However, the author finds these methods [6, 17] waste memory space because in novelty detection application, there are many quantities that do not vary rapidly over space like temperature and pressure. In other robotics work [114], novelty detection is used but it does not address the problem of storing different normal quantities at different locations in the environment. This thesis proposes to address the variation of the normal situation in the mobile robot environment while taking into account the memory consumption to store this information. In addition, the author proposes that the novelty detection system should be adaptable to new changes in the environment to allow on-line learning and inspection, similar to the work in [16] but more challenging since the normal situation affecting a finite space is considered. On top of that, to the best of the author’s knowledge, there is no work on mobile robots that takes advantage of mobility to reduce false alarms. This will also be introduced in this thesis.
9. Page 4 line 8: Add after “... unusual at others.”: A map requires memory and reducing memory size is an important consideration when using onboard memory. Onboard memory is needed especially when a mobile

- robot cannot communicate or transfer data wirelessly due to signal blockage (being underwater, inside a cave etc.) or due to physical constraints that do not allow the robot to carry a wireless module.
10. Page 22: Add a new paragraph after para 2 (after line 10 from the top): To summarize what has been discussed in this section, the limitation of space-driven maps such as grid maps and Quadtrees require predefined boundaries before they can be used and this information would not be available for an unknown environment. Grid maps also have a fixed size and thus require a maximum amount of memory. A quad tree map could change size but it still wastes memory by allocating unused regions for areas not visited by the robot. A map using landmark locations is not suitable to represent regional data as it requires a number of locations which can use as much storage as a grid map or perception based map to represent a region. Map representation using the geometry of objects is restricted to systems that have sensors that can extract geometry information from the environment. Perception based maps might waste memory by storing the same information redundantly in a region as samples are indexed at regular intervals. Lastly, novelty detection systems that use no map are restricted to environments with a single normal condition. As we can see, these methods of mapping have limitations in terms of memory requirement as well as practicality issues for novelty detection application. These memory issues can be solved if the maps are data driven and at the same time have flexible and adaptable region size. For this reasons, a mapping system where size is flexible, adaptable, data driven and suitable for storing different types of measurements for novelty detection systems is proposed.
 11. Page 24: Add at the end of para 2: This relatively high standard deviation setting allows fast convergence during initialization and it does not affect the performance of the localization system in the simple environment used for the experiment.
 12. Page 26: line 1: replace “detail” with “detailed”
 13. Page 27: line 9 from the bottom: Add after “... is used here”: (see Section 2.5 for a detailed explanation)
 14. Page 29: Add at the end of para: The expansion of a region happens when the measurement taken from areas near a region is similar to the measurement taken from within the region.
 15. Page 30 line 4: replace “direction” with “directions”
 16. Page 33 line 3 from the top: Replace n with nr
 17. Page 33 Equation (2.15): Replace n with nr
 18. Fig 2.11 : replace “believe” with “believes”, “fro” with “from” and “becau” with “because”
 19. Page 43 line 6 from the bottom: replace “reduced” with reduce”. line 4 from the bottom: replace “used” with “use”
 20. Page 50 line 4 from the bottom: Add after “accuracy is calculated.”: The minimum region tolerance can be calculated using Equation (2.32).
 21. Page 55 line 3 from the bottom: Delete: From the author’s experience, in such situations, objects as small as $0.1m^2$ can be readily detected if the object is about a meter from the laser range finder
 22. Page 61 para 1 line 3: Add after “ambient temperature of $24^{\circ}C$.”: The sensor was allowed to stabilize for a minute before taking a measurement at each marked distance from the source.
 23. Page 63 Algorithm 2.1 Between coding line12 and line13: Add: End
 24. Page 68 line 2 from the bottom: Add after “are shown in Table 2.4.”: From the table, door 1 could be in the open or closed state when the robot took the measurement (both are considered normal) and since there is no other alternative state, the unusual state is not applicable (n/a).
 25. Page 68: Add at the bottom of the page: In environments where walls are rough and uneven such as caves the number of regions will reduce little for certain measurements such as laser range scans. However, there will be quantities that do not vary very rapidly (such as temperature and pressure) and for these a flexible region map will be useful.
 26. Page 68 line 3 from the top: Add after “... into several regions”: (R_{o1} , R_{o2} and R_{o3})
 27. Page 85 para 2 line 1: replace “describe” with “described”
 28. Page 87 line10 from the top: Add after “(GWR)” : [16]
 29. Page 90 line2 from the bottom: Add after “... introduced.”: An ‘epoch’ here means one tour of the entire robot environment.
 30. Page 99 line 2: replace “detail” with “detailed”
 31. Page 103: Add at the end of para 3: The clustering deals with different data (anomaly points) taken from different locations by any single type of sensor.

32. Page 107 Add at the end of para 2: The data values plotted in the figures were calculated. Note that accuracy here shows the degree of closeness of measurements of a quantity to its actual value. The figures do not show accuracy with respect to number of samples. Rather, they show how the accuracy could change when the number of affected sectors and the distance of the object from the sensor are varied. For Figure 4.5, the calculation is normalised to the maximum measurement of the laser i.e. when the object surface is close to the laser's maximum range. For Figure 4.7, the calculation is normalised to the maximum difference between the surface of the object and the value of the anomaly point.
33. Page 123: line1 from the bottom - Add after "...to each other.": Clustering has a useful effect for a moving object depending on the rate of measurement. If the rate is low, a moving object would not be detected; hence the algorithm could act as a filter for identifying only non moving objects. If the moving object moves about within the same area, there is a possibility that the anomaly points will be scattered and fail to be clustered. One possible solution is to increase the rate of measurement until the system can track the movement of the object.

By using the repetitive observation strategy, it would take a considerable amount of noise to produce a cluster. This reduces the possibility of false detection.

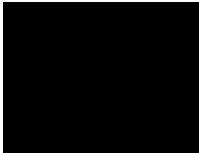
In general, relatively old and new data are of equal importance for the repetitive observation strategy. However, the system has a finite amount of short term memory, where data are organized in a first in first out (FIFO) manner. Old data that are displaced out of the memory bank would be discarded.

There are possibilities where two or more clusters might be caused by the same as well as different objects. However, in general, for the anomaly detection application, the most important thing is that anomalies can be detected.
34. Page 143: Add at the end of para: As discussed earlier, with respect to the laser scan, scanning convex, non convex or even irregular shaped objects would give different results. The anomaly points would appear closer or further away from the object's surface depending on the surface profile. However, when using the repetitive observation strategy, observations are made from several different viewpoints. As a result, it is expected that, the resulting anomaly points will originate from different regions of the object's surface. For this reason, the clustering results for any relatively compact object are expected to be quite similar.
35. Page 158: Add at the end of para: Over inspect could terminate navigation at non goal points but this will not defeat the purpose of the navigation which is to ensure total inspection coverage.
36. Page 184: In publications number [4] and [5], replace "accepted to" with "in".
37. Page 194: Add a new reference: [114] Bruce MacDonald and Toby Collett, "Novelty processing in human robot interaction," Symposium on Processing Novelty, Elam School of Fine Arts, University of Auckland, New Zealand, April 8 2004.

DECLARATION

I declare that:

1. This thesis contains no material that has been accepted for the award of any other degree or diploma in any university or institution.
2. To the best of my knowledge, it contains no material previously published or written by another person, except when due reference is made in the text of the thesis.



Muhammad Fahmi Miskon
August 16, 2009

Notice 1

Under the Copyright Act 1968, this thesis must be used only under the normal conditions of scholarly fair dealing. In particular no results or conclusions should be extracted from it, nor should it be copied or closely paraphrased in whole or in part without the written consent of the author. Proper written acknowledgement should be made for any assistance obtained from this thesis.

Notice 2

I certify that I have made all reasonable efforts to secure copyright permissions for third-party content included in this thesis and have not knowingly added copyright content to my work without the owner's permission.

ACKNOWLEDGMENT

I would like to express my gratitude to all those who gave me the possibility to complete this thesis. I am deeply indebted to my main supervisor A/Prof. Andy Russell and my associate supervisor A/Prof. Lindsay Kleeman, whose help, stimulating suggestions and encouragement helped me in all the time of research and writing of this thesis.

Another great debt is to my fellow Ph.D. students in the Intelligent Robotics Research Centre (IRRC), Anies Pudmajaja, Alan Zhang, Elizabeth Hartley, Jay Chakravarty, Fredy Tungadi, Dennis Lui, Nghia Ho, Tuan Phan, Wai Ho Li, Om Gupta, David Zhi Li, Sutono Effendi, Lara Kornienko, Damien Browne and Rahul Walia. Thanks for the helps, talks, laughs and friendship.

I appreciate all the care and support from my parents Miskon and Hasnah, brother Fadhli, sister Aishah over the years. Not to forget my parent-in-laws, Nordin and Sharipah, brother and sister in-laws, Angah, Uda, Yana, Eli and Edi.

Finally, I thank Faraizura Nordin whose sacrifice, support, help and encouragement have been unfailing and to Adam and Daania whose joy and laughter keep the stress away.

ABSTRACT

Novelty detection is a method which highlights unusual data gathered from an environment. The use of novelty detection on a mobile system is an attractive idea. An important aspect of an intelligent robot is the ability to monitor changes as this is one of the important capabilities that are possessed by all biological systems. There are many applications that could benefit from this such as surveillance and inspection applications. However, there are also challenges that arise from implementing novelty detection on a mobile platform. One of them is the problem of mapping sensor measurements that are normally perceived (normal data) from the environment. Most conventional maps require some prior information about the environment to construct their structure, thus they are not readily adaptable to any environment. They also require a large amount of storage space and consequently require similar processing capability, and consume more power which as a whole constrains the design and size of the mobile system.

This thesis presents an alternative mapping system for storing and learning normal data in the environment namely the flexible region mapping system. Its structure can change to accommodate the distribution of normal data. As a result, data are mapped where they are measured and according to the size of the affected area. This thesis also investigates approaches for reducing false positives and to estimate the position of anomalous objects by taking advantage of the system's mobility. A close range inspection strategy has also been developed to demonstrate how an autonomous mobile robot could use the results of novelty detection to perform further investigation of anomalous objects.

The work in this thesis has been targeted to be applicable to any mobile systems that could localized themselves, particularly those that have limited resources in terms of data storage, physical size, processing power and power supply. The solution of mapping normal sensor measurements that is demonstrated in this

thesis is most suitable for structured environments but it could be extended to more complex environments.

Experiments were conducted in an artificial L-shaped environment as well as in a real office corridor. A mobile robot that carries different types of sensors particularly a laser range finder, an anemometer, a temperature sensor, an ambient light sensor, a chemical concentration sensor and an electromagnetic radiation sensor was used. The results show that the flexible region map used as few as 0.7% and 3.3% of the storage space required for a conventional grid map and a perception based map. The map can autonomously accommodate to changes in the normal condition of the environment. The implementation of the false positive filter developed in this thesis reduces the false positive rate by up to 20% compared to the unfiltered novelty detection results, when using noisy sensors at the highest sensitivity settings. Apart from that, the close range inspection strategy is shown to be capable of achieving up to 100% close range inspection coverage near the vicinity of an anomaly.

vi | Page

2.2	Related Work	13
2.2.1	Spatial Indexing	14
2.2.2	Maps Used by Mobile Robots.....	16
2.2.3	Summary	22
2.3	Overall System Design.....	23
2.4	Flexible Region Map.....	26
2.4.1	Definition and design considerations	26
2.4.2	Initiation of a region.....	28
2.4.3	Expansion of a region.....	29
2.4.4	Merging two regions	31
2.5	Novelty Detection Mechanism: An Introduction to the Habituating Self Organizing Map	33
2.5.1	Self Organizing Map	35
2.5.2	Habituation function.....	38
2.5.3	Similarity threshold, S_T	38
2.5.4	Measure of the performance of HSOM.....	39
2.6	Implementation of Different Sensor Types.....	40
2.6.1	Determining the Value of the Region Tolerance for the Laser Range Finder	41
2.6.2	Determining the Value of the Region Tolerance for Other Sensor Types	57
2.7	Summary of the Mapping Process	62
2.8	Experiments.....	64
2.8.1	Experiment 1: Memory requirement when using the flexible region map.....	64
2.8.2	Experiment 2: Performance and memory requirements of different sensors	67
2.9	Discussion and Conclusion	74
Chapter 3	Autonomous Mapping.....	76

3.1	Introduction	76
3.2	Region Separation	77
3.2.1	Separation Algorithm	82
3.3	Autonomous Mapping	85
3.3.1	Added Features of the Flexible Region Map	85
3.3.2	Autonomous Mapping Algorithm	87
3.3.3	Mapping with Minimal Supervision	89
3.4	Experiments.....	89
3.5	Discussions and Conclusions	97
Chapter 4	Repetitive Observation Strategy	99
4.1	Introduction	99
4.2	Related work	101
4.3	System Overview	103
4.4	Estimating the Position of the Source of Novelty	104
4.4.1	Directional Sensors	104
4.4.2	Modeling the Distribution of Laser Range Finder Anomaly Points ..	114
4.4.3	Anomaly Points using Data from Other Types of Sensors	118
4.5	Clustering Anomaly Points	119
4.5.1	Similarity Measures	120
4.5.2	Challenges of On-line Clustering.....	122
4.6	Discussion and Conclusions.....	123
Chapter 5	False Positive Filter.....	125
5.1	Introduction	125
5.2	Related Work	126
5.3	System Overview	127
5.4	Filtering false positive detections.....	128
5.5	Experiments.....	131

5.6	Discussion and Conclusions.....	142
Chapter 6	Close Range Inspection Strategy	144
6.1	Introduction	144
6.2	Related work	145
6.3	System Overview	147
6.4	Close Range Inspection.....	148
6.4.1	Problem Definition.....	148
6.4.2	Navigation Strategy.....	149
6.4.3	Practical Consideration for Terminating Navigation at a Goal Point	152
6.4.4	Algorithm for Close Range Inspection	153
6.5	Experiments.....	156
6.6	Demonstration of using Sensors with Limited Work Range	160
6.7	Discussion and Conclusions.....	163
Chapter 7	Discussion and Conclusion	165
7.1	An Overview of the Thesis	165
7.2	What is New in this Thesis	166
7.3	Limitations and Future Work.....	167
7.3.1	A More Flexible Region Structure.....	167
7.3.2	Multi-sensor Synergy	167
7.3.3	Extracting Information from Sensors.....	168
7.3.4	Commercialization: Novelty Detection Standalone Module	168
7.4	Conclusion	169
Appendix A	Electromagnetic Radiation Sensor	171
A.1	Introduction.....	171
A.2	Sensor Design	172
A.3	Data Processing.....	173
A.4	Performance	177

A.5 Discussion about the EMR sensor.....	182
Appendix B List of Publications	184
References.....	185

LIST OF TABLES

Table 2.1: Confusion matrix representing the possible outcomes of the novelty detection.....	39
Table 2.2: Comparison between simulation and theoretical Euclidean distance values in different robot poses.	49
Table 2.3: The storage requirements when using different mapping approaches for mapping the environment shown in Figure 2.26.	67
Table 2.4: Environmental setup.....	68
Table 2.5: The storage requirements when using different mapping approaches for mapping different type of measured quantities in the environment shown in Figure 2.29.....	70
Table 4.1: A guide to determine the input parameter for estimating the distribution of the anomaly points.....	116
Table 4.2: The comparison between the distribution of the anomaly points from the model and from the actual detection for 3 different cases of observation span.	117
Table 5.1: Environmental settings during the experiments.	132
Table A.1: The signature of devices used in the experiments recorded over 60 seconds.....	178
Table A.2: Results of 40 measurements to recognize different devices using the time between peak signatures.	178
Table A.3: Examples of the attributes used for the signature and the scoring scheme of the CD player and HP1 based on the histogram in Figure A.5.	181

Table A.4: Result of 10 measurements to recognize different devices using the time between peak signature and the histogram.	182
--	-----

LIST OF FIGURES

Figure 1.1: The proposed novelty detection system.	6
Figure 1.2: Overview of the autonomous mobile novelty detection system with indication of where the subsystems are presented in the thesis. The supporting subsystems (with no chapter label) that are employed for conducting the experiments are described in Chapter 2.....	8
Figure 2.1: Possible number of cells and their arrangement when storing normal sensor measurements using different map representations. The path of the robot is shown as dashed lines.	17
Figure 2.2: Example of a map representation using landmark locations (red dots) and point obstacles (green dots that appear as lines). The positions of the robot when it takes the laser measurements are represented as the white squares. Courtesy of Fredy Tungadi of the Intelligent Robotic Research Centre (IRRC) at Monash University.	19
Figure 2.3: An example of a map representation using planes (left) with the texture of the planes (right). Courtesy of Nghia Ho of the Intelligent Robotic Research Centre (IRRC) at Monash University [48].	20
Figure 2.4: Possible number of cells and their arrangement when storing different types of normal sensor measurements using the flexible region map.	23
Figure 2.5: Functional diagram of the surveillance robot with its main system components for performing novelty detection and mapping normal data using a flexible region map.	24
Figure 2.6: The Pioneer 3 mobile robot used for the experiments and the positioning of its various sensors.....	25

Figure 2.7: Initiation of a region.....	29
Figure 2.8: Expansion of a region.....	30
Figure 2.9: Merging two neighboring regions.....	33
Figure 2.10: A neural network consisting of an input layer, a hidden layer and an output layer.	35
Figure 2.11: The effect of path-following accuracy and odometry error on the laser range finder pose.....	42
Figure 2.12: An example of an HSOM network that takes inputs from laser range finder measurements. In this example, the angular range of the sensor is divided into M=3 sectors, producing 3 average readings.	44
Figure 2.13: Defining the input vector from the Hokuyo URG-04LX laser scan.	45
Figure 2.14: The MobileSim simulation is shown in the figure on the left. The figure on the right shows the laser beams, the value of the simulated robot's position and heading together with the Euclidean distance between the laser measurement and the measurement taken from the center of the room.	49
Figure 2.15: The effect of object size on the Euclidean distance between measurements when there is no object and when an object exists. The object is modeled as a portion of a sector.	52
Figure 2.16: An object is modelled as a portion of a sector.	54
Figure 2.17: As the robot travels past an object, different sectors of its laser scan are affected by the object.....	55
Figure 2.18: Effect on the value of Euclidean distance of using different sizes of sector (sector size = 10 degree is shown in the simulation example above the graph) when detecting a 400X400 mm ² box.	56
Figure 2.19: The corridor environment where the sensor measurements were taken. This corridor is used in one of the experiments.....	57

Figure 2.20: Light intensity measurements (taken when the robot was travelling along the path shown in Figure 2.19). The LDR output voltage was produced by the circuit shown in the figure. L1, L2 and L3 indicate the positions of the light sources.	58
Figure 2.21: Ambient temperature measurements (taken when the robot was travelling along the path shown in Figure 2.19).	59
Figure 2.22: Airflow velocity measurements (taken when the robot was travelling along the path shown in Figure 2.19).	60
Figure 2.23: Airflow direction measurements (taken when the robot was travelling along the path shown in Figure 2.19). Note: Air flow direction is not meaningful when there is no measurable velocity.	61
Figure 2.24: The ethanol concentration in a room with still air reduces almost linearly over distance before it stabilizes at a distance of more than 500 mm. The TGS2600 output voltage was produced by the circuit shown in the figure.	62
Figure 2.25: The L-shaped environment used for the first experiment.	65
Figure 2.26: The flexible regions created for mapping normal laser measurement. The maps shown were created using different region tolerance (R_T) settings. ..	66
Figure 2.27: The effect of changing the region tolerance, R_T value to the number of regions created and the minimum detectable object size as shown in Equation (2.33) and Equation (2.41) with the following parameter values: $\alpha = 1, \theta_{sect} = 20$ and $N = 10$	66
Figure 2.28: The corridor environment.	68
Figure 2.29: The corridor environment in its normal condition.	69
Figure 2.30: The regions created for different types of sensors. The rectangles shown are the regions which associate the location with normal conditions. The smallest dots on the inspection route indicate where the robot detected unusual measurements using one or more of its sensors.	72

Figure 2.31: The corridor in its unusual condition and the results of novelty detection using the laser range finder, ambient light sensor and anemometer. The red lines indicates the source of novelty; including the open door, the position of the lights, and the expected areas where the wind changes.....	73
Figure 3.1: An example of how it perceives new measurement (left) and how a robot deviates from its path (middle) while travelling inside region R_o . As a result, three separated regions are created (right).....	78
Figure 3.2: Examples of three forms of overlapping.....	79
Figure 3.3: Decaying novelty function with thresholds.....	86
Figure 3.4: Environmental setup for the experiment. The lines coming out from the robots (the red circles) are the average laser measurements from 8 sector divisions of the 270° laser angular range.	91
Figure 3.5: Results show new regions and the resulting separated regions during epoch 6 (displayed in several frames for better visualization). New region 2 separated region 1 into regions 3, 4 and 5. Region 6 separated three regions. Region 2 was separated into regions 7 and 8, region 4 into 9 and 10 and finally region 3 into 11 and 12.	92
Figure 3.6: Values of novelty measures over 15 learning epochs. The discontinuation of old lines or the start of new lines is due to the deletion of regions or creation of new regions. When a new region is first created, its novelty measure is 0.81.	93
Figure 3.7: Individual graphs showing the novelty measure of all regions.....	94
Figure 3.8: Results of novelty detection during epoch 15. The location of normal measurements (red dots where the block used to be) and unusual measurements (black dots indicating a portion of the wall that usually cannot be detected) are determined using the repetitive observation strategy described in Chapter 4. ...	95
Figure 3.9: Results of autonomous mapping due to deviation from the original path. Temperature data is used to make the visualization of the regions easier.....	96

Figure 3.10: Values of novelty measures for 15 epochs. Region 6 is eventually deleted after it was inaccessible by the robot for several epochs.	97
Figure 4.1: System overview.	104
Figure 4.2: The laser angular range is divided into 8 sectors where the average value of laser measurements from Sector 2 is shown to have the highest dissimilarity. The vector \mathbf{d} carries the directional information and average distance value of the detected anomaly.	105
Figure 4.3: The magnitude of the vector \mathbf{d} , depends on the relation between the average value of the laser measurements taken during inspection \mathbf{di} and during the normal situation, \mathbf{dn}	106
Figure 4.4: Examples of the resulting anomaly points as the position of the anomaly surface was varied.	108
Figure 4.5: The accuracy of the anomaly point decreases when the difference between distance to the surface and the rest of the laser scan increases.	108
Figure 4.6: Examples of anomaly points when the number of laser scans affected by the object is varied.	109
Figure 4.7: The accuracy of the estimated position of an anomaly point increases when the number of affected laser scans in a sector increases.	110
Figure 4.8: Convex, neutral and concave surfaces detected within a sector of a laser range finder scan.	111
Figure 4.9: Test environment for investigating the difference between the average of laser measurements within a sector and the actual measurement at the center of the sector. A rectangular shaped object is shifted 10mm at a time along the bold line shown in the figure.	112
Figure 4.10: Comparison between the average laser measurement in two neighboring sectors and the actual laser measurement at the center of each sector.	113

Figure 4.11: Results of anomaly detection from three inspection steps. The lines coming out from the robot show the average value of laser measurements within the respective sectors. The angle of each line is positioned at the center of each sector. The average distance is longer than the actual distance to the object. ..	113
Figure 4.12: Anomaly point model of a rectangle shaped anomalous object.....	115
Figure 4.13: Comparison of ellipses generated using the model and actual distributions when the robot is moving in different directions. The model data is presented using the blue circular dots and dashed ellipses. Experimental data is indicated with red dots and solid red ellipses.	118
Figure 4.14: The robot observes anomalies from different positions on its route using a laser range finder. The distribution of the anomaly points approximates the shape of the surface of the object.	120
Figure 4.15: An example of the drawback of using the distance threshold for creation of a new cluster. Ideally, point no. 3 should be grouped into the first cluster. The numbering represents the order of data presentation.	122
Figure 5.1: The system for filtering false positives.	128
Figure 5.2: The robot observes anomalies from different positions on its route using a laser range finder. The single anomaly point that forms Group 1 is from a false positive detection.	129
Figure 5.3: The filter is only applicable to groups of anomaly points that are already out of the working range of the laser range finder (shown using the black dots). The white dots are anomaly points which are still within the working range of the sensor.	131
Figure 5.4: State of the robot's environment in its normal state. Door D1 was normally both closed and open while door D2 was always closed. Rectangular box labeled P1 represents the approximate position of the rubbish bin which was introduced during the experiment.	132

Figure 5.5: Examples of detection results using the Singleton Cluster Filter. The clustering process groups nearby estimated anomaly points (the red dots) and represents the groups visually using ellipses. Note that in (a), some of the estimated anomaly points appear to be on the far side of the wall and others inside the box. This is mainly due to the fact that the laser measurements are taken as average readings.	134
Figure 5.6: Comparison of ROC curves for RHSOM and RHSOM with SCF.	136
Figure 5.7: Results of different sensitivity tuning. The anomaly points are represented by the red dots while the purple dots represent singleton clusters. The ellipses created near the rubbish bin indicated by the box are considered to represent true positive detection.	138
Figure 5.8: Comparison of ROC curves for RHSOM with SCF, RHSOM with 2CF and RHSOM with 3CF.	139
Figure 5.9: Filtering using SCF and 2CF. By filtering clusters with 2 or less anomaly points, a lower false positive rate was achieved but the true positive rate was also reduced. Although the true positive rate was reduced, as a result of many observations the anomalous object was still highlighted.	139
Figure 5.10: The maximum neighbor distance parameter d_{\max} affects the size of the groups formed.	140
Figure 5.11: ROC curves for the RHSOM with SCF when using different values for d_{\max} (value indicated by the numbers near the markers).	141
Figure 5.12: Filtering false positives for novelty detection of airflow velocity.	142
Figure 5.13: Filtering false positives resulting from novelty detection of ambient light measurements.	142
Figure 6.1: Overall close range inspection strategy.	147

Figure 6.2: Coverage is defined using the length of the accessible perimeter path. 100% coverage is achieved if the robot encircles the whole object by following the path.....	149
Figure 6.3: The accessible perimeter of an object could be constrained by an adjacent wall and the minimum safety distance to objects.	151
Figure 6.4: The anomaly points represent part of the perimeter of an anomalous object.....	151
Figure 6.5: Illustration of the close range inspection algorithm.	156
Figure 6.6: Positions of the anomalous object introduced into or missing from the environment.	157
Figure 6.7: The resulting inspection path when the anomalous object is on the wall. The circled red dots indicate inspection starting and termination points.	158
Figure 6.8: The resulting inspection path when the object is fully accessible. The circled red dots indicate inspection starting and termination points.....	159
Figure 6.9: The resulting inspection path when performing close range inspection on a missing object.	159
Figure 6.10: Electromagnetic radiation sensor mounted on the mobile robot.....	160
Figure 6.11: The EMR sensor system.....	161
Figure 6.12: Positioning of the anomalous objects introduced into the environment.	162
Figure 6.13: Outcome of the demonstration of a close range inspection using the EMR sensor.	163
Figure A.1: The EMR signature sensor system, the electronic device and the inductively coupled magnetic field between them.	173
Figure A.2: The waveform of the CD player (top) and the mobile phone (bottom) EMR.....	174

Figure A.3: A close up look at the mobile phone's waveform.	174
Figure A.4: The illustration of the time between peak algorithm.....	175
Figure A.5: The histogram of time between peaks from 0 to more than 450 ms.	179
Figure A.6: The histogram of time between peaks from 0 to more than 45 ms.	180
Figure A.7: The mobile robot with the sensor attached is moved past several boxes that contain different electronic devices. Box A contains HP1 and box B contains a CD player. Box C is empty while box D contains HP2.	181

LIST OF ALGORITHMS

Algorithm 2.1: The creation and expansion of the thematic map using flexible regions.....	62
Algorithm 2.2: The mergence process.....	63
Algorithm 2.3: Novelty detection using the flexible region map.	63
Algorithm 3.1: Region separation.....	82
Algorithm 3.2: Find_IS and all affected regions (separation due to the creation of a new region)	82
Algorithm 3.3: Find_IS and all affected regions (separation due to deviation of robot from its path).....	83
Algorithm 3.4: Find_IR	84
Algorithm 3.5: Find_PRS (intersection between I_S and I_R).	84
Algorithm 3.6: Determine_xywl of separated regions	84
Algorithm 3.7: Autonomous mapping using a flexible region map.	87
Algorithm 3.8: Mark visited regions	88
Algorithm 3.9: Update region status.....	88
Algorithm 4.1: Clustering algorithm.	121
Algorithm 4.2: Combining nearby groups.....	122
Algorithm 6.1: Close Range Inspection (see illustration in Figure 6.5):.....	153
Algorithm A.1: Time between peaks (TBP).....	176

Algorithm A.2: Number of Peaks.....	176
Algorithm A.3: Minimum and Maximum Time between successive peaks.	176
Algorithm A.4: Time between peaks histogram.....	177

Chapter 1

Introduction

This chapter presents the motivation and objectives of this research project. The philosophy behind the design of the various elements of this project is detailed to give an idea of the expected results. The contributions of the research are also described here. This chapter ends with an overview of the structure of the thesis.

1.1 What is Novelty Detection?

The adjective ‘novel’ is defined in Merriam-Webster [1] as:

new and not resembling something formerly known or used,

and novelty is defined as:

the quality of being novel.

Novelty detection is the process of identifying new/unusual/abnormal data gathered from an environment. As described by the definition of the adjective ‘novel’, in order to identify new/unusual data, the novelty detection system must have knowledge of what is normal beforehand. The term ‘normal’ is used to describe the *regular pattern or the norm*. In this thesis, the normal condition of the environment is known through supervised or unsupervised learning. For supervised learning, a human supervisor sets a period of time where any measurement taken during the period is considered as normal. For unsupervised learning, a robot makes

repeated observation of the same environment and considers a regularly observed quantity over the many observations as normal.

1.2 Motivation and aim

There are many applications such as fault detection [2, 3], identification of masses in mammograms [4] and internet security [5] that would benefit from using novelty detection. For such applications, unusual data are scarce as faults or errors only happen occasionally which makes it difficult to gather data for training purposes. Also, sometimes it is difficult to determine in advance the features which indicate the items of interest to the detection system. For that reason, it is more practical to use a novelty detection approach and learn normal data instead of the abnormal data. Then any new data which differ from the normal data are considered as anomalies.

Recently, the novelty detection approach is becoming more popular among researchers from the mobile robot field. Several works have been reported using novelty detection for collision detection [6-8] and to assist a learning process [9, 10]. Others have used novelty detection for focusing a robot's attention [11, 12] and for inspection and surveillance tasks [11, 13-17]. Brooks in his paper [18] suggested that, in order to appear intelligent, a robot needs to display a number of different behaviors that operate in parallel, with more complex behaviors subsuming more primitive behaviors as required by the application and environment. The behaviors were ranked using different level of competence of which the higher level implies a more desired behavior that is expected from an intelligent robot when reacting to its environment. Some of the behaviors (in order of the level of competence) include avoiding objects, wander around the environment, explore and build maps of the environment. Placed at level 5 of his suggested task achieving behaviors is monitoring changes, of which novelty detection is an important example. This is why, in the future all domestic/office robots should be generally aware of their environment and although they may be cleaning/delivering/etc. robots, they should also be able to monitor changes and report anomalies just as we would expect a human doing the same task to do.

The work described in this thesis is motivated by the many benefits and challenges of developing an autonomous mobile robot system that employs novelty detection. Some of the challenges and benefits will be describe in the following subsections.

1.2.1 The benefits

There are many benefits of performing novelty detection using a mobile robot. The mobility of the novelty detection system overcomes the limitations of using static sensors. For example, it is easier to implement mobile robot surveillance than to setup and adapt static sensors to a new environment. It does not require the installation of fixtures on the building structure. Mobility also increases the effective working range of a sensor. As a consequence, it opens up the possibility of using sensors that have a very limited work range [19-21]. For these sensors, static installation would be impractical as too many units would be required to cover the whole environment [22] and they will cost too much. By using a mobile robot, a single expensive sensor can be used to monitor many locations in the environment.

Sensing from close range benefits almost any sensor because in general the closer a sensor is to the source of the sensed entity, the more sensitive it will be. For example, chemical concentration is more diluted the further from the source it is measured. The same holds true for radiation level, magnetic field and light sources. Even with images from a camera, a close range viewpoint will highlight more detailed features such as the fine texture of the object surface. Apart from bringing sensors close to the object of interest, the mobile robot could also diversify the angle of perception of the sensors. A camera would certainly benefit from this, as any object usually looks different from different angles. Other examples where change of viewpoint can benefit perception include the situation where the airflow carries a chemical plume in a specific direction.

Another advantage of using an autonomous mobile novelty detection system is that immediate action can be taken upon detecting an unusual situation. The action

could be further investigation of the detected entity. In a scenario which involves intruders, the mere presence of the robot would certainly discourage the intruders and the robot could also pursue or intercept them [23].

1.2.2 The challenges

In order to perform novelty detection in an extended environment, a robot needs to refer to a map, which associates locations in the environment with their normal condition. Without a map, the robot will have difficulty evaluating conditions which are normal at one place but unusual at others. The size and dimension of a conventional grid based map need to be predefined. It also requires a lot of memory, which in turn constrains the robot minimum physical size, limits the size of the environment for any given memory, demands more computational resources, as well as consumes more energy. Hence, one of the challenges is to make the mapping data driven so that no prior knowledge of the environment is needed and to reduce the memory requirement of a map for novelty detection without sacrificing the detection performance.

Another challenge is that the performance of novelty detection is affected by robot localization errors and deviation from a predefined inspection route. As a consequence, a great many false positives would be detected especially when the measured entity is sensitive to change in the sensor's pose.

Last but not least, learning the normal condition of an environment is a time consuming effort. The problem is exacerbated by the fact that the environment may change from time to time. The challenge is how to make the surveillance system easily adaptable to a new or a changed environment.

1.2.3 The aim of this thesis

The overall aim of this research project is to investigate how to overcome the challenges and how to benefit from using novelty detection on a mobile robot. To be more specific, the following is a list of the objectives of this thesis:

1. To reduce the memory requirements of a novelty detection map from what is required by the conventional mapping approach use by the current mobile robot system.
2. To make the mapping data driven by adjusting the map to the needs of the normal measurements produced by different types of sensors in different locations in an environment.
3. To make novelty detection maps autonomously adaptable to a new or changed environment.
4. To reduce the number of false alarms from the results of the novelty detection by benefiting from the mobility of the surveillance system.
5. To develop a method to allow a robot to perform close range inspection near the perimeter of the detected anomalous object using information from novelty detection.

1.3 Design philosophy

The author proposes a spatial novelty detection system which can function as a supporting subsystem. This will result in a system which could be easily added to any mobile robot system at any stage of the robot's life. The proposed system is indicated in Figure 1.1 and requires no prior information about the environment. The only information it requires is its current sensor measurements and the robot's pose. The output of the system is the condition of the environment and perhaps a sample of what is taken to be the normal sensor measurements at specific location in the environment (in case that the robot learns what is normal in the environment by

itself). Training of the spatial novelty detection system should also be made autonomous. Without any modification to the robot's original task, the proposed system should be capable of autonomously learning the normal condition of the environment with a minimum or even no supervision.

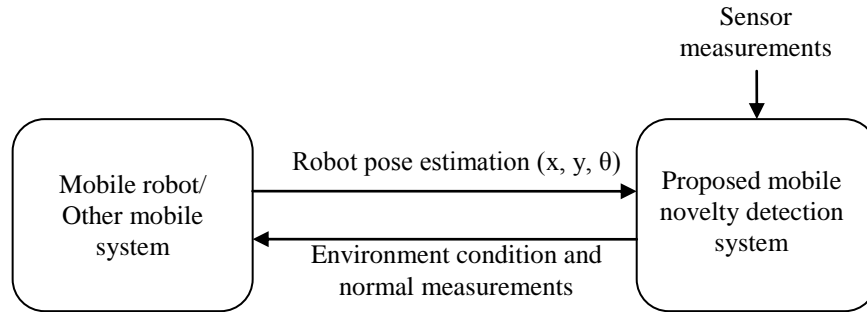


Figure 1.1: The proposed novelty detection system.

The author believes that there are many applications which would benefit from this design philosophy. For example, a robot's ability to monitor changes could be easily enhanced with new sensors. As a result, an old but functional robot could be retrofitted, a current inspection robot could be upgraded with new sensing technology [24] or any mobile robot could be designed without the need to allocate resources from its main system for monitoring changes. As the system does not require prior information about its environment and due to its ability to adapt, it could be easily used by any mass produced mobile robot without any knowledge of their future working environment.

In addition to that, as depicted in Figure 1.1, any mobile object like vehicles, humans, cyborgs or even animals could be mounted with the system as long as they could localize themselves, probably by using GPS, beacons or other methods. Rats for example could be trained (or tricked) to follow a certain route in sewers or pipes. When mounted with the novelty detection system, they could be used to monitor the chemical content of the sewage or inspect cracks in pipes. Pets at home could carry the novelty detection system to monitor changes in noise level, temperature, smells and other parameters. When a novelty is detected the owner could be informed directly through wireless communication, perhaps direct to his/her mobile phone.

Apart from monitoring changes, another possible use from this novelty detection system is perhaps for observing the distribution of normal conditions in the environment. For example, cars that travel to work every weekday using the same route at about the same time could be used to observe the normal average speed pattern along different segments of the route. This information would be useful for the development of semi-autonomous ‘smart’ car which has become popular lately.

As a supporting subsystem, the novelty detection system is preferably made standalone and external to the main system. As a result, this puts some constraints on the storage size, processing capability, power supply, cost and the physical size of the system, especially if the mobile system that carries the novelty detection system has space and weight limitations. This problem has been addressed before as one of the challenges of this project.

1.4 Contributions of the Research

The proposed autonomous mobile novelty detection system is illustrated in Figure 1.2 where the main contributions and their related chapters are highlighted using bold text. The following subsections describe the contribution of this project.

1.4.1 Development of flexible region map systems for novelty detection

The main contribution of this thesis is a new approach for mapping normal data gathered from an environment, namely the flexible region map. This map acts as a reference for a mobile novelty detection system. The original idea about the map is that the size of its regions can change to accommodate the requirements of the entity that is mapped. The significant contribution of the map is that it reduces the amount of memory required to map normal data while maintaining the performance of the novelty detection system.

As part of the contribution, a detail theoretical study of the use of a laser range finder sensor and the Flexible Region Map on the mobile novelty detection

system is also presented. There is also consideration of novelty detection with other sensors including an anemometer, ambient light sensor, gas concentration and temperature sensors.

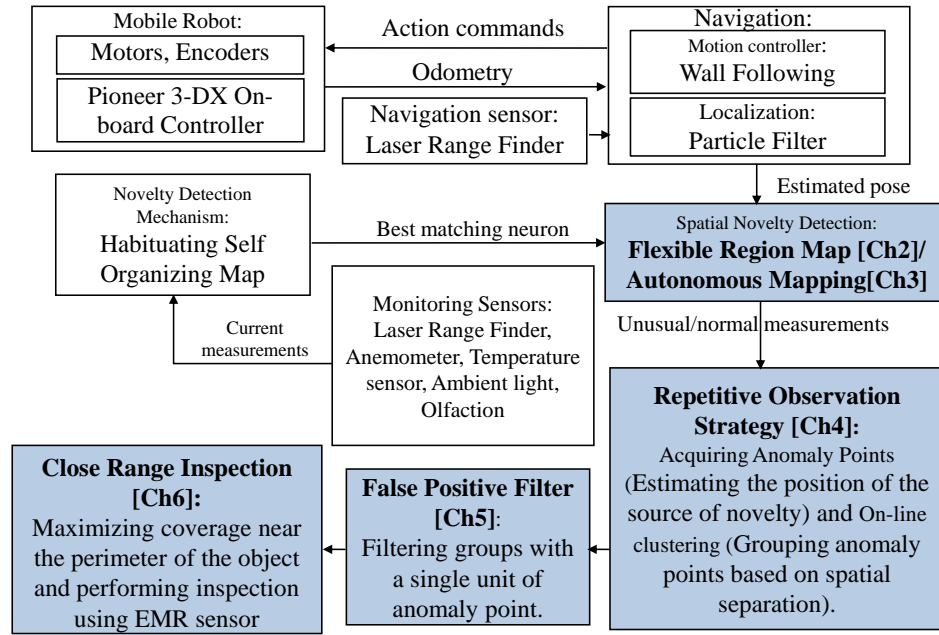


Figure 1.2: Overview of the autonomous mobile novelty detection system with indication of where the subsystems are presented in the thesis. The supporting subsystems (with no chapter label) that are employed for conducting the experiments are described in Chapter 2.

1.4.2 Autonomous mapping using a flexible region map

The next contribution of this thesis is the development of a method for making a flexible region map autonomously adapt to a new or changed environment. The map accommodates to changes in the environment by resizing, separating, creating or deleting region cells as well associating each cell with a normality measure.

1.4.3 Repetitive observation strategy: Confirming the presence of an anomaly

The repetitive observation strategy was also developed as part of this project. This strategy is a method which filters out false positive detections by rejecting isolated

events. A true detection is confirmed after repeated detection of an anomaly from the same vicinity.

1.4.4 Close range inspection strategy

This thesis also introduces a navigation strategy for close range inspection. By using the strategy, a robot would be able to navigate near the perimeter of anomalous objects. In contrast with the work by others, the aim of the path planning is to increase the inspection coverage near the perimeter of the object and not to find the shortest route from one point to another. The strategy uses information gathered from the novelty detection system when using the laser range finder. As part of the contribution of this thesis, an electromagnetic sensor which can sense electronic devices in packages was developed to demonstrate the close range inspection strategy.

1.5 Thesis Organization

In Chapter 2, the statement of the problem of mapping for novelty detection is described after providing a review of different map structure commonly used by traditional mobile robot system. Then the proposed flexible region mapping system is presented. Chapter 3 presents an extension of the work in Chapter2 where a method that allows the flexible region map to be autonomously updated is given.

Chapter 4 discusses the repetitive observation strategy which takes advantage of the capability of a mobile robot which can take measurement from different position in the environment. Then a noise filtering method based on the repetitive observation strategy is presented in Chapter 5 where a filter which can reduce the number of false positive from the results of the novelty detection is described.

Chapter 6 describes the close range inspection strategy which uses the system developed based on the work in Chapter 2 to Chapter 5 to perform inspection near

the vicinity of the detected anomalous object. Finally, Chapter 7 concludes the thesis with a discussion and some future direction for the research.

Since a number of different topics are discussed in this thesis, the associated literature review is presented at the beginning of each chapter.

Chapter 2

Flexible Region Map

This chapter presents the main contribution of this dissertation; the flexible region map. The chapter starts with an overview of the application area. Then the flexible region map is presented. Following that the novelty detection mechanism used in this project and the practical considerations when mapping different types of sensor measurements are discussed. Experimental results show how the flexible region map can be adjusted to suit different types of measured entity as well as different novelty detection sensitivity settings while still achieving good performance.

2.1 Introduction

In order for novelty detection to be used on a mobile platform, the normal data from sensor measurements need to be associated with a map because they usually vary from place to place. Without a map, false detections might occur due to misclassification of data which is normal only at certain places in the environment. Producing a map as a reference for performing novelty detection is not a trivial task. The challenge is that, in some environments, the normal data for some quantity such as the ambient temperature is very much the same throughout the environment. In this case using a map seems to be unnecessary. However, sometimes there are exceptions at certain places in the environment, such as at locations near a heater. In such environments with isolated hot spots, by not using a map, false positives might occur if only a cool temperature is registered as normal. False negatives might occur if both the cooler temperature and the hotter temperature near the heater are

registered as normal for the whole environment and a hot temperature is detected at locations far from the heater. However, if a grid based map is employed, memory will be wasted to store large amounts of redundant information about a quantity that varies only for a few distinct locations.

Although memory size is not an issue for some applications, there are many where this is a constraint due to some limiting factor. One of the limiting factors is to minimize cost when the system is mass produced. Other factors, which are more technical, include limited computing resources, physical weight, physical size and power supply of the robot. For example, flying miniature robots or other micrometer or nanometer size robots might be very particular on the shape and weight of its physical body and there is a limitation on the power supply that they could carry. So, even though memory is cheap nowadays, the designer of these types of robots still considers ways which could optimize the robot's resources. In addition to that, given any particular size of memory, reducing the amount of memory required per area means more area can be mapped. This is especially important for multi-purpose robots, which perform novelty detection as well as other processes which form their main task.

Motivated by this challenge, the author has proposed a new mapping method called the flexible region map. This map can adjust the size of its cells which divide up the mapped space depending on the distribution of the normal condition in the environment. The flexible region map adjusts its memory requirements depending on the characteristics of the entity being mapped. In addition, the performance of novelty detection (i.e. measured using sensitivity) when using the flexible region map is comparable to using a grid based map. Sensitivity is defined as the proportion of actual positives which are correctly identified as such. The goal is to create a general spatial referencing method which could be used for any type of data for novelty detection purposes.

This chapter presents a detail description of the flexible region map and practical aspects that must be considered when implementing novelty detection using the map. An in depth investigation of the use of the main sensor for this project (i.e.

the laser range finder) is given. Discussions of how to map normal data from entities detected by other sensors such as ambient light, ambient temperature, combustible gas concentration, electromagnetic radiation and wind data are also provided.

The remainder of this chapter is organized as follows. Section 2.2 presents related work concerning map building and the uses of novelty detection in mobile robot applications. An overview of the mobile robot novelty detection system is given in Section 2.3. Section 2.4 describes the flexible region map approach. Section 2.5 introduces the type of novelty detection used for this project. Section 2.6.1 discusses case studies used to determine the parameters of the novelty detection system particularly for laser range finder data. In Section 2.6.2 details of other sensors that are used in this project are presented. Section 2.7 gives experimental results and this is followed by discussion and conclusions in the last section.

2.2 Related Work

A lot of previous work has been done in the area of mapping of spatial information. This section is dedicated to reviewing literature related to map representations in general. The main purpose of the review is to consider the available map representations especially those that are used by mobile robots, in order to find the most appropriate map for storing novelty detection data (normal data gathered from the environment which is used for performing novelty detection). An example scenario and the requirements of novelty detection data will be considered to give an idea of the advantages and limitations of some of the map representations. The map that is sought should be able to accommodate different kinds of novelty detection data from different types of sensors and be as general as possible.

The maps used for novelty detection will be thematic maps. A thematic map is a map which associates theme or feature information to their spatial location. In [25], Petchenik described thematic maps as "in place, about space". What illustrates the main difference between thematic maps and general reference maps is that while the general reference maps show where something is in space, thematic maps tell a

story about the place. For novelty detection, the theme is the *normal data* which comes from the robot's sensors (such as temperature, distance, air flow velocity and direction, ambient light etc.) and which are taken in the robot's environment. Some maps used for navigation could also be called thematic maps since the robot indirectly uses mapped signatures (list of features) perceived in the environment to determine its position [26].

There are many forms of thematic maps. The user of the map and the main purpose of the map help characterize the most suitable representation for a thematic map. Thematic maps are traditionally used in the field of geography to show the distribution of data such as population densities, barometric pressure, land elevation and other uses [27]. The main difference between these maps and the ones described here is the audience, as well as the cartographer. While all the traditional thematic maps are created by humans for humans, the cartographer and the audience of the novelty detection map is the robot itself.

The measured quantities of any entity will not deviate too much if they are observed from within a region of a certain size. This is especially true for ambient entities like room temperature, light intensity and air flow velocity. This can also be true for measurements that are pose sensitive such as laser range finder measurements, by lowering the sensitivity of the novelty detection in exchange of allowing a small difference in measurements at neighboring poses. In this light, a regional thematic map is more appropriate for novelty detection applications. The following section will discuss different representations of maps especially for storing data affecting a region.

2.2.1 Spatial Indexing

The problem of spatial databases and indexing has been explored extensively especially in the field of computer science. A spatial database is a database that is optimized to store and query data related to objects in space while spatial indexes are used by spatial databases to optimize spatial queries. As the main concern is to

optimize spatial queries, a major part of the work in this field focuses on developing reference system which could be accessed or searched easily and on developing efficient searching algorithms. Although these are some of the motivations of the work in this chapter, the main concern is to find a suitable map representation for data to be used for novelty detection. For this reason, attention is given to map representations covered in the field of spatial indexing. Common spatial indexing methods that could represent data in regions include grids [28], Quadrees [29, 30] and R-trees [31-33].

A grid is a 2-D surface that is divided into a series of contiguous cells. The shape of the cells can be in many forms such as triangular and hexagonal [28]. However, square or rectangular grids are the most commonly used for their simplicity of representation using Cartesian coordinate. The grid map is perhaps the simplest form of spatial indexing to manage as its cell size and arrangement are fixed, and independent of the data.

Quadrees [29, 30] are a form of grid map where the resolution is varied according to the position and distribution of the data to be fitted. They are based on the successive subdivision of a 2-D region into four equally sized quadrants. Another commonly used variant of Quadrees is the Octree where 3-D space is partitioned by subdividing it into eight octants. Although quadrees and their variants reduce the storage space compared to a grid, they still have rigid geometries and relatively coarse steps of resolution.

Unlike grids and Quadrees, R-trees [31-33] have flexible geometry. When using R-trees, data are grouped using the minimum bounding rectangle (MBR). The MBR is an expression of the maximum extent of a 2-dimensional object within its 2-D (x, y) coordinate system, (i.e. $\min(x)$, $\max(x)$, $\min(y)$, $\max(y)$). One of the advantages of using R-trees for spatial indexing is that the size and the number of MBRs used is determined by the data. This means the storage size as well as the cells resolution is optimized to fit the data by contrast with grids or Quadrees.

In summary, some spatial index methods are ‘space driven’ like the grids, others like R-trees are ‘data driven’. While space driven indexing is easier to create,

the data driven approach is more storage efficient. The following section will discuss how some of the popular approaches involving spatial indexes and other methods are employed to produce maps that are used for mobile robot applications.

2.2.2 Maps Used by Mobile Robots

In the field of mobile robotics, a lot of work relating to mapping is mostly for navigation purposes. Maps for navigation are used to determine the robot position in the environment and also for performing path planning. Maps are also used by robots for purposes other than navigation such as to perform novelty detection. Although many of the examples given are related to simultaneous localization and mapping (SLAM) problems and some are related to path-planning, this chapter does not address these problems. The main purpose of the review is to see how different maps are represented. This will help the choice of the most suitable representation for storing novelty detection data.

Different robot mapping approaches and their respective map representations are discussed in [34]. These include the Occupancy Grid [35, 36] which uses grid (or metric) maps and Kalman filtering [37, 38] that stores landmark locations. Others that specifically use laser scanner data like Lu/Millios [39] and Expectation Maximization [40] represent the map using point obstacles. There are also multi-planar maps [41, 42] that store the geometry of objects instead of grids. For path planning, maps such as grids and Quadtrees [43] are used. These maps will be discussed from the perspective of how they are constructed and in terms of the amount of storage space required.

2.2.2.1 Space-Driven Maps

Grid maps (see Figure 2.1(a)) are one of the most common map representations for mobile robot use. They are commonly used to represent the presence of obstacles and free space at locations in the environment. One of the popular approaches is to associate each grid element in the grid map with its state of occupancy. This is often

presented probabilistically. Elfes and Moravec were among the first to use this approach. The map was named the occupancy grid map [35] and has been widely use by many others [44, 45]. Other researchers also employ grid based maps to map other physical entities such as gas plumes [46].

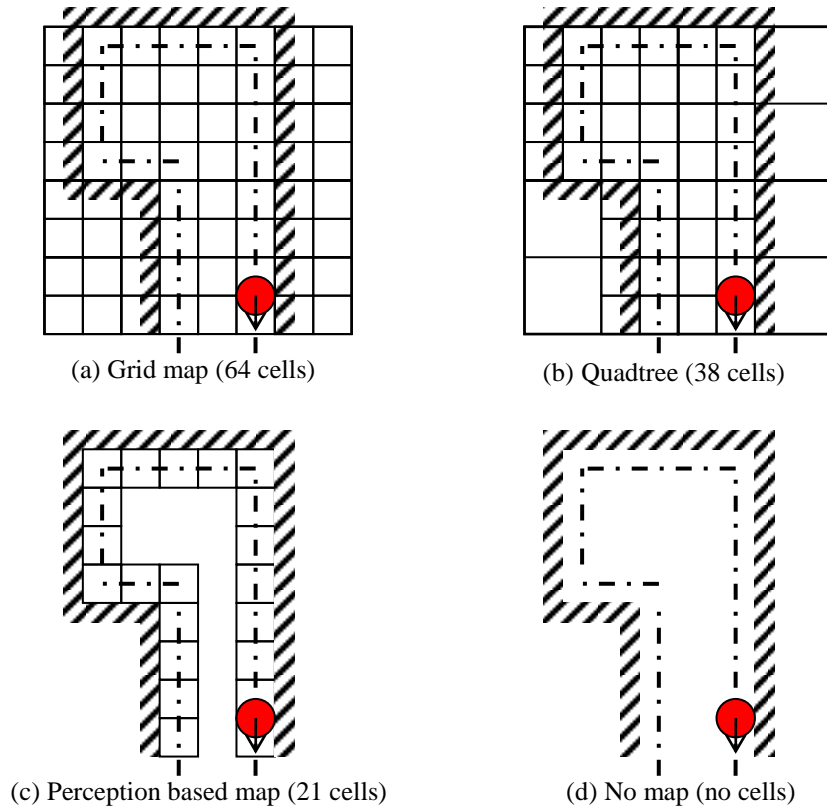


Figure 2.1: Possible number of cells and their arrangement when storing normal sensor measurements using different map representations. The path of the robot is shown as dashed lines.

As mention before, grid maps are the easiest to create and manage since the map consists of evenly spaced grid elements and the size and the boundary of each grid element is predefined before the map is created. However, this also means that the memory requirement to store information in the grids is fixed and maximized. The resolution of the grid influences the accuracy of the spatial distribution of the information. This means that in order to gain a more accurate representation, more memory is required. As an example, as reported in [47], the state space to represent

an environment of size $30 \times 30\text{m}^2$ with an angular resolution of 2° and cell size of $15 \times 15\text{cm}^2$ consists of $(30 \times 0.15)^2 \times (360/2) = 7,200,000$ states. Handling such a large number of states requires a lot of processing time and is a very demanding task with current computer speeds.

Quadtrees reduce the amount of space required compared with grid maps and provides a means to efficiently access stored data and to be able to adjust the resolution of its cells. Like grids, the initial square cell of Quadtrees is predefined with a size that should cover the whole environment. The cell is divided into four equal areas if the data it needs to store is affecting only part of the cell. This is repeated until the data can be represented by a single cell or until the division meets the highest map resolution. Although this will reduce some storage space, as can be seen from the example in Figure 2.1(b), due to its rigid geometry and coarse step resolution, some cells are still unnecessarily created. As shown in the example in Figure 2.1, for some mobile robot applications, the robot navigation route may be planned such that it does not visit most of the reachable area covered by the map. This will waste the memory required to map unvisited areas. It is natural for a surveillance robot to follow a predefined route [17] or to use wall following behavior [16] as many human security officers do. The reason is that to visit all discreet positions in the environment would take too much time and effort.

2.2.2.2 Data-Driven Map

Some maps used by mobile robots only store information when and where it becomes available. The advantage of this is that no memory is wasted for empty cells as with the grid map or Quadtrees. Examples of such map representations includes landmark locations [37, 38] and the geometry of objects [41, 42]. As the representations are data dependent, the types of representations are chosen to suit the nature and purpose of the data. Landmark locations refer to the points where features are extracted from vision or laser range finder data in 2-d or 3-d space (see the example in Figure 2.2). However, landmark data is represented at points which means that this method is not suitable for representing data affecting a region.

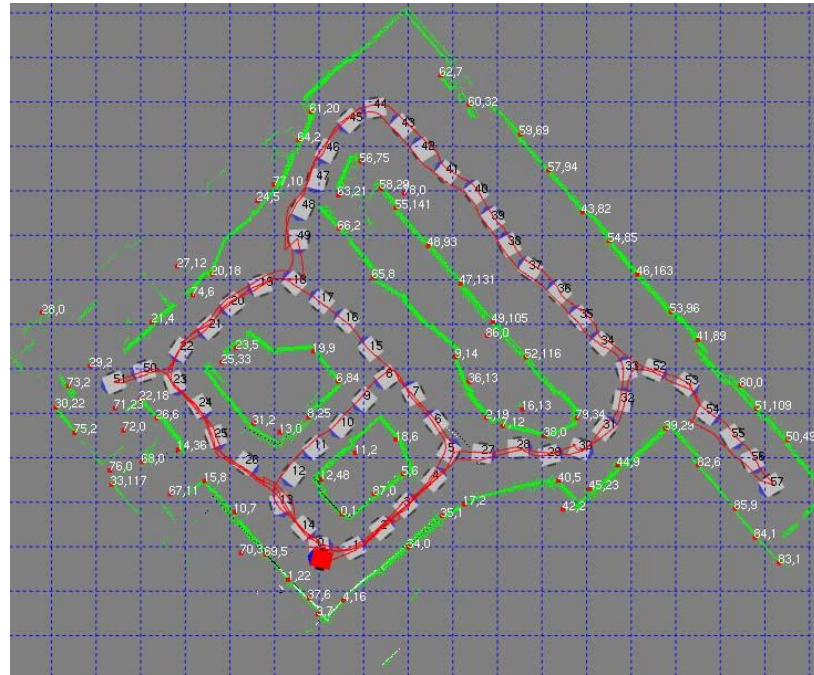


Figure 2.2: Example of a map representation using landmark locations (red dots) and point obstacles (green dots that appear as lines). The positions of the robot when it takes the laser measurements are represented as the white squares. Courtesy of Fredy Tungadi of the Intelligent Robotic Research Centre (IRRC) at Monash University.

An example of representations using the geometry of objects is shown in Figure 2.3. The surface of objects such as walls and doors are represented using planes. In addition to that, other characteristics such as their textures are associated with these planes. This map representation could be used to represent regional data such as the texture given in the example. However, its application is limited to representing the position of structured objects in space and a range sensor such as the laser range finder is required to acquire the geometry of the plane.

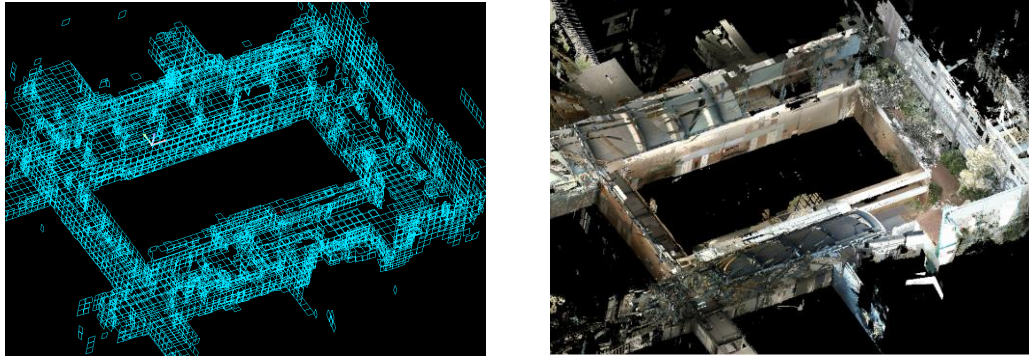


Figure 2.3: An example of a map representation using planes (left) with the texture of the planes (right). Courtesy of Nghia Ho of the Intelligent Robotic Research Centre (IRRC) at Monash University [48].

As the novelty detection task is actually to compare perceptions taken at a certain location but at different times, a perception based map is perhaps more suitable for representing the data. This means that the information is simply referenced to the position where the robot acquires it. One example of this type of representation is called point obstacles (see the example in Figure 2.2). Point obstacle representation is used in [49] where the laser measurements are indexed at the position of the robot when it takes the measurements. For point obstacle representation, the laser measurements need to be taken and indexed at closely spaced points. This is done to allow a high percentage of overlapping to align and correct the laser scans.

Another example of a perception based map is described in [17] and is actually used for novelty detection. The robot navigates by following a path, and information which is observed from the route is mapped onto the position of the robot. This type of map is illustrated in Figure 2.1 (c). Unlike grid maps, this map saves a large amount of memory by only storing information on the robot path. In this particular example, panoramic images are stored at regular intervals along the route, as it is expected that in most environments this information is sensitive to changes in position.

From these examples of perception based representation, it can be seen that due to requirement of the techniques and/or the sensors, samples are indexed at

regular intervals. However, many sensed quantities such as ambient temperature and combustible chemical concentration can have the same value throughout an area such as an office environment, except for certain exceptional locations. Even high dimensional sensors return the same measurement in certain situations. For example, successive laser range finder distance measurements are similar in a long corridor. Another example is the histogram features of images taken by a camera in a monotonous colored room which will look the same. In such situations, storing perceptions at a regular interval will waste memory by storing redundant information in neighboring positions when these elements could actually be merged together. The following section will discuss some related work which uses no map when performing novelty detection in these types of situation.

2.2.2.3 Mobile Novelty Detection Using No Map

In some environments, all data are assumed to be distributed evenly or if they are not, it is assumed that each group of data is unique and therefore no referencing to the environment space is needed (see Figure 2.1(d)). Examples of this can be found in Marsland's work for novelty detection purposes [16, 50, 51].

In these examples, the possible unusual data is assumed to have no resemblance to the normal data. While this approach minimizes the memory requirement, the assumption made is limited to environments like inside pipes or sewers. In most environments such as in corridor and offices, there are many different conditions which are normally observed in the environment but might be unusual at certain locations.

In [52], Marsland introduces an approach suggesting how to select the appropriate novelty filter (each novelty filter stores normal data related to a specific environment) to use in different environments by using a familiarity vector. However, this approach requires the robot to travel a certain distance before it has enough confidence to select the appropriate novelty filter. By the time it is able to

choose the appropriate filter to use it might already have missed highlighting some unusual measurements.

2.2.3 Summary

Different types of map representations have been discussed, especially ones that are commonly used in the mobile robotic field. From the literature many maps used for navigation are available but only a few are used for novelty detection, as novelty detection is not often implemented on a mobile robot. To the best of the author's knowledge, no effort has been given to investigating the type of map representation that is suitable for novelty detection applications and is sufficiently general that it can be used for referencing different types of data in a wide range of situations.

The proposed map representation for novelty detection using a mobile robot is as follows:

1. Data driven indexing like the R-tree is used, although the hierarchical aspect (the tree) is not implemented as optimized searching of data is beyond the scope of this work. To the best of the author's knowledge, it has never been used before for novelty detection using a mobile robot.
2. Regions that have a flexible size are used to accommodate the requirement of different types of data in a range of possible situations.
3. Minimum Bounding Rectangle (MBR) is used for representing the region as it is the computationally simplest of all linear bounding containers [53].
4. Regions can be changed (created, expand, merge and separated) in response to dynamic data.

The expected kind of maps that store measurements from different sensors are illustrated in Figure 2.4.

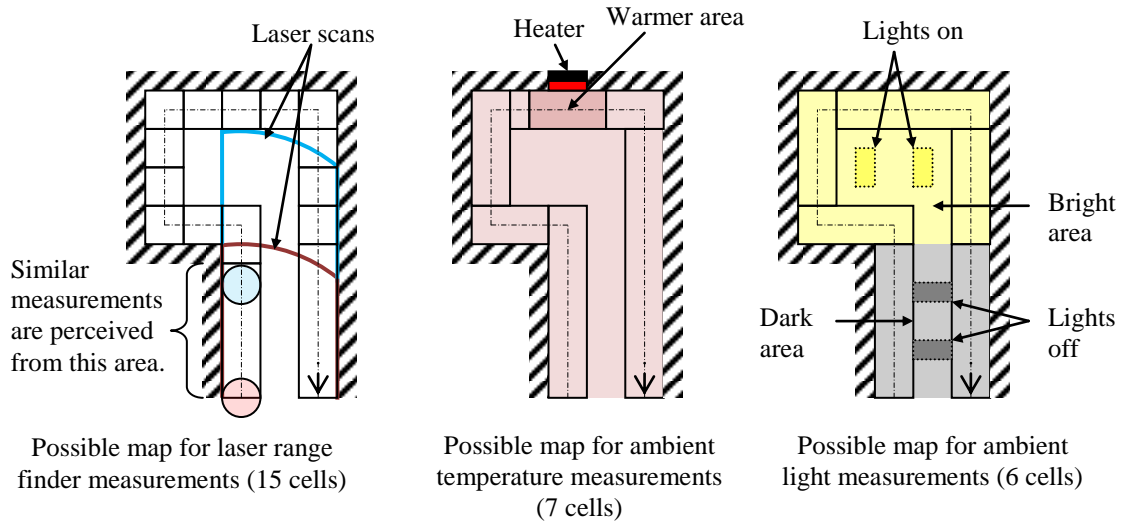


Figure 2.4: Possible number of cells and their arrangement when storing different types of normal sensor measurements using the flexible region map.

2.3 Overall System Design

This section provides a description of the overall system. A schematic diagram of the functional system design is shown in Figure 2.5. This consists of three main components; the navigation system, thematic mapping/referencing system and novelty detection mechanism.

The navigation system provides position and heading information to the main controller. The robot determines its position using odometry and corrects accumulated position errors using a particle filter localization approach. The availability of the hardware and software for developing the particle filter localization made the author chose the technique over others. In practice, any localization technique can be use instead of the particle filter approach.

The robot navigates with a wall-following behavior using feedback from its laser range finder as described in [54]. It maintains a distance of 400 mm from the wall either on its left or on its right, depending on the direction of travel. During inspection from the starting point to the stopping point, the robot pauses every 100

mm of travel and then aligns itself parallel to the wall before taking measurements from its sensors.

Particle filter localization was used to determine the position of the robot. A detail explanation of the approach is presented in [55]. For this project, laser measurements were employed as the sensory information used by the method. A constant number of 1000 particles was used and the weighted mean of the states of these particles was used to estimate the robot position. The position estimate is accepted only if the standard deviation of the distribution of the robot position in x and y directions are both below 100 mm and 5° for the heading.

The main contribution of this chapter is in the development of the thematic mapping system. It requires two types of information; robot heading and position together with normal sensor measurements. Any type of novelty detection mechanism can be employed to represent the normal sensor measurement. For this project, the Habituating Self Organizing Map was employed. The novelty detection mechanism and the flexible region map are described in detail in the following sections.

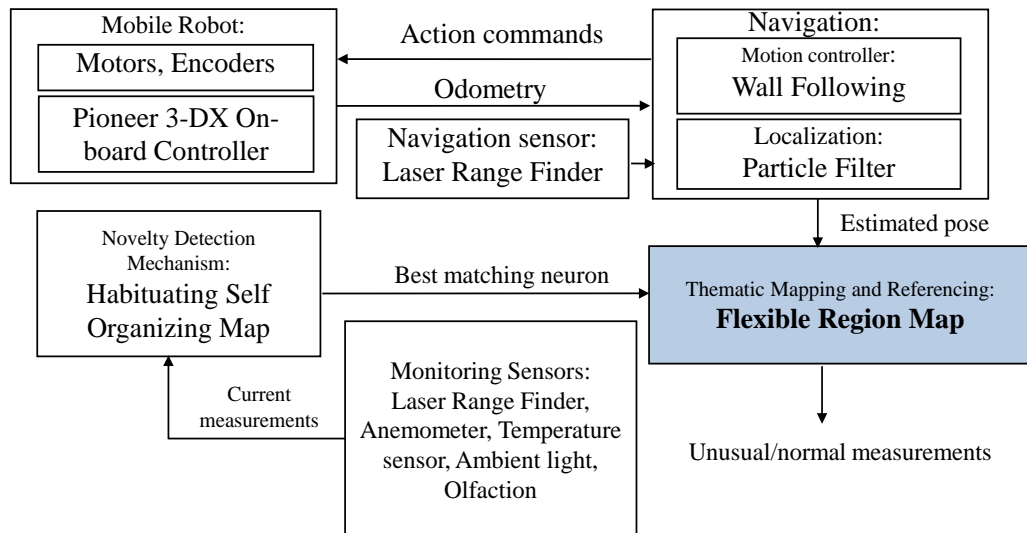


Figure 2.5: Functional diagram of the surveillance robot with its main system components for performing novelty detection and mapping normal data using a flexible region map.

The mobile robot used for the experiments was a Pioneer 3 DX manufactured by MobileRobots Inc. The robot carries several sensors including a Hokuyo URG-400LX laser range finder, a TGS2600 chemical sensor, an LDR for measuring light intensity, a TS8000 Anemometer and a SMT 160-30 ambient temperature sensor. The detail features of the sensors are mentioned in Section 2.6 *Implementation of Different Sensor Types*.

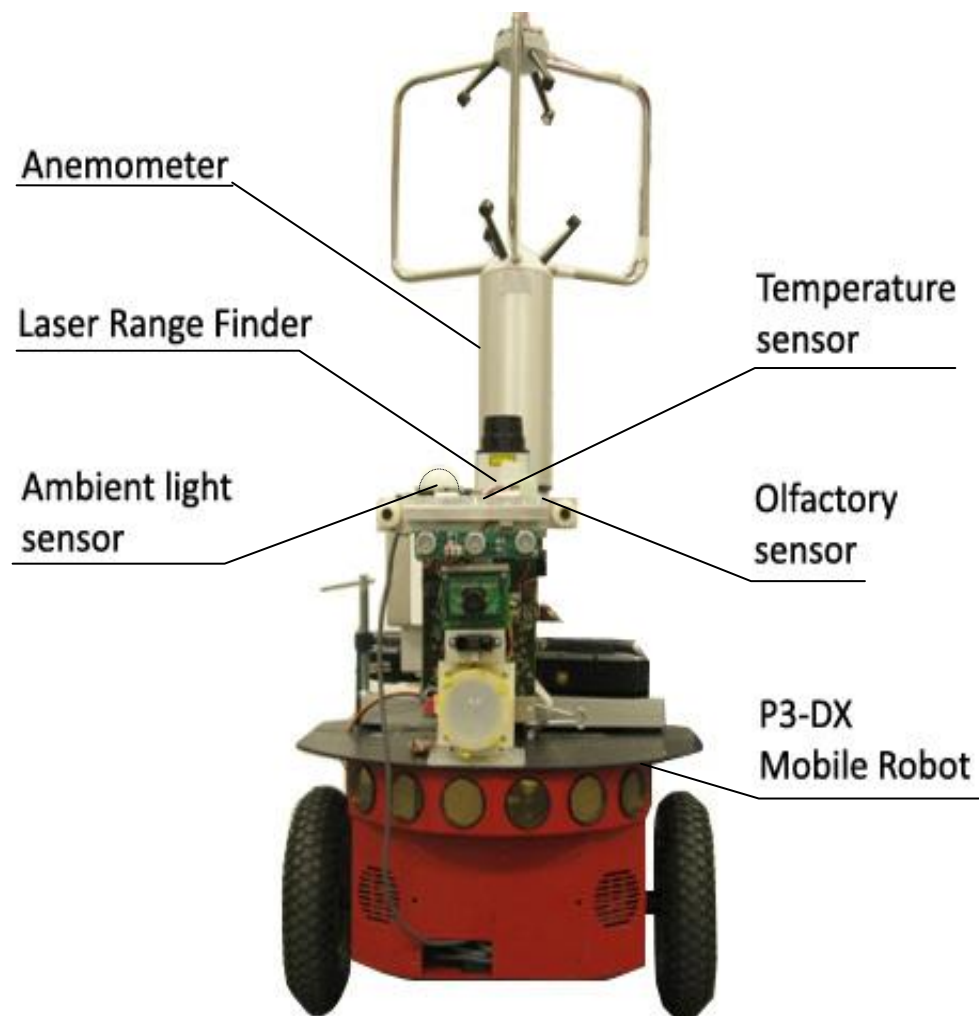


Figure 2.6: The Pioneer 3 mobile robot used for the experiments and the positioning of its various sensors.

2.4 Flexible Region Map

This section presents a detail description of the flexible region map which is the main contribution of this thesis.

2.4.1 Definition and design considerations

2.4.1.1 Definition

A flexible region is defined as a geometrically specified area which can change its size to shrink or grow, as well as merge with other regions. These changes are performed based on the similarity between perceptions at neighboring spatial positions of the robot.

2.4.1.2 Shape and description of a region

In principal a flexible region could be represented using any spatial footprints like a bounding diamond, the minimum bounding parallelogram, the convex hull, the bounding circle or bounding ball, and the bounding ellipse. For this project, the bounding box, also known as Minimum Bounding Rectangle (MBR) is used as it is known to be the computationally simplest of all the linear bounding containers [53]. Rectangular shapes are also relatively easy to combine into a map compared to other shapes. Another reason is that since grid based maps and perception based maps use rectangular cells as well, direct comparison could be made between these maps and the flexible region maps. A rectangle is described using its width, w and length, l extending from a reference point $(P_{x_region}, P_{y_region})$.

2.4.1.3 Information associated with a region

1. Reference point $(P_{x_region}, P_{y_region})$ - A reference point referred to the bottom left corner of a rectangle.

2. Region size - The size of a region is described using the width and the length extending from the reference point (P_{x_region} , P_{y_region}).
3. Heading states – The robot's heading also needs to be associated with the map especially if a sensor measurement is sensitive to the change of the robot's heading. In this project, laser range finder and air flow direction measurements are two of the measurement types that are sensitive to change of the robot's heading. As the intended working environment for the surveillance robot developed for this project is mostly rectangular in shape, the author decided that it was sufficient to reduce the number of states for the robot heading to 4 i.e. 0° , 90° , 180° and 270° .
4. Normal measurements - Normal measurements are sensor measurements that are commonly observed (autonomously by robot) or labeled as normal by a human expert. In this project, normal sensor measurements are represented using neurons in a Habituating Self Organizing Map (HSOM). The HSOM is discussed in detail in Section 2.5 Novelty Detection Mechanism: An Introduction to the Habituating Self Organizing Map.

2.4.1.4 Region tolerance, R_T

Region tolerance, R_T is the maximum allowable difference between measurements taken (or 'neurons' since neural network based novelty detection is used here) from anywhere in a region and measurement at the centre of the region when it is initially created. In the case where a measured quantity should remain unchanged, there are 3 reasons why measurements at the same position could differ from each other:

1. Robot localization error – the deviation between the robot actual position and estimated position.
2. Robot path-following repeatability – the degree of offset between the robot actual path and the planned path.
3. Sensor measurement error and fluctuation.

These are the factors to be considered in choosing the value of a region tolerance.

A more general form of region tolerance is the similarity threshold, S_T . S_T is the maximum allowable difference between two measurements that belong to the same group. More information about the similarity threshold is provided in Section 2.5 *Novelty Detection Mechanism: An Introduction to the Habituating Self Organizing Map*.

2.4.1.5 Trade-off between number of regions and sensitivity of detection

Region tolerance can be set higher than its minimum value so that measurements at neighboring locations that are less similar to each other can be referenced using one region. This decreases memory requirement by reducing the number of regions in the map. However, by doing this the sensitivity of the novelty detection will also be reduced. A detail explanation of the concept of sensitivity relating to novelty detection is given in Section 2.5.4 *Measure of the performance of HSOM*.

2.4.2 Initiation of a region

When required, a new region (R_i) is initiated by establishing a w_{init} mm wide and l_{init} mm long rectangle with the centre being the position of the sensor (see Figure 2.7). As mention earlier, the values of the initial width, w_{init} and the initial length, l_{init} depend on the minimum value of the region tolerance.

A region is initiated if both of the following conditions are true:

1. At the current robot position, the robot observes a normal sensor measurement.
2. There is no existing region at the current robot position which maps the normal sensor measurement.

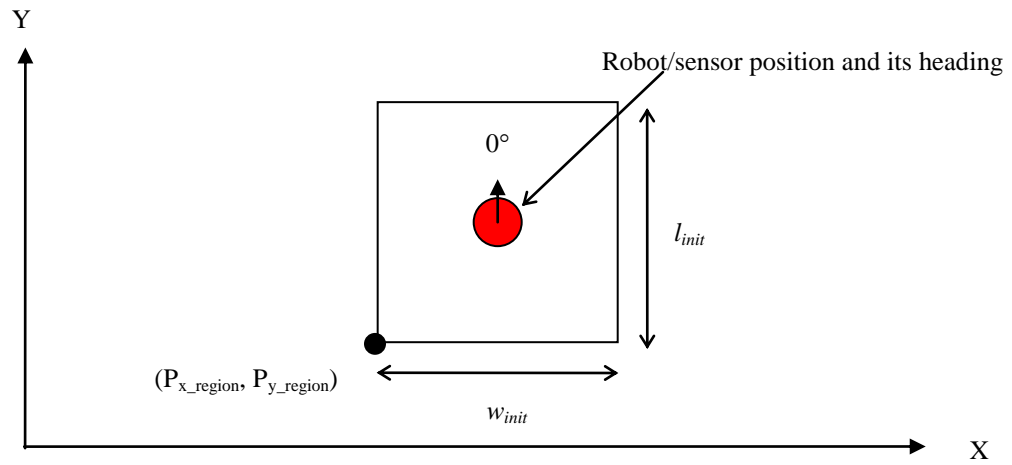


Figure 2.7: Initiation of a region.

2.4.3 Expansion of a region

A region grows by increasing its width or length by the width or length extension value, δw or δl (see region R_i in Figure 2.8). The sensor receptive angle influences the expansion direction of the region unless the sensor is insensitive to direction. A region should be expanded if the difference between a measurement taken immediately outside of a region and measurement at the center of the initial region is less than the region tolerance, R_T .

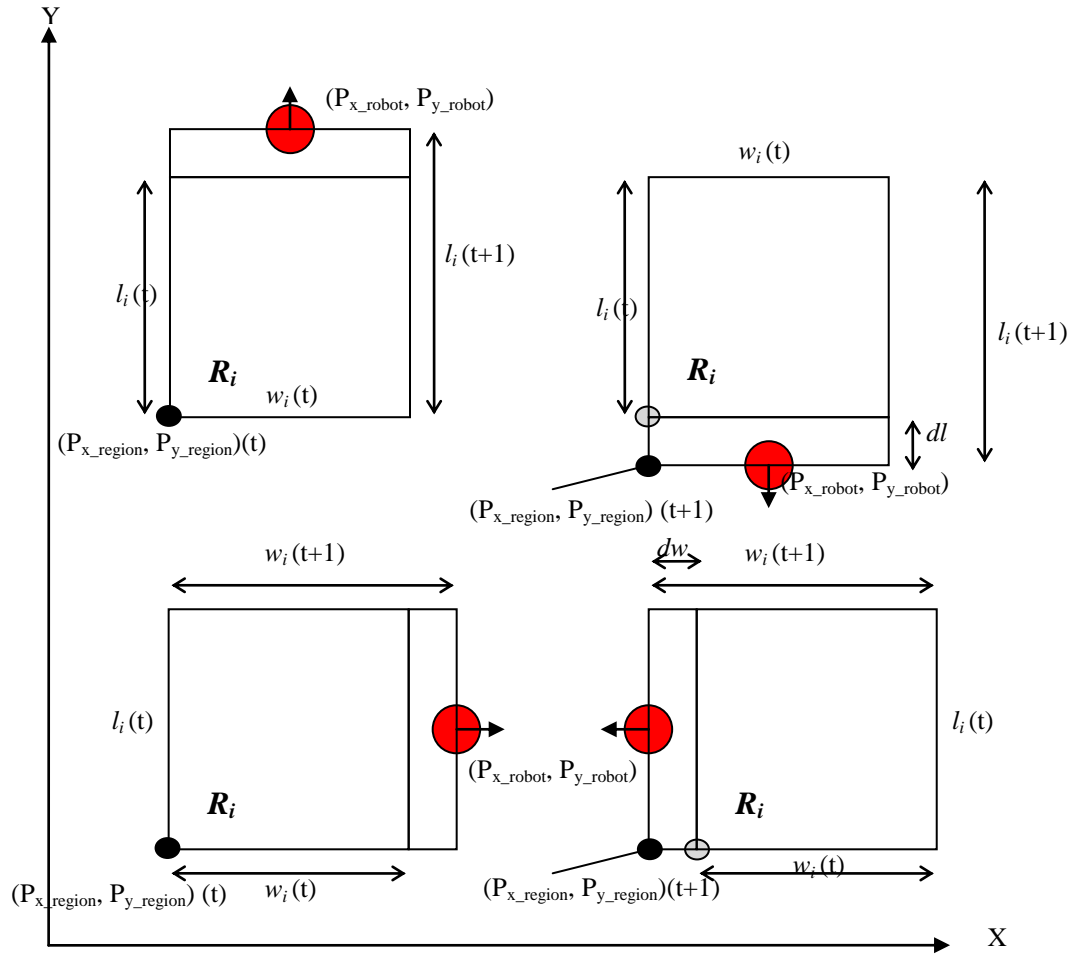


Figure 2.8: Expansion of a region.

The parameter that needs to be changed (P_{x_region} , P_{y_region} , l or w) and the amount by which it changes depends on the direction of expansion. The main consideration is that the region tolerance is maintained below its set value. The following are the parameter values that need to change for different direction of extension.

1. If the extension is in the positive y direction.

$$l_i(t+1) = |P_{y_robot} - P_{y_region}| \quad (2.1)$$

2. If the extension is in the positive x direction.

$$w(t+1) = |P_{x_{robot}} - P_{x_{region}}| \quad (2.2)$$

3. If the extension is in the negative y direction.

$$\delta l = |P_{y_{region}} - P_{y_{robot}}| \quad (2.3)$$

$$l(t+1) = l(t) + \delta l \quad (2.4)$$

$$P_{y_{region}}(t+1) = P_{y_{region_prev}}(t) - \delta l \quad (2.5)$$

4. If the extension is in the negative x direction.

$$\delta w = |P_{x_{region}} - P_{x_{robot}}| \quad (2.6)$$

$$w(t+1) = w(t) + \delta w \quad (2.7)$$

$$P_{x_{region}}(t+1) = P_{x_{region_prev}}(t) - \delta w \quad (2.8)$$

2.4.4 Merging two regions

Two regions R_i and R_j (see Figure 2.9 for an example) are merged by combining either the width or the length of both regions. The regions R_i and R_j could be merged if they fulfill the following requirements:

1. Both are close to each other, such that the gap between both regions, Δn is less than a threshold, Δn_T . Depending on the direction of the merge, the threshold value is taken to be half of the region's initial width or length. As explained earlier, this is to ensure that the region tolerance is maintained to be below the set value.

$$\left| (P_{x_Ri} + w_i) - P_{x_Rj} \right| \leq 0.5w_{init} \quad (2.9)$$

$$\left| (P_{x_Rj} + w_j) - P_{x_Ri} \right| \leq 0.5w_{init} \quad (2.10)$$

$$\left| (P_{y_Ri} + l_i) - P_{y_Rj} \right| \leq 0.5l_{init} \quad (2.11)$$

$$\left| (P_{y_Rj} + l_j) - P_{y_Ri} \right| \leq 0.5l_{init} \quad (2.12)$$

2. The length of both regions is about the same size given that their y coordinates are similar, or the width of both regions is about the same size given that their x coordinates are similar as shown in Equation (2.13) and Equation (2.14).

$$|w_i - w_j| \leq 0.5w_{init} \text{ given that } |P_{x_Ri} - P_{x_Rj}| < 0.5w_{init} \quad (2.13)$$

or

$$|l_i - l_j| \leq 0.5l_{init} \text{ given that } |P_{y_Ri} - P_{y_Rj}| < 0.5l_{init} \quad (2.14)$$

3. Both regions contain the same set of neurons as shown in Equation (2.15) where N_i and N_j are two sets of data from region R_i and region R_j respectively which consist of the value of normal neurons n observed from within the regions.

$$N_i = N_j = \{n_1, n_2, \dots, n_n\} \quad (2.15)$$

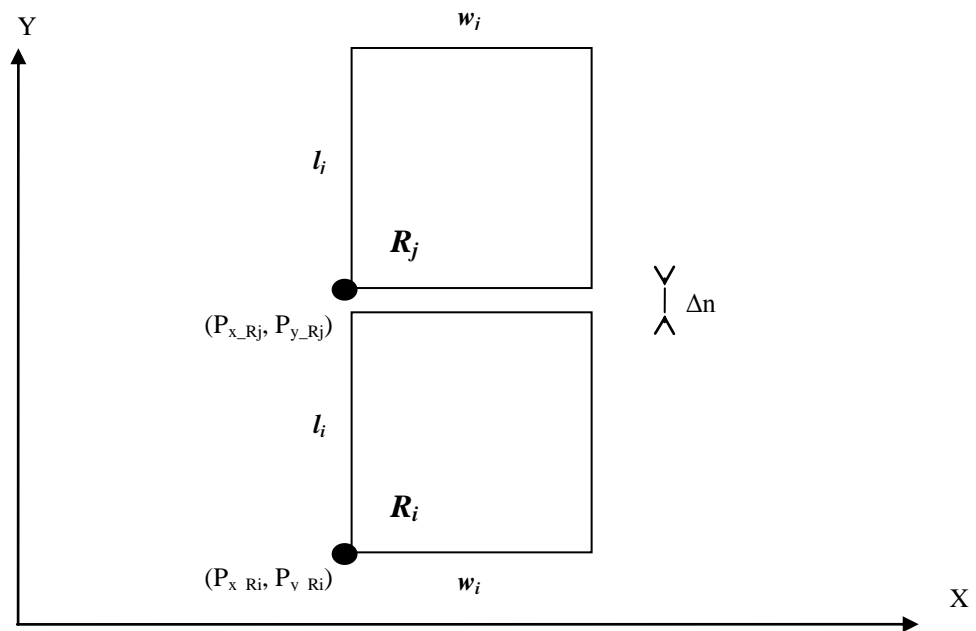


Figure 2.9: Merging two neighboring regions.

2.5 Novelty Detection Mechanism: An Introduction to the Habituating Self Organizing Map

This section describes the novelty detection mechanism that is used in this project. As mentioned before, novelty detection is a mechanism which highlights sensor measurements that deviate from the normal condition of the environment. The considerations that should be taken into account when selecting an appropriate

novelty detection method vary from case to case and depend on the type of application [56-58]. In this project, the main considerations are:

1. The novelty detection is implemented on a mobile platform.
2. Many different types of data are used including laser distance measurements, temperature, humidity, air flow direction, air flow velocity and chemical concentration.

Based on these considerations, the Habituating Self Organizing Map (HSOM) [51] was chosen. HSOM is a neural network type novelty detection mechanism which can readily adapt to a new environment. A small number of runs are sufficient for the system to learn the pattern of measurements found in an environment. This makes the learning process for different types of sensor measurements relatively simple. HSOM also has been proven to work for mobile robot applications [51].

Figure 2.10 illustrates an example of an Habituating Self Organizing Map (HSOM) neural network consisting of 4 neurons in its hidden layer. It is a novelty detection mechanism based on the Self Organizing Map (SOM) and consists of two separate parts:

1. A clustering network (i.e. SOM)
2. A set of habituating synapses that connect the network neurons to the output neuron (i.e. habituation function).

As can be seen from the figure, each of its neurons is connected to the output via an habituable synapse. The output neuron carries the value of the habituable synapse of the best matching neuron, n_{BMU} . The input measurement is considered as normal if the value is below the habituation threshold, h_T .

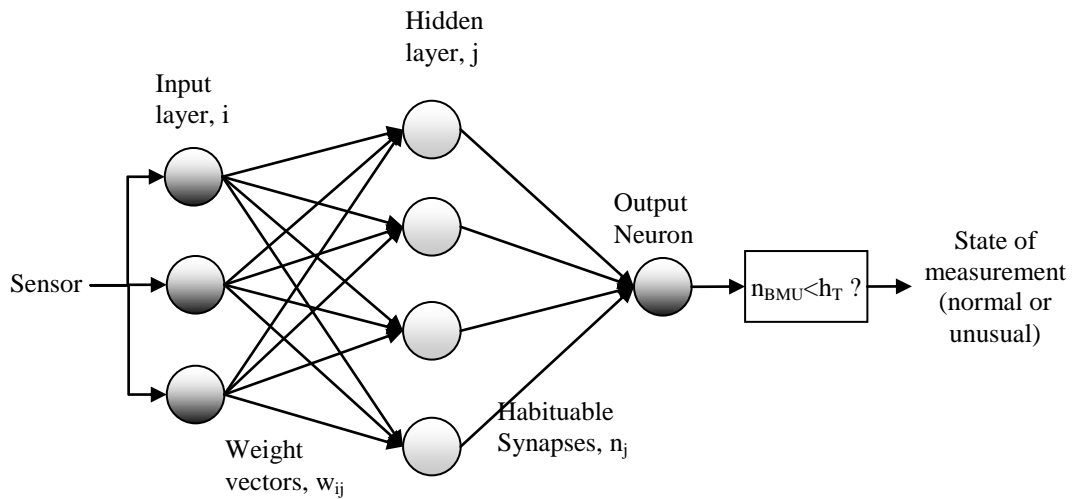


Figure 2.10: A neural network consisting of an input layer, a hidden layer and an output layer.

2.5.1 Self Organizing Map

The Self Organizing Map (SOM) [59] is one of the most commonly used unsupervised neural networks. Its function is to cluster input measurements from each of the sensors by adapting its neuron weight vectors to resemble the different input patterns. Instead of just adapting the winning neuron, the SOM also adapts the neurons that are similar to the winner, although to a lesser extent. Because of this, a SOM network has the self organization property. This means that similar perceptions are close to each other in the neural network map space or in other words, it is topology preserving. The benefit of this is that the novelty detection mechanism can generalize between similar perceptions.

Weight initialization.

Prior to performing the clustering process, the neuron weight vectors need to be initialized. One of the limiting factors when using a SOM is that its success in representing the environment depends on a good initialization of its weight vectors. For this reason, in this project the weight vector of each neuron is initiated by applying *K-mean clustering* [60] on data gathered from the environment. This is done

to ensure that the distribution of the weight vector lies within the principal component of the data gathered from the environment.

Clustering process.

The clustering can be performed either online or offline. In this project, this process is performed offline. This means that, the sensor measurements were gathered from several passes through the environment and following that they were used as the input to the SOM network. In this project, data from each sensor are treated separately and each sensor has its own SOM network.

The SOM clustering process is as follows:

1. For a given input, i , the distance between the input and each neuron in the hidden layer, j is calculated using the Euclidean distance measure, d_j as given by Equation (2.16) where v_i is a component of the input vector and w_{ij} is a component of the neuron weight vector (refer to Figure 2.10).

$$d_j = \sqrt{\sum_{i=1}^N (v_i(t) - w_{ij}(t))^2} \quad (2.16)$$

2. The neuron that has the minimum distance is selected as the winner, or the Best Matching Unit (BMU).
3. The weight for the BMU and its neighbors (i.e. neurons that have a distance similar to the BMU) are updated using Equation (2.17). In the equation, Θ is the neighborhood function which describes the relationship between the BMU and its neighbors and α is the learning rate.

$$w_{ij}(t+1) = w_{ij}(t) + \Theta(t)\alpha(t)(v_i(t) - w_{ij}(t)) \quad (2.17)$$

Neighborhood and learning function.

To ensure that the SOM network preserves its topological ordering, the adaptation of its weight vectors is controlled by a neighborhood function, θ and a learning function, α . The neighborhood function defines the amount of influence a BMU has over its neighbors. The more similar a neuron is to the BMU, the higher the value of θ . The similarity between a neuron weight vector and a BMU weight vector is calculated using the Euclidean distance as given by Equation (2.18).

$$d_{jBMU}(w_{ij}) = \sqrt{\sum_{i=1}^N (w_{ij} - w_{iBMU})^2} \quad (2.18)$$

The neighborhood size, r also decreases over time to make the network stabilize after some times as given by Equation (2.19) where τ is a constant the controls the rate of the decay.

$$r(t) = e^{\left(\frac{-t}{\tau}\right)} \quad (2.19)$$

The neighborhood function, $\theta(d,r)$ takes the form of a Gaussian function and is given by Equation (2.20) where d is the distance between the weight vector of a neuron and the BMU and r is the neighborhood size.

$$\theta(d,r) = e^{-\frac{d}{2r^2}} \quad (2.20)$$

The learning function, α is given by Equation (2.21) where τ_1 is a constant that controls the rate of decay.

$$\alpha(t) = e^{\frac{-t}{\tau_1}} \quad (2.21)$$

2.5.2 Habituation function

The second part of the Habituating Self Organizing Map (HSOM) is the habituation function. To modify a SOM network to become a HSOM, each of the neurons in the hidden layer is linked to the output through an habituable synapse (refer to Figure 2.10). The synapse habituates every time a neuron becomes the best matching unit (BMU).

There are various models of habituation described in the literature [61-63]. However, as commented by Marsland in [13], all that is required for simulating an habituation behavior is a curve that shows decay as the number of perceptions increases. For that reason, in this thesis, a decaying exponential function is used for habituating the synapses, given by Equation (2.22). In the equation, o is the number of times the neuron becomes the BMU and τ_2 is a time constant which governs the rate of habituation. A neuron is considered as normal if its habituation synapse, $n_j(o)$ is less than the habituation threshold, h_T (see Figure 2.10).

$$n_j(o) = e^{\frac{-o}{\tau_2}} \quad (2.22)$$

2.5.3 Similarity threshold, S_T

Similarity threshold, S_T is the maximum allowable difference between two measurements that belong in the same group. If the similarity measure between an

input vector and a neuron weight vector is bigger than S_T , the pair is not considered as a significant match.

One of the limitations of the Habituating Self Organizing Map (HSOM) is that when it finds the best matching neuron, even a very poor match can become the best match. In this project, this drawback is resolved by rejecting a match that is not significant. In this case, the input measurement should be classified as a novel measurement.

2.5.4 Measure of the performance of HSOM

Sensitivity is a common performance measure of a binary classification test such as the Habituating Self Organizing Map novelty filter. In order to clarify the concept of sensitivity, imagine a surveillance scenario where an environment is tested for the presence of a novel object. The test outcome can be positive (a novel object is present) or negative (a novel object is not present), while the actual status of the environment may be different. In that setting the following can be defined:

True positive (TP): Environment that has a novel object is correctly observed to have a novel object.

False positive (FP): Environment that does not have a novel object is wrongly identified as having a novel object.

True negative (TN): Environment that does not have a novel object is correctly recognized as having no novel object.

False negative (FN): Environment that has a novel object is wrongly identified as having no novel object.

The state of detection as described in the previous list is summarized using a confusion matrix as shown in Table 2.1.

Table 2.1: Confusion matrix representing the possible outcomes of the novelty detection.

Is the state novel?		Actual state	
		Yes	No
Measured state	Yes	TP	FP
	No	FN	TN

Based on the confusion matrix, the sensitivity is given as:

$$Sensitivity = \frac{\text{number of TP}}{\text{number of TP} + \text{number of FN}} \quad (2.23)$$

2.6 Implementation of Different Sensor Types

This section discusses the issues relating to the sensors used in this project. As mentioned before, region tolerance, R_T is affected by:

1. Localization error
2. Path-following error
3. Sensor measurement error and fluctuation.

First, as part of the contribution of this thesis, this section presents the effect of robot localization error and path-following error on the value of the region tolerance for laser range finder normal measurements. There follows an evaluation of the minimum size of a new object that a HSOM novelty filter of the laser range finder measurement could detect. Finally, this section discusses ways to determine the value of region tolerance for other sensor measurements.

2.6.1 Determining the Value of the Region Tolerance for the Laser Range Finder

The laser range finder is considered in more depth compared to the other types of sensors that are used in this project for two reasons:

1. The laser range finder is the main sensor used in this project
2. Being sensitive to changes in position and direction, it provides a good example to consider when using novelty detection on a mobile platform.

2.6.1.1 Problem definition

Figure 2.11 shows an example of a region in a flexible region map of a corridor environment. Normal reference pose is the position and heading of the robot when it maps the normal sensor measurements.

Laser range finder measurements are affected by any change in the sensor's pose. As depicted in Figure 2.11, the pose of a laser range finder could differ from the normal reference pose due to robot localization error and poor path-following repeatability.

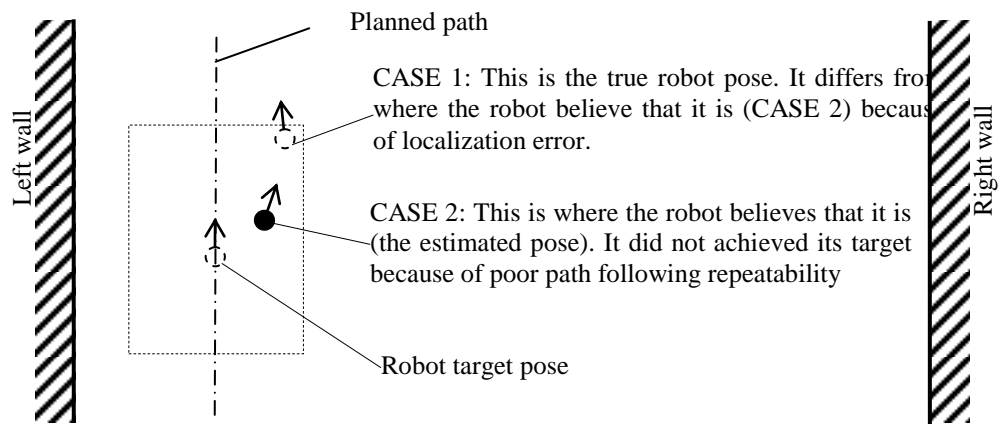


Figure 2.11: The effect of path-following accuracy and odometry error on the laser range finder pose.

This section examines the minimum value of the region tolerance, R_T of a laser range finder measurement after considering the robot localization error and limitation of its path-following repeatability. Since there is a trade-off between region tolerance and detection sensitivity, the study also looks into the effect of variation in the value of the region tolerance on the sensitivity of detection. The following are the objectives of the study:

1. To determine the difference between the laser range finder measurements at the true pose and at the estimated pose.
2. To determine the difference between the laser range finder measurements on the true path and on an estimated path.
3. To estimate the minimum detectable size of object after considering the region tolerance.

The outcomes of the study are vital for:

1. Choosing the appropriate region tolerance, R_T to classify normal or unusual sensor readings.
2. Identifying the initial size of the length, l_i and the width, w_i of a flexible region.

3. Identifying the effect of translational and rotational displacement on the laser range finder measurements.

2.6.1.2 Modeling the average laser distance measurement, d_{ave_i}

The Hokuyo URG-04LX has an angular resolution of 0.315° . This project used 240° of its angular range which consists of exactly 682 adjacent laser measurements. The angular range is divided into M sectors. Each sector contains an equal number of laser measurements, N . The average measurement from each sector, d_{ave_i} forms the input vector for the neural network (see Figure 2.12).

In a real world application, one could say that a laser range finder allows the construction of the detailed surface geometry of any objects in the field of view, and their localization in the model frame of reference. If such low resolution data is desired, cheaper sensors such as low-end sonar systems may be more appropriate. One of the major advantages of the laser range finder is its measurement accuracy; applying a naive sample averaging technique to such data loses this major strength. By dividing laser range measurements into sectors, it may seem that the system does not take full advantage of having such high resolution information. However, there are several strong reasons why in this project the laser measurements are down sampled. First, the sensitivity of the laser needs to be reduced to allow for variations of measurements especially due to the robot's inability to achieve the target pose (refer CASE 2 in Figure 2.11). Second, one of the motivations of the work in this thesis is to reduced storage, and averaging groups of sensor readings would certainly reduce the amount of storage required by the system. Third, the down sampling demonstrates that the system is robust for used with other cheaper but less accurate alternatives like sonar and infra red sensors. Finally, all the calculations are presented in a general form so that the user can decide the appropriate size of a sector (from 1 up to the maximum number of laser measurements available).

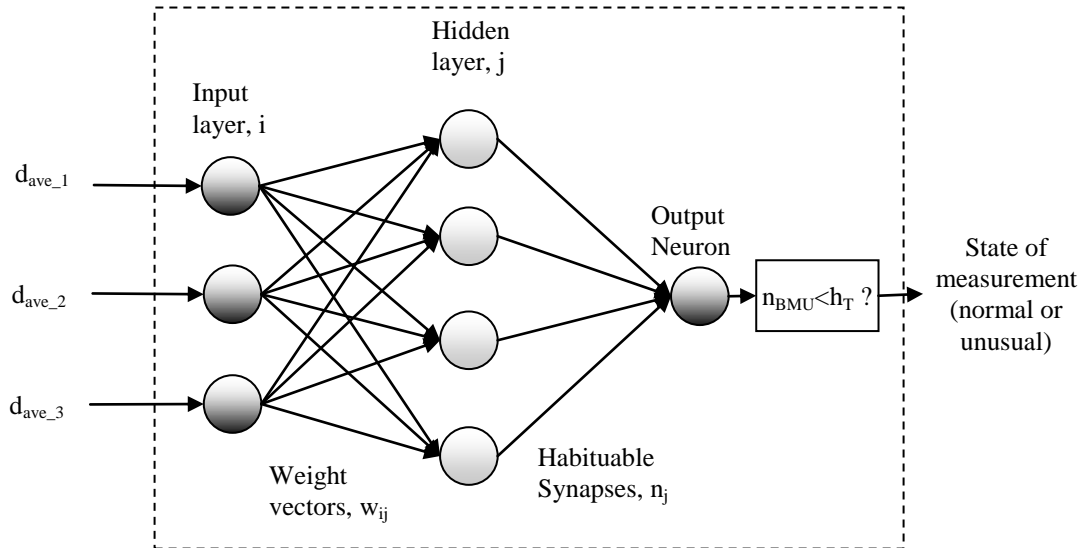


Figure 2.12: An example of an HSOM network that takes inputs from laser range finder measurements. In this example, the angular range of the sensor is divided into $M=3$ sectors, producing 3 average readings.

The decision regarding the number of sectors to use depends on the particular project's requirement. If the angular range is divided into too many sectors, the size of the input vector will be increased and this will increase the memory requirement as well as reducing processing speed. If the angular range is divided into too few sectors, the environment will be poorly represented and the system will not be sensitive to small objects.

In this project, for the benefit of easier explanation and to show that the system is robust, most of the examples in this thesis divide the Hokuyo URG-04LX laser angular range into 8 sectors. Through the analysis introduced in a later section, as well as through experience, it was found that this setting allows the detection of objects as small as 0.1m^2 (such as bags, trash bins and small boxes) from about a meter away from the sensor. This is sufficient to detect the changing patterns introduced in the project's experimental environment as well as in a typical surveillance task.

Figure 2.13 depicts an example of a laser range finder measurement where the pose of the sensor is denoted by x_l, y_l and θ_l . The laser angular range is divided into 8 sectors.

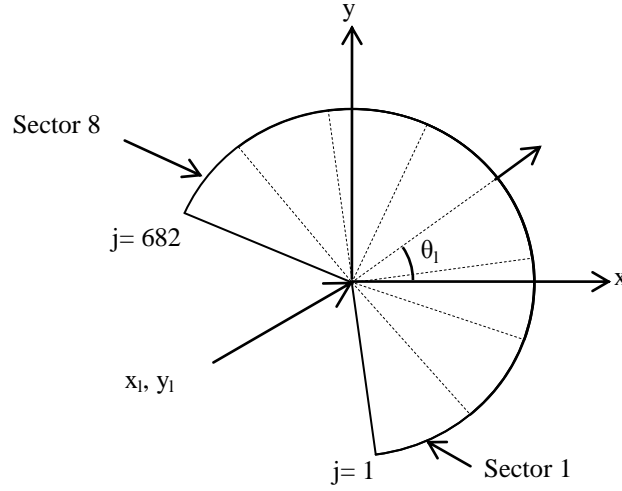


Figure 2.13: Defining the input vector from the Hokuyo URG-04LX laser scan.

The path of the laser beam for any particular measurement j is modeled by a linear equation (see Equation (2.24)) where slope, m is calculated using Equation (2.25) and y-intercept, c is found using Equation (2.26). The laser angular resolution is denoted by α .

$$y = m_j x + c_j \quad (2.24)$$

$$m_j = \tan((j - 1)\alpha + \theta_l) \quad (2.25)$$

$$c_j = y_l - m_j x_l \quad (2.26)$$

In order to estimate the minimum value of the region tolerance, a rectangular room was considered with dimensions not exceeding the maximum range of the laser

range finder. The author chose a rectangular room because rotational and translational error in any direction will affect the laser range finder measurements. Another reason is that a rectangular shaped room is similar to the shape of the intended working environment for the system which will consist of offices and corridors. To model a rectangular room, the walls of the room are represented by 4 straight lines (Equation (2.27)) where k denotes the 4 rectangle edges.

$$y = m_k x + c_k \quad (2.27)$$

By solving Equation (2.24) and Equation (2.27) simultaneously, the intersection between both lines can be determined. The intersection between the line representing laser beam j and the line representing the walls is shown by Equation (2.28) and Equation (2.29).

$$y_{int} = \frac{-\frac{m_j}{m_k} c_k + c_j}{1 - \frac{m_j}{m_k}} \quad (2.28)$$

$$x_{int} = \frac{y_{int} - c_k}{m_k} \quad (2.29)$$

The distance value of the individual laser beam, r_j is calculated using Equation (2.30) where r_{max} is the maximum laser range.

$$r_j = \begin{cases} \sqrt{(x_{int} - x_l)^2 + (y_{int} - y_l)^2}, & r_j < r_{max} \\ r_{max}, & r_j \geq r_{max} \end{cases} \quad (2.30)$$

The average laser distance measurement in a sector i which consists of N laser measurements is calculated using Equation (2.31).

$$d_{ave_i} = \frac{1}{N} \sum_{s=1}^N r_j \quad \text{where } j = s + N(i - 1) \quad (2.31)$$

2.6.1.3 Difference between Laser Measurements from the Estimated and Actual Sensor Pose

The average laser distance measurement taken at the actual pose, $d_{ave_i_actual}$ can be calculated by replacing x_l, y_l and θ_l in Equation (2.24), Equation (2.25), Equation (2.26) and Equation (2.30) with the actual pose of the laser x_{actual}, y_{actual} and θ_{actual} . Similarly, the average laser distance measurement taken at the estimated pose with localization error, $d_{ave_i_error}$ can be found by replacing x_l, y_l and θ_l with the estimated pose $x_{estimate}, y_{estimate}$ and $\theta_{estimate}$.

The difference between the laser range finder measurements at the actual pose and at the estimated pose can be calculated using the Euclidean distance similarity measure as given by Equation (2.32), where $d_{ave_i_error}$ represents the laser measurement when there is error in the robot's pose estimation and $d_{ave_i_actual}$ represents the laser measurement taken at the robot actual pose. M is the number of sectors.

$$d_{euc} = \sqrt{\sum_{i=1}^M |d_{ave_i_error} - d_{ave_i_actual}|^2} \quad (2.32)$$

At this stage, by assuming that the path-following is perfect, the actual pose of the sensor should be same as the target pose as shown before in Figure 2.11.

2.6.1.4 Validating the Average Laser Distance Measurement Model

The model was validated by comparing theoretical and simulation results (see Table 2.2). The same actual and estimated poses were introduced to both theoretical and simulation models. The theoretical values were calculated by using the equations described in the previous sections.

The simulations were carried out using MobileSim i.e. simulation software provided by MobileRobots Inc. for simulating robots and their environment. This software is used for debugging and experimentation purposes. The software only provides a simulation of the SICK LMS-200 laser range finder. Its specifications are slightly different from the laser range finder that was used for this project i.e. Hokuyo UR-04LX. The SICK LMS-200 provides either 100 or 180 degree angular range with 0.25, 0.5 or 1.0 degree angular resolution. However, as comparison is made between theoretical and simulation analyses, as long as both theory and simulation use the same type of sensor, the comparison is considered as valid.

A 4m² square room was constructed using the Mapper 3 (Basic) software which is also provided by MobileRobots Inc. The robot/SICK laser system was positioned at the center of the room (see Figure 2.14) and this is considered as the actual pose of the sensor. Poses other than this are taken as estimated poses with localization error.

For theoretical calculations, the square room was modeled using 4 straight line equations as given by Equation (2.27).

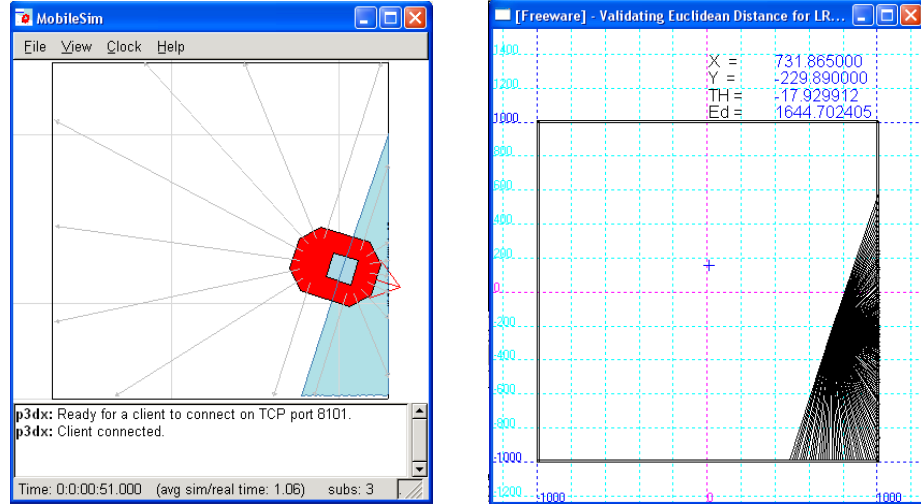


Figure 2.14: The MobileSim simulation is shown in the figure on the left. The figure on the right shows the laser beams, the value of the simulated robot's position and heading together with the Euclidean distance between the laser measurement and the measurement taken from the center of the room.

The Euclidean distance value is normalized over the maximum possible value of the Euclidean distance. In the simulation, the maximum range was set to be 4000mm with 180 range values measured over 180° which is the maximum angular range for the SICK LMS-200 laser range finder. The laser measurements are divided evenly into 6 sectors. Using Equation (2.32), given that the input measurement when there is no localization error, $d_{ave_i_actual}$ has a minimum value (at the center of the square room) and the input measurement when there is localization error, $d_{ave_i_error}$ has a maximum value (at one corner of the room), the maximum possible difference between these parameters is $\sqrt{4000^2 \times 6} = 9798\text{mm}$.

The actual values of the robot pose at the center of the room are $x_{actual} = 0\text{mm}$, $y_{actual} = 0\text{mm}$ and $\theta_{actual} = 0^\circ$. The results of the comparison between the theoretical and simulation Euclidean distance values are given in Table 2.2.

Table 2.2: Comparison between simulation and theoretical Euclidean distance values in different robot poses.

	$x_{error} = 63.5mm$ $y_{error} = 34.6mm$ $\theta_{error} = 28.9^\circ$		$x_{error} = 555.8mm$ $y_{error} = -546.6mm$ $\theta_{error} = -44.9^\circ$		$x_{error} = 10.7mm$ $y_{error} = -53.8mm$ $\theta_{error} = -78.9^\circ$	
	Theory	Simulation	Theory	Simulation	Theory	Simulation
Euclidean distance, d_{euc}	473.0	453.5	1542.4	1535.5	192.0	182.7
Normalized Euclidean distance, d_{euc_norm}	0.048	0.046	0.157	0.156	0.019	0.018

2.6.1.5 Estimating the Region Tolerance Due to Localization Error and Path-following Error

In this project, the robot localizes itself by using Particle Filter localization. At any given localization step, the robot only accepts heading and position estimates when the particle standard deviation is not more than ± 100 mm in the x and y directions and $\pm 5^\circ$ for the heading.

Due to path-following error, the robot and hence the laser range finder can be offset from the planned route. A wall following behavior is used by the robot to navigate and a wall alignment behavior aligns the robot's heading parallel to the wall. This strategy allows the robot to maintain its pose within the limits of ± 100 mm in x and y directions and $\pm 5^\circ$ for the heading from the intended route.

The Euclidean distance value due to localization error, plus the path-following accuracy is calculated. By setting the actual values of the robot pose i.e. $x_{actual} = 0mm$, $y_{actual} = 0mm$ and $\theta_{actual} = 0^\circ$ and using the maximum deviation of Particle Filter localization plus the path-following error as the maximum error i.e. $x_{error} = 200mm$, $y_{error} = 200mm$ and $\theta_{error} = 10^\circ$, we get a minimum region

tolerance value of $R_T = 824.67\text{mm}$ (normalized to 0.084 i.e. over the maximum possible value of the Euclidean distance of 9798mm as described in the previous section).

2.6.1.6 Region Initial Dimension

When a region is initiated the robot should ensure that any measurement taken within the boundary of the region should be below the region tolerance. In this project, based on the values of localization error and path-following error of the robot, the total error is expected to be $\pm 200\text{mm}$ in x and y directions and $\pm 10^\circ$ for the heading. Since the position of the robot is at the center of a region when it is first created, the robot needs to ensure that the difference between the sensed quantities taken at the center and at the furthest position in that region is less than the region tolerance value. With this in mind the initial width and length of the laser flexible region can be defined to be 400 mm (i.e. $\pm 200\text{mm}$ from the center of the region). The maximum difference of the heading of the robot should be $\pm 10^\circ$ from the actual state of the heading (i.e. 0° , 90° , 180° or 270°).

2.6.1.7 Estimating minimum detectable object size in the worst case scenario

An object is most difficult to detect when it is near to the outer most boundary of the laser scan area and when it lies in-between two sectors as shown in Figure 2.15. For this reason, in order to find the minimum detectable size of an object, the object is modeled as a portion of a sector, with an area defined by Equation (2.33). In this equation, θ_{sect} is the angle of the sector influenced by the object, R is the maximum laser range and l_{obj} is the object length in a radial direction.

$$A = \frac{\theta_{sect}}{360} \pi (R^2 - r^2) \quad \text{where } r = R - l_{obj} \quad (2.33)$$

In a circular room as depicted in Figure 2.15 where room radius is equal to laser maximum range and the laser range finder is positioned at the center of the

circle, the average laser reading within each sector that does not contain an object is equal to the maximum laser range i.e. 4000 mm. Thus Euclidean distance from Equation (2.32) can be simplified to be Equation (2.34) where P is the maximum laser range.

$$d_{euc} = \sqrt{\sum_{i=1}^M |d_{ave_i} - P|^2} \quad (2.34)$$

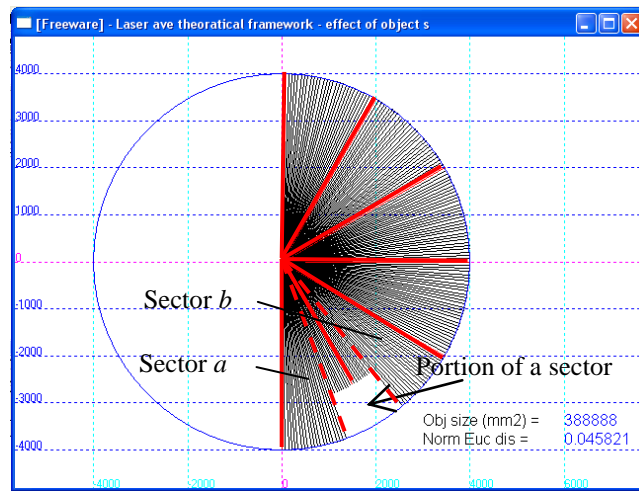


Figure 2.15: The effect of object size on the Euclidean distance between measurements when there is no object and when an object exists. The object is modeled as a portion of a sector.

As the object in Figure 2.15 affects two sectors only, Equation (2.34) can be simplified to become Equation (2.35) where d_a and d_b are the average laser readings in the two affected sectors.

$$d_{euc}^2 = (d_a - P)^2 + (d_b - P)^2 \quad (2.35)$$

Given that the minimum Euclidean distance is achieved when d_a and d_b have the same value, Equation (2.35) can be further simplified to Equation (2.36) by equating $d_a = d_b = d_{ave_i}$:

$$d_{euc}^2 = 2(d_{ave_i} - P)^2 \quad (2.36)$$

By referring to Equation (2.33), the relationship between the object size and the average laser reading d is given by Equation (2.37).

$$\begin{aligned} \theta_{sect} &\propto d, & \text{given } l_{obj} \text{ is fixed} \\ &\text{or} & \\ l_{obj} &\propto d, & \text{given } \theta_{sect} \text{ is fixed} \end{aligned} \quad (2.37)$$

By fixing the sector angle, θ_{sect} , the average laser distance measurement in sector i which consists of N laser readings is calculated using Equation (2.38). The distance value of the individual laser reading, r_j is calculated using Equation (2.30).

$$d_{ave_i} = \frac{1}{N} \sum_{s=1}^N r_j \quad (2.38)$$

The distance values of the individual laser beams, r_j in the affected sector are of two types; one that is affected by the object and the other that is not. The one that is not affected by the object has the maximum range of the laser, $r = R$ and the one that is affected has the value of $r = R - l_{obj}$. By referring to Figure 2.16, given that the laser angular resolution is α , the number of laser readings that are affected by the object in a sector (either sector a or b) is given by $\theta_{sect}/2\alpha$. Equation (2.38) then can be expanded to Equation (2.39).

$$d_{ave_i} = \frac{1}{N} \left(\sum_{s=1}^{\frac{\theta_{sect}}{2\alpha}} (R - l_{obj}) + \sum_{s=\frac{\theta_{sect}}{2\alpha}}^N R \right) \quad (2.39)$$

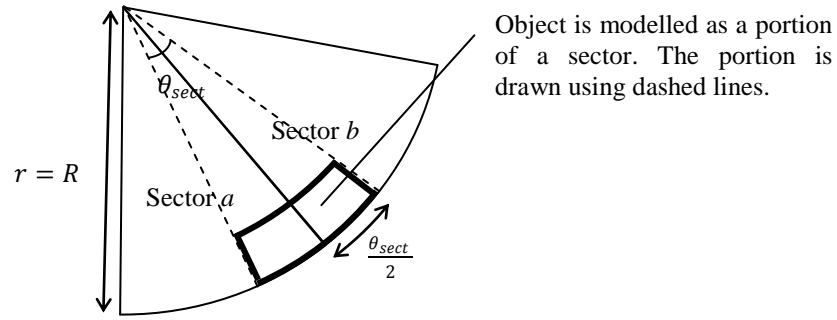


Figure 2.16: An object is modelled as a portion of a sector.

Equation (2.39) can be simplified to produce Equation (2.40) by multiplying the number of laser measurements (with and without object) by their length.

$$d_{ave_i} = \frac{1}{N} \left(\frac{\theta_{sect}}{2\alpha} (R - l_{obj}) + \left(N - \frac{\theta_{sect}}{2\alpha} \right) R \right) \quad (2.40)$$

By using Equation (2.40), to replace d_{ave_i} in Equation (2.36) and knowing that $P=R$, l_{obj} becomes:

$$l_{obj} = -\frac{N2\alpha}{\sqrt{2}\theta_{sect}} d_{euc} \quad (2.41)$$

In the previous section, the value of the minimum region tolerance after considering localization error was found to be $d_{euc_err} = 824.67\text{mm}$. This means

that the maximum allowable difference between two measurements that belong to a region is $d_{euc_err} = 824.67\text{mm}$. By solving Equation (2.41) using this value together with other parameter values, $\alpha = 1$, $\theta_{sect} = 20^\circ$ and $N = 30$, the object length, $l_{obj} = 1749.13\text{mm}$ is determined. A minimum detectable object size of approximately 1.91m^2 is determined by substituting this value into Equation (2.33).

It should be pointed out that this value is the minimum size in the worst case scenario. In practice, there are ways to improve the minimum detectable object size including reducing the sector size (N) and using a higher resolution (smaller value of α). For example, with $\alpha = 0.356$ and $N = 10$, the object length becomes $l_{obj} = 207.56\text{ mm}$ with object size of $A = 0.27\text{m}^2$. On top of this, there are a lot of situations where the robot can perform a laser scan while it is closer to the object and where the object lies fully within a sector as depicted in Figure 2.17. As can be seen from the figure, the average value of Sector 1 and Sector 2 changed depending on the position of the object with respect to the sector. The Euclidean distance value is highest when the object fully lies within Sector 2. From the author's experience, in such situations, objects as small as 0.1m^2 can be readily detected if the object is about a meter from the laser range finder.

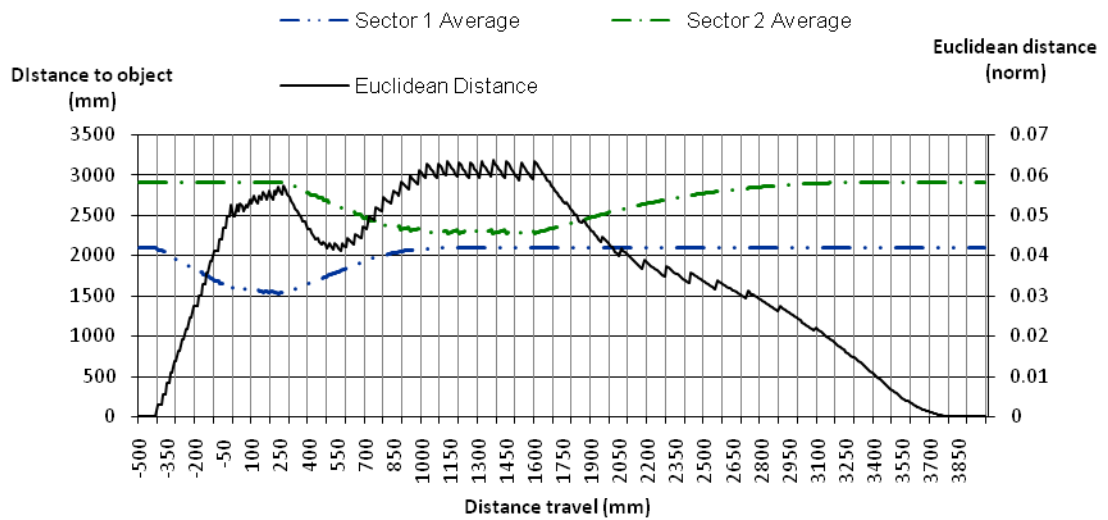


Figure 2.17: As the robot travels past an object, different sectors of its laser scan are affected by the object.

Another major factor that can influence the ability to detect an object is the size of the sector. As can be seen from Figure 2.18, the test result shows that the size of the sector influenced the value of the Euclidean distance when detecting a 0.16m^2 box. The graph shows that the smaller the size of the sector, the more sensitive the system will be.

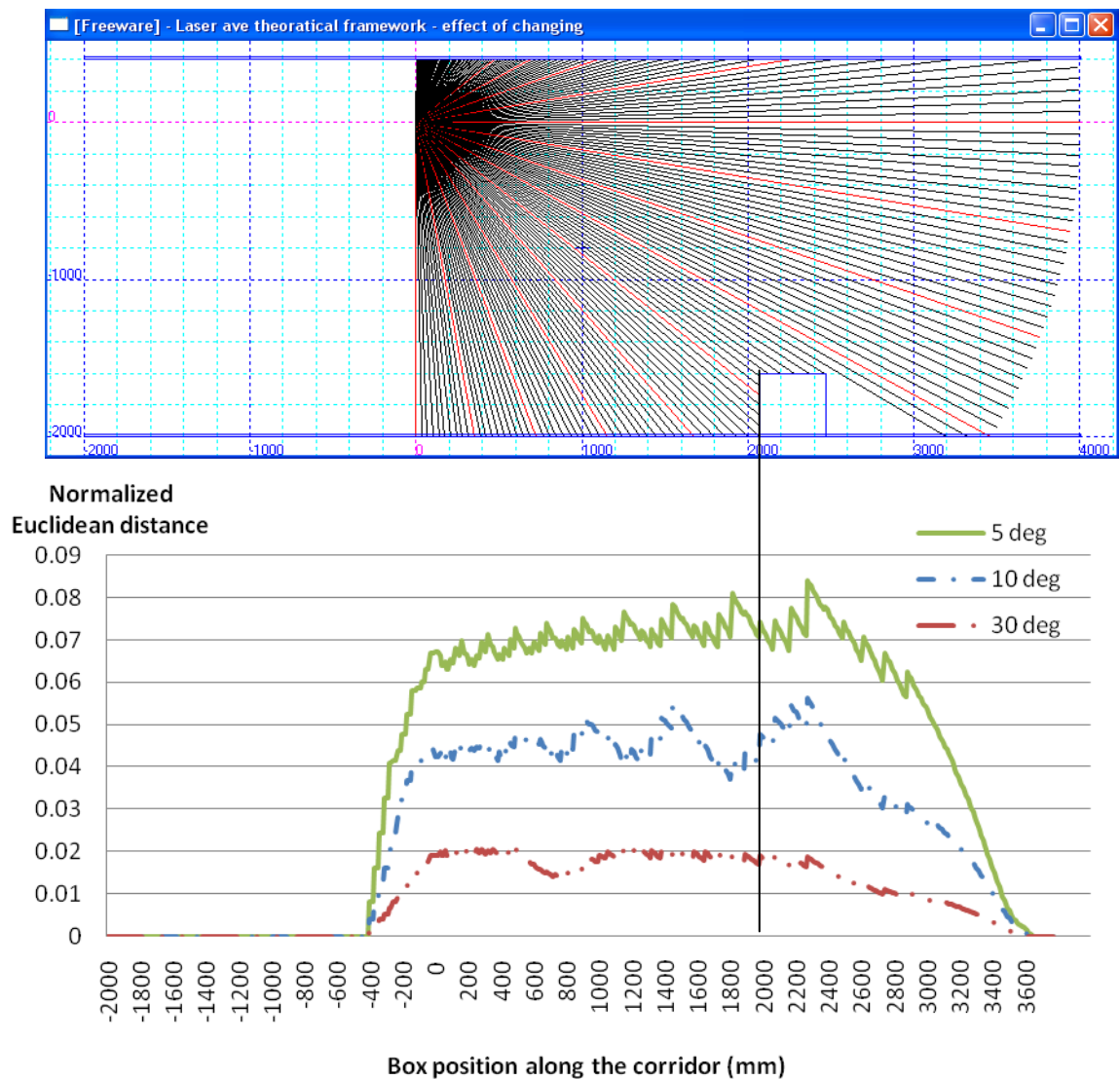


Figure 2.18: Effect on the value of Euclidean distance of using different sizes of sector (sector size = 10 degree is shown in the simulation example above the graph) when detecting a $400 \times 400 \text{ mm}^2$ box.

2.6.2 Determining the Value of the Region Tolerance for Other Sensor Types

This section presents the work done to find suitable region tolerances for objects measured by the other sensors used in this project. As mention before in the detailed discussion of the laser range finder, the value of the region tolerance will influence novelty detection sensitivity. In turn, the sensitivity of the novelty detection will influence the number of false positives produced during inspection [64]. The more sensitive a system is, where even a small change will be highlighted, the higher the number of false positives.

The factor that influences the region tolerance for the sensors described in this section is measurement fluctuation, and not localization error and path-following error. As many of the types of quantity being measured for this section are ambient quantities (except for air flow direction) and insensitive to direction, localization and path-following error do not affect the sensed quantity very much. The appropriate values of region tolerance are determined by observing the sensor measurements at different positions along the robot inspection route in the test environment as depicted in Figure 2.19 (except for gas concentration sensor measurements).

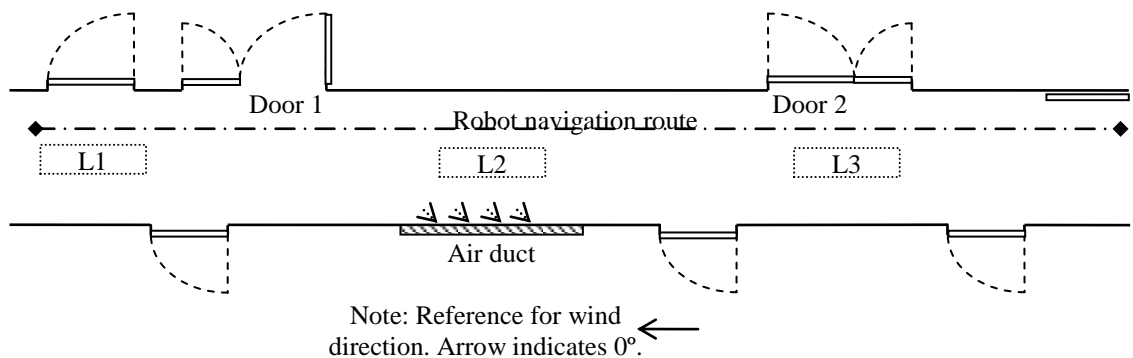


Figure 2.19: The corridor environment where the sensor measurements were taken. This corridor is used in one of the experiments.

2.6.2.1 Ambient light

Ambient light is measured using a light dependent resistor (LDR). As depicted in Figure 2.20, the output voltage of the LDR circuit was a local maximum when the sensor was directly beneath the light. The output voltage decreased gradually as the sensor moved further away from the light source until it became near to zero. However, if there is another light source nearby, the output voltage will decrease to a local minimum before it rises up again as now it is influenced by the nearby light source. Using the circuit shown in Figure 2.20, the difference in output voltage between well-lit and poorly-lit areas of the corridor is greater than 0.25 V. For this reason the minimum value of the region tolerance for the ambient light sensor measurement was set to be $R_T = 0.25$.

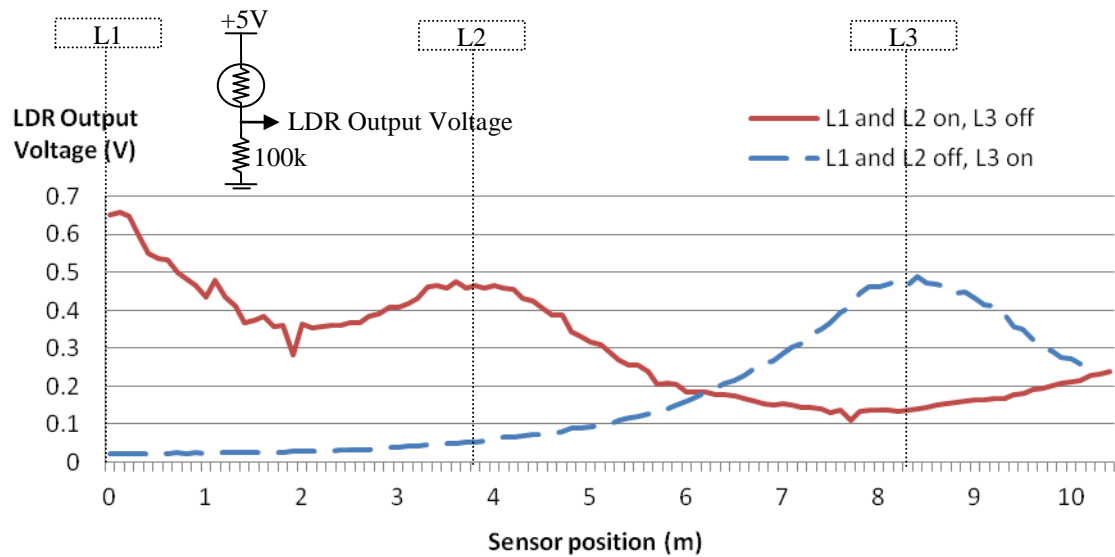


Figure 2.20: Light intensity measurements (taken when the robot was travelling along the path shown in Figure 2.19). The LDR output voltage was produced by the circuit shown in the figure. L1, L2 and L3 indicate the positions of the light sources.

2.6.2.2 Ambient temperature

The ambient temperature is measured using the SMT 160-30 temperature sensor. The ambient temperature in the environment changes when the ventilation system is in

operation. Temperature readings shown in Figure 2.21 were gathered on two different days; Day A and Day B. As can be seen, on one day, the normal temperature in the environment was 21.5°C while on the other day; the temperature was about 1°C higher.

The day when the corridor temperature was a bit low, the ventilation unit was turned off. This explains why the temperature was the same throughout the corridor. However, the day with the slightly higher temperature, the ventilation unit was turned on and sucked in air, mostly fresh air coming from the West end of the corridor in Figure 2.19. As can be seen from Figure 2.21, the air flow cools the corridor temperature from 22.5°C down to 21.5°C . However, since there is little air flowing at the East end of the corridor, the temperature in that area remained the same.

Under these conditions, it can be seen that the data fluctuated. The minimum value of the region tolerance for the ambient temperature is set based on the maximum fluctuation about the average value which was about 0.5°C .

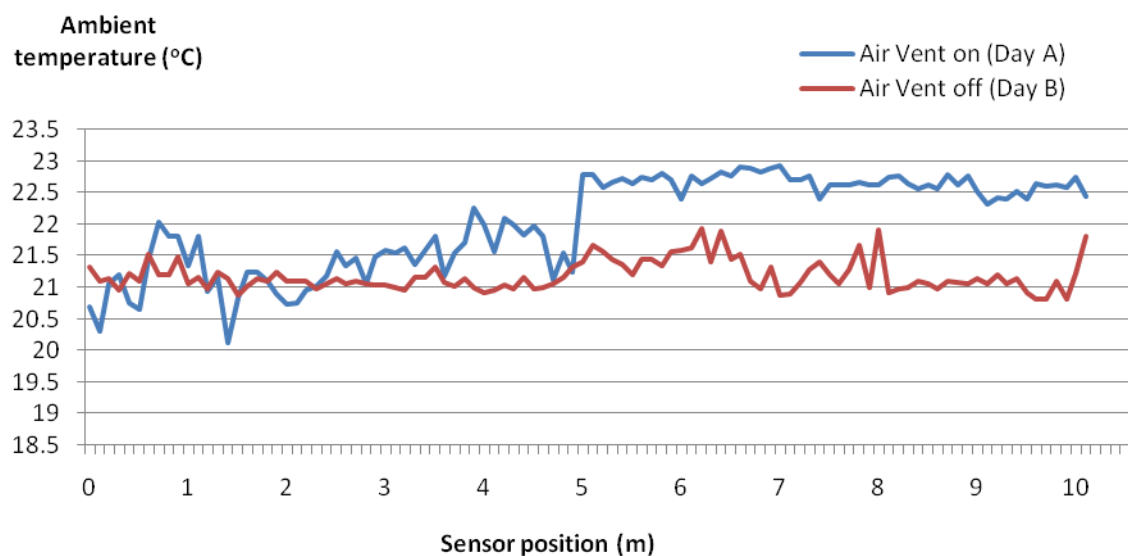


Figure 2.21: Ambient temperature measurements (taken when the robot was travelling along the path shown in Figure 2.19).

2.6.2.3 Air flow velocity and direction

Air flow velocity and direction are measured using a Young Model 81000 anemometer. As shown in Figure 2.22, the airflow in the environment is below measurable limits when the air ventilation is turned off (the air flows to the air duct as indicated in Figure 2.19), thus registering 0m/s for air velocity and no air flow direction. When the air ventilation unit is turned on and exhausting air, the air seems to flow mainly from the West end of the corridor (Figure 2.19) which explains why the air velocity in that region is about 1m/s but in the rest of the corridor, the velocity is less and in certain places, 0m/s. In the area where the air is flowing, the air flow direction fluctuated between 150° and 200° (refer to Figure 2.19 to see the reference air flow direction). Since air flow is so dynamic, in this project, the minimum value of the region tolerance of the air flow velocity and direction was determined by ensuring that they are above the average fluctuation of both quantities which is approximately 0.5m/s and 50° .

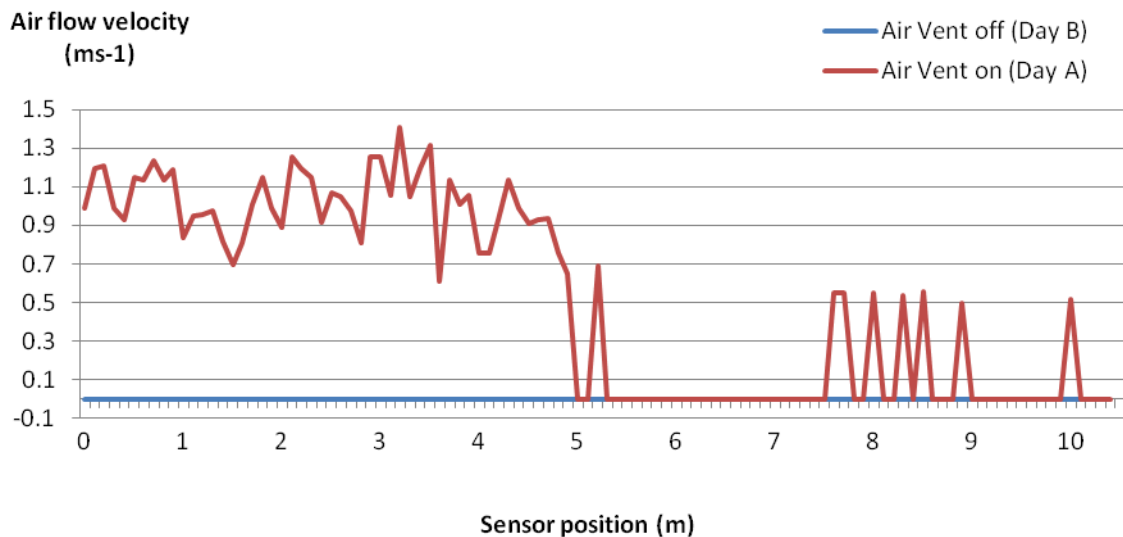


Figure 2.22: Airflow velocity measurements (taken when the robot was travelling along the path shown in Figure 2.19).

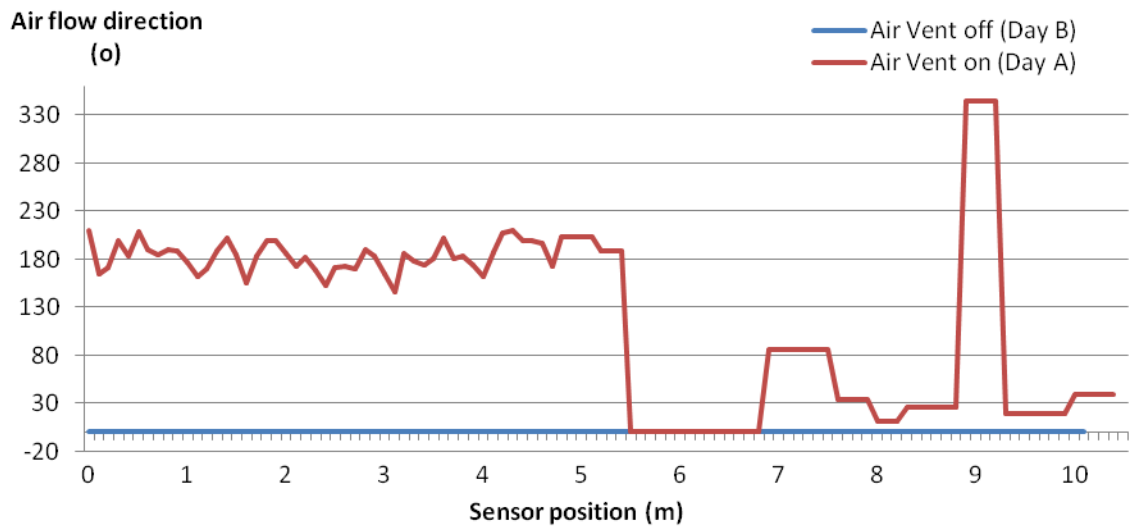


Figure 2.23: Airflow direction measurements (taken when the robot was travelling along the path shown in Figure 2.19). Note: Air flow direction is not meaningful when there is no measurable velocity.

2.6.2.4 Combustible gas concentration

An experiment was conducted to see how a TGS2600 chemical sensor reacts to ethanol from different distances to the source. The experiment was conducted in a controlled environment with still air and ambient temperature of 24°C. As depicted in Figure 2.24, the sensor's output voltage reduces as the source is further away from the sensor. The relationship is almost linear to a distance of 500 mm. After 500 mm, the reading is about the same even though the source of ethanol is taken further away from the sensor. From this it can be seen that the sensor is only sensitive to the ethanol concentration when the source is a short distance (about 500mm) from the sensor. Within that distance the gradient is approximately 0.005V/mm. Since during navigation, the robot's inspection step size is 100mm, it is expected that the reading should change at most by 0.5V after each step. For this reason, the minimum value for the region tolerance for the gas concentration measurement is set to 0.5V.

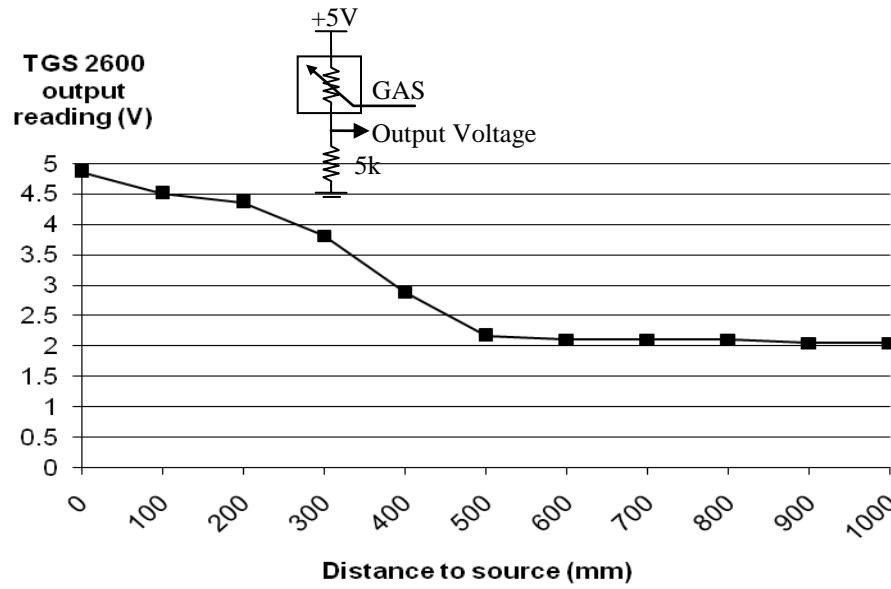


Figure 2.24: The ethanol concentration in a room with still air reduces almost linearly over distance before it stabilizes at a distance of more than 500 mm. The TGS2600 output voltage was produced by the circuit shown in the figure.

2.7 Summary of the Mapping Process

This section summarizes the process of creating, expanding, merging and using the flexible regions. The HSOM network should be trained prior to performing this process.

Algorithm 2.1: The creation and expansion of the thematic map using flexible regions.

Notation:

HSOM – Habituating Self Organizing Map

BMU – Best matching unit

d_{BMU} – Euclidean distance between input and the BMU

S_T – Similarity threshold

R_T – Region tolerance

N_{BMU} – Novelty measure of the BMU

H_T – Habituation threshold

d_{Nmax} – Maximum Euclidean distance between the current input and any of the region's neurons

1: Get trained HSOM neurons

2: Get new input

```

3: Find BMU
4: If ( $d_{BMU} < S_T$ ) AND ( $N_{BMU} > H_T$ )
5:   If (a region exists at the location)
6:     If ( $d_{Nmax} < R_T$ )
7:       If (input was taken at the boundary of the
           region)
8:         Expand region
9:       Else
10:        Include BMU as normal member of region
11:      Else
12:        Create a new region
13:    Else
14:      Create new region
15:    End
16:  End

```

Algorithm 2.2: The merge process.

```

1: Repeat for all regions
2: Find the nearest neighboring region
3: If ( neighboring region has same content ) AND (
    neighbors are aligned with each other )
4:   Merge regions
5: End

```

Algorithm 2.3: Novelty detection using the flexible region map.

```

1: Get input
2: Find the BMU
3: If ( $d_{BMU} > S_T$ )
4:   Novelty = 1
5: Else
6:   If (a region exist at location)
7:     If (BMU is normal in region)
8:       Novelty = 0
9:     Else
10:      Novelty = 1
11:    Else
12:      Novelty = 0 // No decision because of having
                  no reference
13:    End
14:  End

```

2.8 Experiments

2.8.1 Experiment 1: Memory requirement when using the flexible region map

The first experiment was conducted in the L-shaped environment shown in Figure 2.25 that was constructed from polystyrene blocks. The dimensions of the L-shaped environment are shown in Figure 2.26. The objectives of this experiment were:

1. To see the effect of changing the value of the region tolerance, R_T on the number of regions created.
2. To determine the amount of memory required for storing information when using a flexible region map and to compare this with memory required when using a grid based map, a perception based map and when not using a map at all.

Figure 2.26 shows the distribution of flexible regions in the environment used for mapping normal conditions of laser range finder measurements. It can be seen how the regions only cover places visited along the path-following route of the robot. Some of the regions are elongated as a result of region expansion and mergence.

The maps in Figure 2.26 were created using different values of region tolerance, R_T . Increasing R_T decreases the sensitivity of classification between different input patterns. As a result, smaller numbers of regions were created. Generally, it can be seen that in areas where the measurement varies highly with change of position, such as near the corners or at a dead end, many regions were created. However, this was not the case with maps created using a higher R_T . As depicted in Figure 2.27, increasing the region tolerance, R_T will decrease the number of regions but at the same time will sacrifice the sensitivity of the system. Nevertheless, in places where the sensor measurements do not vary much over space, such as in long corridor, the number of regions required to map the normal patterns is always reduced.

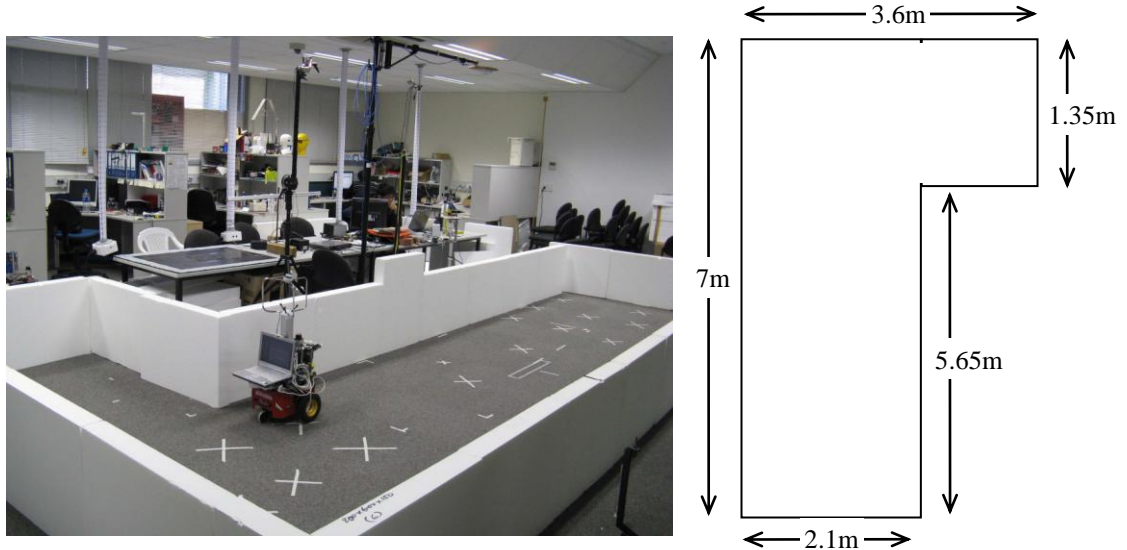


Figure 2.25: The L-shaped environment used for the first experiment.

Some of the regions shown in Figure 2.26 overlapped with other regions. One of the reasons was two regions were created for different robot headings particularly at the corners in the L-shaped environment. In practice, only one of the regions will be referred to at any current state of the robot as the robot will find the region which matches its current position as well as its heading. Another reason of the overlapping was that different values were measured at the same position and heading but at different times during the training, prompting the robot to create new or expand available regions. In this case, a position can have two or more normal conditions (see more examples in Figure 2.30 (a) near Door A).

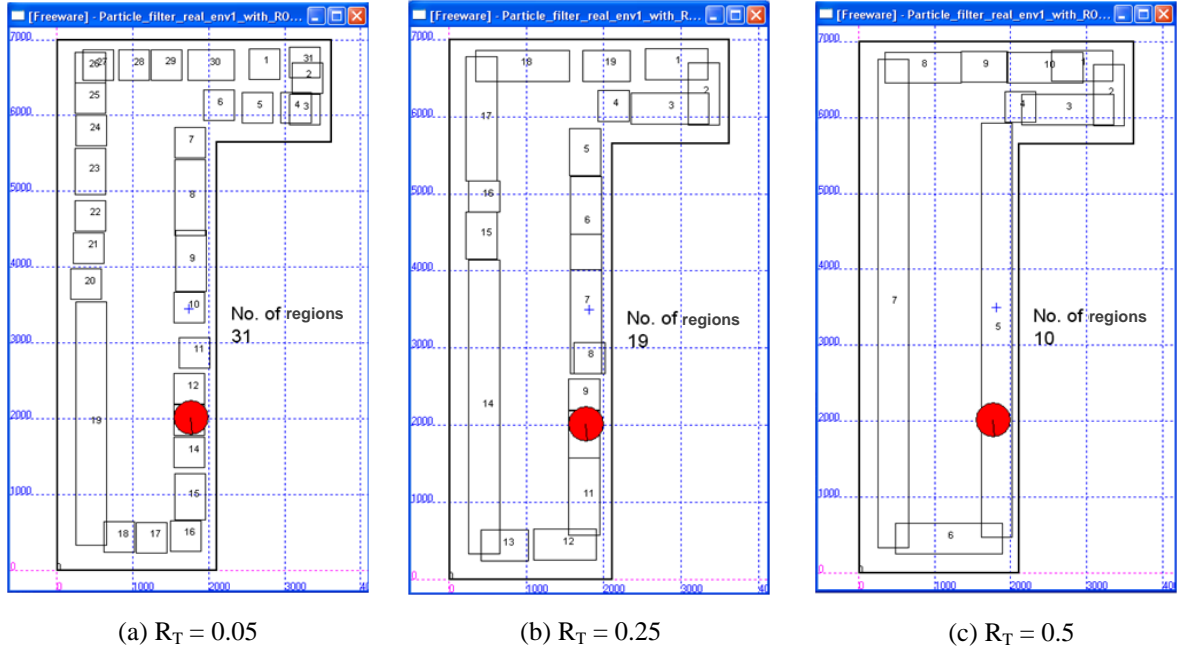


Figure 2.26: The flexible regions created for mapping normal laser measurement. The maps shown were created using different region tolerance (R_T) settings.

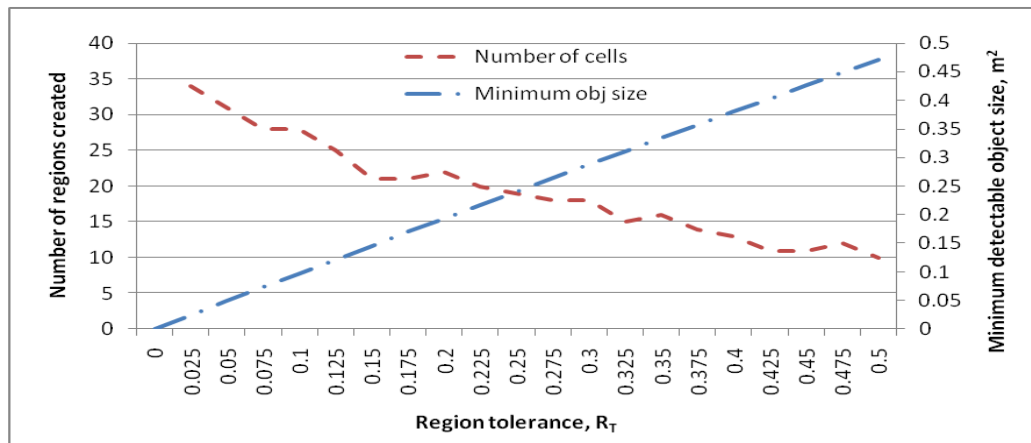


Figure 2.27: The effect of changing the region tolerance, R_T value to the number of regions created and the minimum detectable object size as shown in Equation (2.33) and Equation (2.41) with the following parameter values: $\alpha = 1$, $\theta_{sect} = 20$ and $N = 10$.

For the grid based and the perception based mapping approaches, the number of grid cells used to map information is predefined. Thus the amount of memory required when using these approaches can easily be estimated by dividing the

environment area by the minimum size of a region/cell. The size of the cells for these maps was set to be equal to the initial grid size of the flexible region map since this has taken into account the localization error and the path-following error of the robot. A grid map has a fixed number of cells and requires the maximum amount of storage. Perception based maps also have a fixed number of cells but less than the grid map because they only map information perceived from the robot route. The result of the comparison of the memory size required by different mapping approaches is given in Table 2.3.

As shown in Table 2.3, the number of cells required for the flexible region map depends on the distribution of the pattern of measurements in the environment. For sensors which are highly sensitive to change in position and direction such as the laser range finder, at a lower region tolerance settings ($R_T = 0.05$), the flexible region map only used 24.6% and 62% of the storage required for the grid map and the perception based map. At a higher region tolerance setting ($R_T = 0.5$), the flexible region map reduced the storage further by only used 9.4% and 20% of what was required by the grid and perception based map. The results show that the flexible region map gives the user the flexibility to reduce the storage size by changing the value of the region tolerance. However, as increasing region tolerance value reduces the sensitivity of the novelty detection, there is a trade-off between reducing the storage size and acquiring higher detection sensitivity.

Table 2.3: The storage requirements when using different mapping approaches for mapping the environment shown in Figure 2.26.

Type of sensor	Storage requirement (no. of regions)					No map
	Grid map	Perception based map	Flexible region (S_T)			
			0.05	0.25	0.5	
Laser range finder	106	50	31	19	10	1

2.8.2 Experiment 2: Performance and memory requirements of different sensors

The objectives of the second experiment are:

1. To see how the flexible region map accommodates the requirements of different types of sensor in the same environment.
2. To evaluate the performance of novelty detection when normal data is mapped using the flexible region map.

The second experiment was conducted in a real environment in a corridor in front of Room G10 in Building 36 at Monash University (see Figure 2.28). The learning was partly supervised in the sense that the robot was ‘told’ that the conditions in which it gathered information during HSOM training and during the creation of the flexible region map was normal. The anomalies which were introduced after training the normal condition are shown in Table 2.4. The corridor in its normal state is depicted in Figure 2.29.



Figure 2.28: The corridor environment.

Table 2.4: Environmental setup.

		States	
		Normal	Unusual
Object	Door 1	Open and Closed	n/a
	Door 2	Closed	Open
	Lighting	L1, L2 = off, L3 = on	L1, L2 = on, L3 = off
	Air ventilation	Off	On

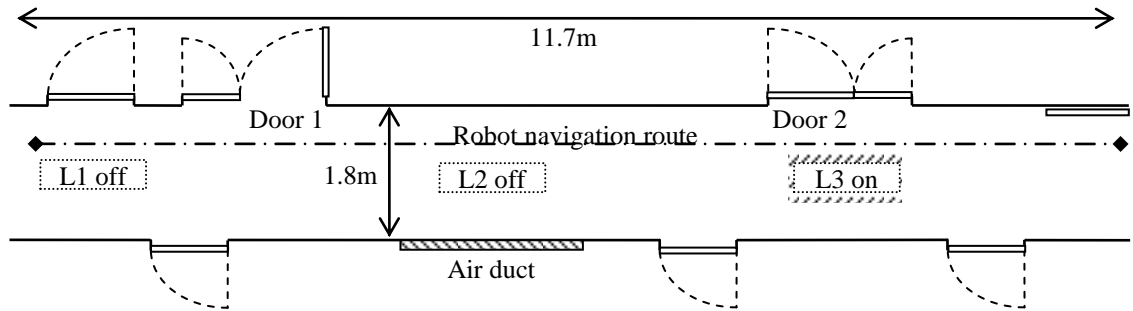


Figure 2.29: The corridor environment in its normal condition.

Figure 2.30 shows the regions created for different types of sensors and the novelty inspection results when unusual conditions were introduced. When compared to the laser range finder, the storage requirement is much less when mapping ambient entities such as temperature, ambient light, air flow direction and air flow velocity. In a stable environment such as in office corridors, these entities usually have a single fixed value except for exceptions at a few unusual locations such as near an air duct or a heater.

Table 2.5 shows how the flexible region map accommodated to the different storage requirement from different types of measured quantities in the environment. The number of regions required by the grid and the perception based map are estimated based on the dimension of the corridor and the minimum size of a region. As can be seen, to store the temperature, air flow velocity, air flow direction and chemical concentration measurements, the flexible region map only used 0.7% and 3.3% of the storage size required for the grid and the perception based map. To map the laser range finder data, the flexible region map used 4% and 20% of the storage required for the grid and the perception based map. Finally, to map the ambient light measurements, the flexible region map used 2.7% and 13.3% of what was required for the grid and the perception based map. Overall, the results show that the flexible region map made a significant reduction in the amount of storage space required to store the normal sensor measurement when compared to the conventional maps

particularly the grid and the perception based map. This is particularly true for quantities that are the same throughout the environment.

Table 2.5: The storage requirements when using different mapping approaches for mapping different type of measured quantities in the environment shown in Figure 2.29.

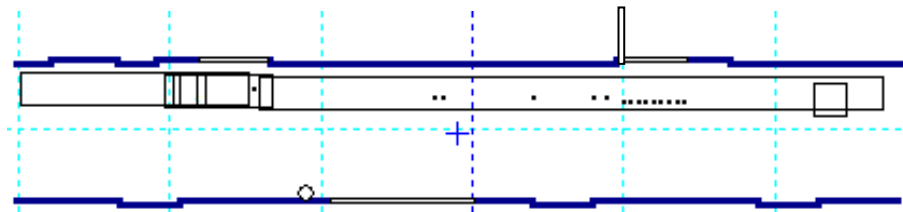
Sensor Type	Storage requirement (no. of regions)			
	Grid Map	Perception based map	Flexible region map	No map
Laser Range Finder	150	30	6	1
Temperature			1	
Air Flow Velocity			1	
Air Flow Direction			1	
Chemical Concentration			1	
Ambient light			4	

The corridor with its unusual conditions and the results of novelty detection are depicted in Figure 2.31. Without a map, the difference between laser measurements at Door 1 and Door 2 when both are open or closed cannot be determined. Since both locations have different normal states, by not knowing which states belong to which position, a false alarm will be given or even worse, a false negative which means the inability to detect true anomalies. This problem was overcome by using a map. In all mapped areas, anomalies have been detected successfully.

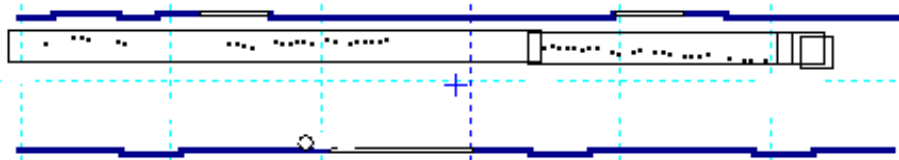
The sources of novelty represented by using the red lines are an indicator of where the quantities being measured were changed. It is an estimate of where the robot should highlight anomalies when the state of the environment was changed. The author realizes that the position of some of the highlighted anomalies do not exactly match his expectation. This is due to the fact that it is almost impossible to predict the complex behavior of the different quantities being measured especially as they reacted with the rest of the environment.

For example, in the situation where lights L1 and L2 are turned on and light L3 is turned off, the combination of light from sources L1 and L2 increased the level

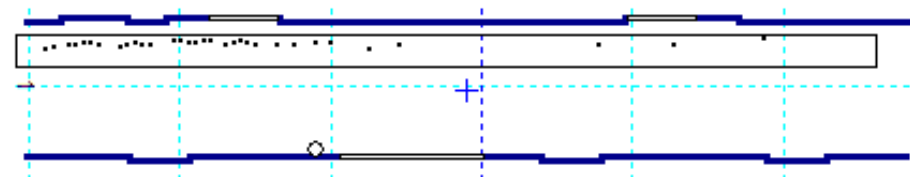
of illumination in the area in between them. Similarly, illumination is also reduced at the position directly under L2 because of the absence of light from L3. Another example is the air flow velocity measurement. The air always flows from the West end of the corridor and not so much from the East end when the ventilation unit is turned on. Acquiring prior knowledge of all of the quantities being measured in all possible scenarios is difficult. This demonstrates exactly why novelty detection using a mobile robot and a thematic map is a worthwhile study because the scheme only requires normal data to model the environment.



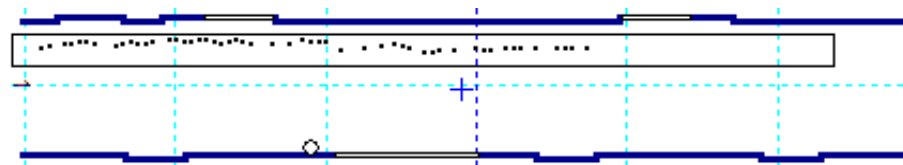
(a) Sensor: Laser range finder. An unusual situation where door D2 was opened.



(b) Sensor: Ambient light sensor. An unusual situation where lights L1 and L2 were turned on while light L3 was turned off. Abnormal measurements were detected at all areas near L1, L2 and L3.



(c) Sensor: Air flow velocity. An unusual situation where the air ventilation was turned on and air was flowing to the air duct.



(d) Sensor: Air flow direction. Similar to the situation in (c).

Figure 2.30: The regions created for different types of sensors. The rectangles shown are the regions which associate the location with normal conditions. The smallest dots on the inspection route indicate where the robot detected unusual measurements using one or more of its sensors.

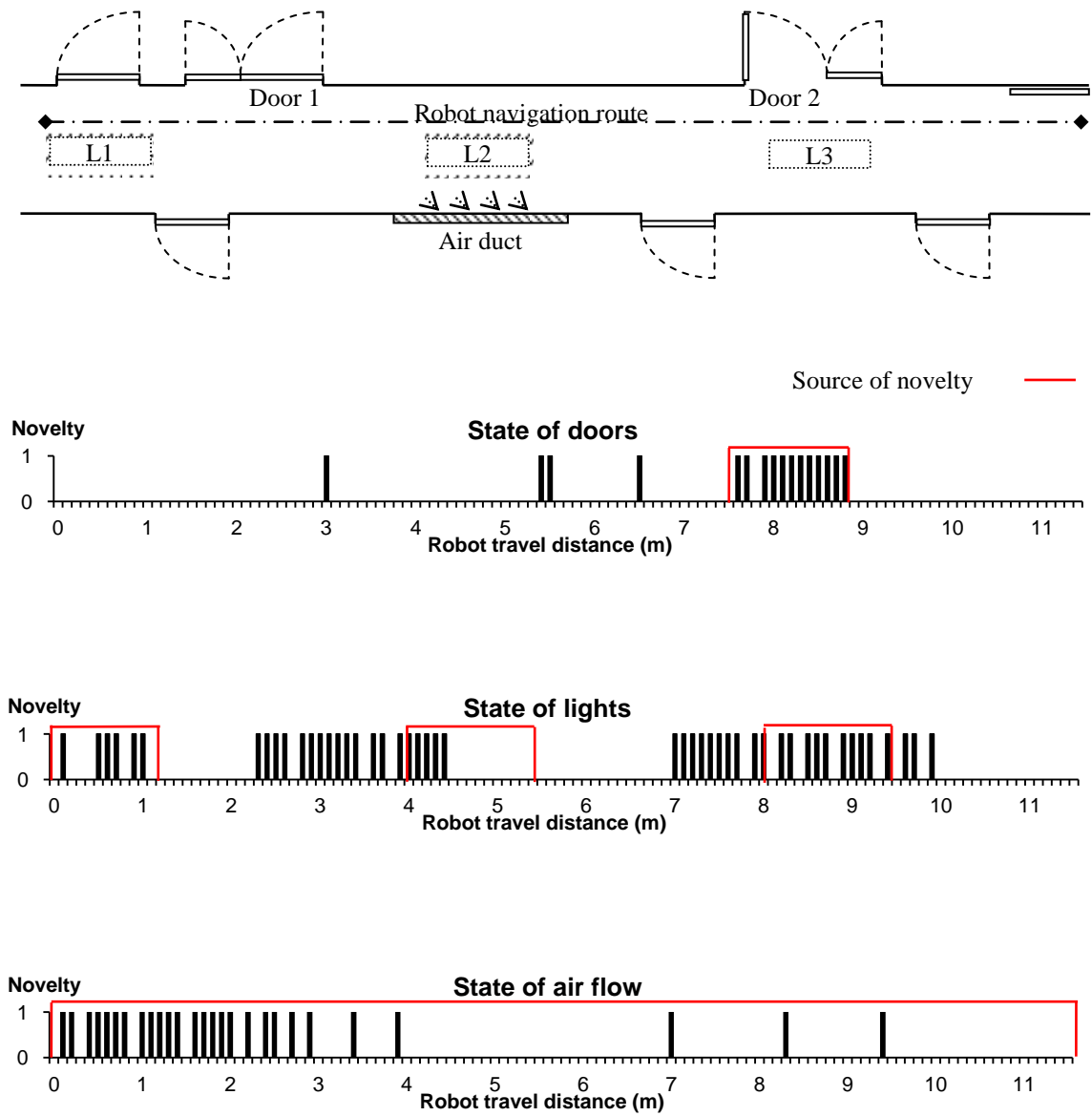


Figure 2.31: The corridor in its unusual condition and the results of novelty detection using the laser range finder, ambient light sensor and anemometer. The red lines indicates the source of novelty; including the open door, the position of the lights, and the expected areas where the wind changes.

2.9 Discussion and Conclusion

The flexible regions reduce the amount of memory required to map information about the environment. In principal, the fewer the changes of sensor measurements over an extended region, the less memory is required to map the region. The amount of memory required to store information is adjusted autonomously according to the requirements of the sensor data and the environment. A flexible region map also needs no pre-allocation of the space of the grids/cells like the space-driven map, making it easier to be used in any new environments. This is particularly useful if the novelty detection system is developed as a standalone system to be used by any used or new mobile robots.

The main objective of having a map is to reduce false negative detections and this has been achieved. The system is now able to detect anomalies which appear normal at other locations in the environment. The performance of novelty detection when using a flexible region map is comparable with using a fixed perception-based map.

Although detail investigation on the processing speed required for different types of maps is beyond the scope of this thesis, it is worth to mention the general expectation of the processing speed of different type of maps. A search will be involved for the data-driven map as they do not associate the data directly to the localization index thus requiring the robot to first find which of the region best match the current robot pose. The speed for accessing data from a flexible region map can be better than other data driven map like the perception based map as if it has fewer number of regions to look for. However, in general, space driven maps like the grid maps have faster accessing speed as there is no search involved to access the data. Nevertheless, as mention in the summary of the related work (Section 2.2.3), with the implementation of the tree structure from the R-tree spatial indexing approaches, the search can be made efficient. This can be one of the possible extension of the work describe in this chapter.

One limitation of the flexible region map is that changing the content of a region is not as easy as updating grid based map cells. This is especially true if the changes only affect part of a region. This limitation is discussed in the following chapter.

For future work, other than surveillance applications, the flexible region map could be useful for scientific exploration in hazardous environments such as in caves, deep sea or other planets. For example, Spirit and Opportunity [65] which were the mobile robots used for the Mars exploration project in year 2004, could benefit from the flexible region map for mapping different types of measurement data. For autonomous exploration, the novelty detection mechanism can be used as an attention selection tool, to select appropriate information to process or requiring further investigation. The fact that Mars is a barren planet means many types of quantities being measured such as temperature, images, types of soils and others are similar over extended regions. This information could be mapped in the limited memory space that the autonomous robot carries using the flexible region map.

Chapter 3

Autonomous Mapping

This chapter presents enhancements that were implemented to make a flexible region map adaptable to changes in the environment. The chapter begins with a brief introduction describing the aims and motivation of the work in this chapter. Then the method for changing part of a region in a flexible region map in response to changes in the environment is presented. This is followed by an explanation of the process of updating the map. Experimental results show that autonomous update was achieved by allowing the flexible region to reshape itself to accommodate to changes in the environment.

3.1 Introduction

A flexible region map has the ability to change the size of its regions to suit the distribution of different entities in different situations. However, once a region has been created, updating the normal condition of a mapped area is not a trivial task. A grid based map such as the occupancy grid map [35] has fixed sized cells. Updating them is just a matter of changing the information within each cell. On the other hand, the flexible region map has variable sized regions and this makes it difficult to update a region when the new information only affects part of the region.

Motivated by this challenge this chapter presents an approach to updating a flexible region map. The objectives and contributions of the work in this chapter are:

1. To develop a method that allows changes of information to be made to part of a region within a flexible region map.
2. To produce an autonomous mapping technique using a flexible region map that allows the robot to learn the normal condition of the environment without any human supervision or with minimal supervision.

There are two types of actions that are required to perform autonomous mapping using a flexible region map. The first action is restructuring of the map. In the previous chapter, creation, expansion and merge functions have been described. These functions allow regions in the map to change their size according to the data that they are associated with. In this chapter, an additional separation function is introduced to allow changes to be made to a part of an established region. The second action is updating the status of regions. This action determines the conditions of sensor measurements (normal/novel) represented by regions covering different areas of the environment.

3.2 Region Separation

Region separation is required for updating a flexible region map. A region should hold the same information throughout the space within its boundary. If new changes affected only part of a region or if part of a region is not accessible by a robot anymore, it should be separated into smaller regions. The robot can then update each region's status separately.

The solution discussed here is focused on maps created by a robot that travels by following the same specified route. This means that the regions will be elongated along the route. In the context of autonomous mapping of normal data for novelty detection, there are two situations where a region should be separated. The first situation is when a robot detects a different perception rather than the one that is associated with the region it is currently in. The term *old region* is used here to represent the already created region. The second situation is when the robot deviates from its path due to a blockage or other reasons, which makes it unable to visit part

of the existing region. Examples of both cases are shown in Figure 3.1. As can be seen from the examples, if one of the two situations occurs, the *old region*, R_o , will be separated into several regions.

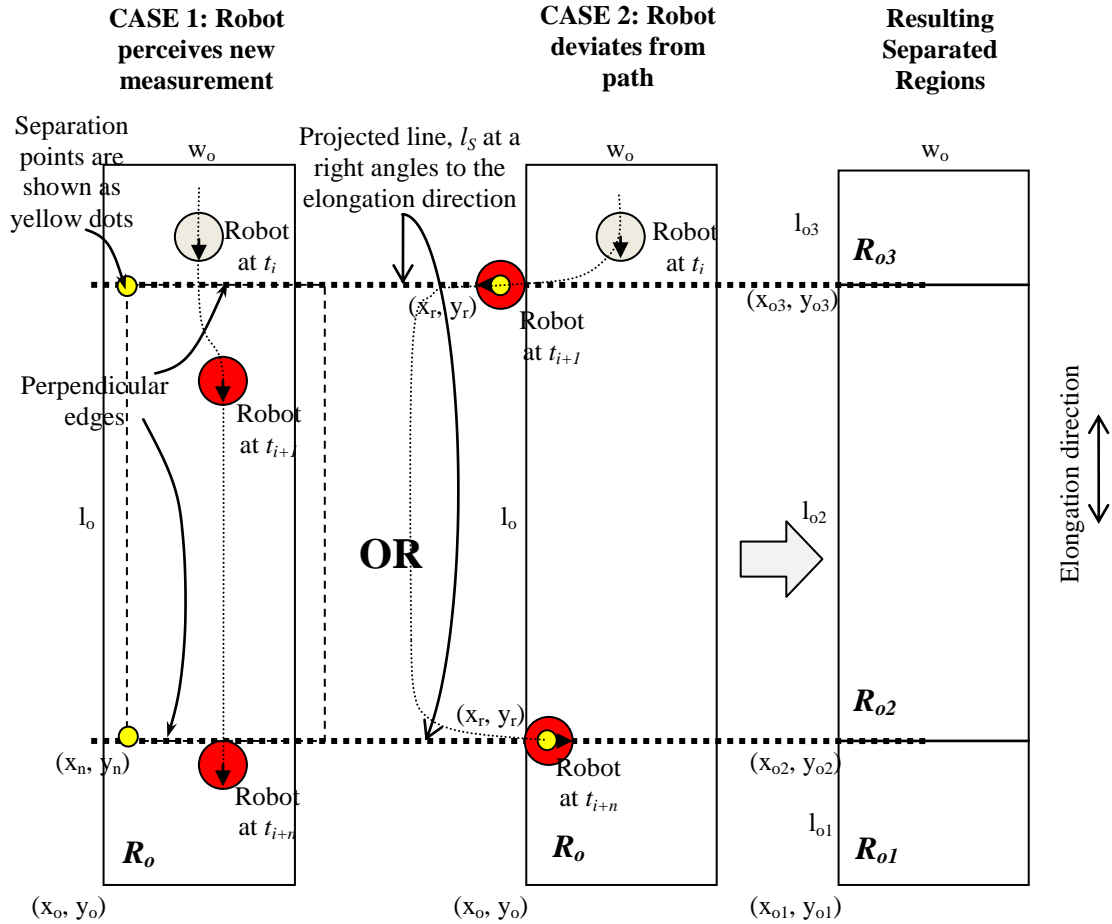


Figure 3.1: An example of how it perceives new measurement (left) and how a robot deviates from its path (middle) while travelling inside region R_o . As a result, three separated regions are created (right).

The separation process proceeds as follows. When a new region, R_n is created it is allowed to expand but only during the epoch it is created. Once R_n stops expanding, any old regions which coincide with one or both (see Figure 3.2) of the R_n edges perpendicular to the old region elongation direction is/are separated. In the case when the robot deviates from its path and is unable to visit the area on its original path, an imaginary line projected perpendicular to the elongation direction of

the old region is established based on the robot position when it exits or enters the old region. This line is used as a guideline to separate the old region.

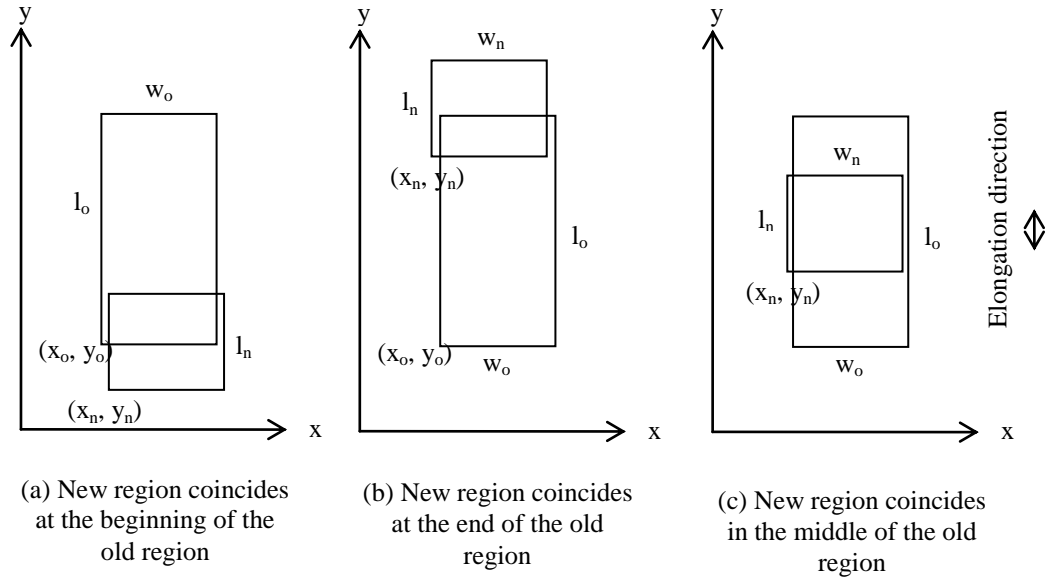


Figure 3.2: Examples of three forms of overlapping.

The method of changing from the old region to the separated regions depends on the situations discussed earlier. For each of the separated regions, the parameters of their bounding box need to be determined but their content is automatically inherited from the old region. In order to determine their parameters, the region elongation line and separation line need to be formulated first. Region elongation line, l_R given by Equation (3.1) is the projected line from the region reference point in the elongation direction and separation line, l_S given by Equation (3.2) is the projected line from the separation point which is perpendicular to l_R . The reference point of the old region is denoted by x_R, y_R, θ_R where θ_R represents the robot heading as well as the elongation direction of the region. In the case where a new region is created, the separation points are (1) the new region reference point and (2) the new region reference point plus its length. In the case where a robot deviates from its path, the separation point is the point where the robot exits from or enters into the side of the old region. The separation point is denoted by x_S, y_S . Given that x_R, y_R, θ_R, x_S and y_S are known; b and d can be determine (see Equation (3.3) and

Equation (3.4)). The reference points of the separated regions x_{R1}, y_{R1} and x_{R2}, y_{R2} could be found where x_{R1}, y_{R1} is equivalent to x_R, y_R and x_{R2}, y_{R2} is the intersection P_{RS} between the two lines (l_S and l_R) given by Equation (3.5).

$$l_R: y = mx + b \quad (3.1)$$

$$l_S: y = -\frac{1}{m}x + d \quad (3.2)$$

$$b = y_R - mx_R \quad (3.3)$$

$$d = y_S + \frac{1}{m}x_S \quad (3.4)$$

$$P_{RS}: x = \frac{m(d - b)}{(1 + m^2)}, \quad y = \frac{m^2(d - b)}{(1 + m^2)} + b \quad (3.5)$$

In this project, Equation (3.1), Equation (3.2) and Equation (3.5) can be simplified due to the fact that the regions are elongated only in four directions 0° , 90° , 180° and 270° which makes the slopes of the equations either zero or non-existent. If the slope is zero (which is the case for 0° and 180°) then l_R and l_S are given by Equation (3.6) and Equation (3.7) and P_{RS} becomes Equation (3.11). On the other hand, if the slope is non-existent (which is the case for 90° and 270°) then l_R and l_S become Equations (3.9) and (3.10) where P_{RS} is given by Equation (3.11).

$$l_R: y = y_R \quad (3.6)$$

$$l_S: x = x_S \quad (3.7)$$

$$P_{RS}: x = x_S, \quad y = y_R \quad (3.8)$$

$$l_R: y = y_S \quad (3.9)$$

$$l_S: x = x_R \quad (3.10)$$

$$P_{RS}: x = x_R, y = y_s \quad (3.11)$$

Now that the reference points for the separated regions R_1 and R_2 have been determined, other parameters which are the width and the length of the separated regions can be identified. For this project, the width and the length are associated with the size of the rectangle edges in x and y directions. For this reason, if the regions are elongated in the 90° or 270° directions, the width remains the same but the length varies. On the other hand, if the regions are elongated in the 0° or 180° directions, the opposite situation occurs. For the first case, the width of both regions w_{R1} and w_{R2} are equal to the width of the old region, w_R as given by Equation (3.12). The length of R_1 , l_{R1} is the distance between x_{R1}, y_{R1} and x_{R2}, y_{R2} which is given by Equation (3.13). The length of R_2 , l_{R2} is the remaining length of the old region after subtracting l_{R1} which is given by Equation (3.14). For the latter case, the length and the width of the regions are given by Equation (3.15), Equation (3.16) and Equation (3.17).

$$w_{R1} = w_{R2} = w_R \quad (3.12)$$

$$l_{R1} = |x_S - x_R| \quad (3.13)$$

$$l_{R2} = l_R - l_{R1} \quad (3.14)$$

$$l_{R1} = l_{R2} = l_R \quad (3.15)$$

$$w_{R1} = |w_S - w_R| \quad (3.16)$$

$$w_{R2} = w_R - w_{R1} \quad (3.17)$$

3.2.1 Separation Algorithm

The following algorithms summarize the discussion on region separation.

Algorithm 3.1: Region separation

```

1:  Separate() {
2:      Find_lS and all affected regions()
3:      Find_lR()
4:      Find_PRS()
5:      Determine_xywl of separated regions()
6:      Delete affected region()
7:  }
```

Algorithm 3.2: Find_lS and all affected regions (separation due to the creation of a new region)

Notation:

sp = separation point
re = region elongation
xy = x or y coordinate
wl = width or length

Algorithm:

```

1:  xy_sp1 = xy_new_region
2:  xy_sp2 = xy_new_region + wl_new_region
3:  For all sp
4:      For all old region i = 1 to N
5:          If (re = 0 OR 180 AND x_region < x_sp AND
              x_sp < (x_region + x_length))
6:              Affected region = region_i
7:              lS = x_sp
8:          EndIf
9:          If (re = 90 OR 270 AND y_region < y_sp AND
              y_sp < (y_region + y_length))
10:             Affected region = region_i
11:             lS = y_sp
12:          EndIf
13:      EndFor
14:  EndFor
```

Algorithm 3.3: Find_IS and all affected regions (separation due to deviation of robot from its path)

Notation:

sp = separation point
 re = region elongation
 xy = x or y coordinate
 wl = width or length

Initialization:

out_of_path = 0

Algorithm:

```

1:  xy_sp = xy_robot
2:  For all old regions i = 1 to N
3:      If (re = 0 OR 180 AND x_region < x_sp AND
          x_sp < (x_region + x_length) )
4:          Affected region = region_i
5:          If (out_of_path == 0 AND robot outside
              region_i)
6:              out_of_path = 1
7:              lS = x_sp
8:          EndIf
9:          If (out_of_path == 1 AND robot inside
              region_i)
10:             out_of_path = 0
11:             lS = x_sp
12:          EndIf
13:      EndIf
14:      If (re = 90 OR 270 AND y_region < y_sp AND
          y_sp < (y_region + y_length) )
15:          Affected region = region_i
16:          If (out_of_path == 0 AND robot outside
              region_i)
17:             out of path = 1
18:             lS = y_sp
19:          EndIf
20:          If (out_of_path == 1 AND robot inside
              region_i)
21:             out of path = 0
22:             lS = y_sp
23:          EndIf
24:      EndIf
25:  EndFor

```

Algorithm 3.4: Find_IR

```

1:   For all affected region
2:     If ( heading = 0 OR 180)
3:       lR = y_region
4:     EndIf
5:     If ( heading = 90 OR 270) {
6:       lR = x_region
7:     EndIf
8:   EndFor

```

Algorithm 3.5: Find_PRS (intersection between l_s and l_R).

```

1:   If ( heading = 0 OR 180)
2:     xRS = lS
3:     yRS = lR
4:   EndIf
5:   If ( heading = 90 OR 270) {
6:     xRS = lR
7:     yRS = lS
8:   EndIf

```

Algorithm 3.6: Determine_xywl of separated regions

```

1:   If ( heading = 0 OR 180)
2:     x1 = x_region
3:     y1 = y_region
4:     w1 = |xRS-x_region|
5:     l1 = l_region
6:     x2 = xRS
7:     y2 = yRS
8:     w2 = |w_region-w1|
9:     l2 = l_region
10:  EndIf
11:  If ( heading = 90 OR 270) {
12:    x1 = x_region
13:    y1 = y_region
14:    w1 = w_region
15:    l1 = |yRS-y_region|
16:    x2 = xRS
17:    y2 = yRS

```

```
18:      w2 = w_region
19:      l2 = |l_region-l1|
20:  EndIf
```

3.3 Autonomous Mapping

A robot that performs noncritical tasks such as cleaning and tour guiding could have full autonomy over the update of its flexible region map. Full autonomy means the robot decides which region should remain and which should be deleted, based on their status as either normal or unusual. For a robot that does more critical tasks such as security and surveillance, autonomous mapping could still be employed but should be closely monitored by a human expert/supervisor.

As mentioned before, the scope of the work describe here is limited to a robot which travels by following a path. The main reason for this is that a normal condition is defined as a measurement that is perceived consistently over a certain number of passes through an environment. In order to make a fair assessment on the status (normal/novel) of each region, the robot should visit all regions within an epoch (i.e. a single pass through its environment). Following a fixed path will ensure that the robot visits all the regions available. A path could be divided into smaller segments so that the robot does not need to wait until it travels through the entire environment. Instead, the robot can update the status of the regions in a segment as it has moved pass the segment.

3.3.1 Added Features of the Flexible Region Map

Several features are added to make the flexible region map described in Chapter 2 able to adapt autonomously to new changes in the previously mapped environment. First, each region is associated with a novelty measure, n as given by Equation (2.22) where o denotes the number of occurrences of an event and τ is a time constant

which controls the rate of habituation. A novelty measure graph is depicted in Figure 3.3.

The concept of habituation is described in Chapter 2. By using habituation, the greater the number of perceptions that match the information stored about a region, the less novel the region becomes. The principal of habituation is based upon the accumulation of observations over time. In this work, a unit of time is a learning epoch, or a single pass of a robot along its path in the environment. Occurrence, o of a region is updated only once during each epoch, regardless of the region size. This means that larger regions that are visited more often during a single pass than a smaller sized region will be habituated at the same rate as the smaller sized region.

$$n(o) = e^{\frac{-o}{\tau}} \quad (3.18)$$

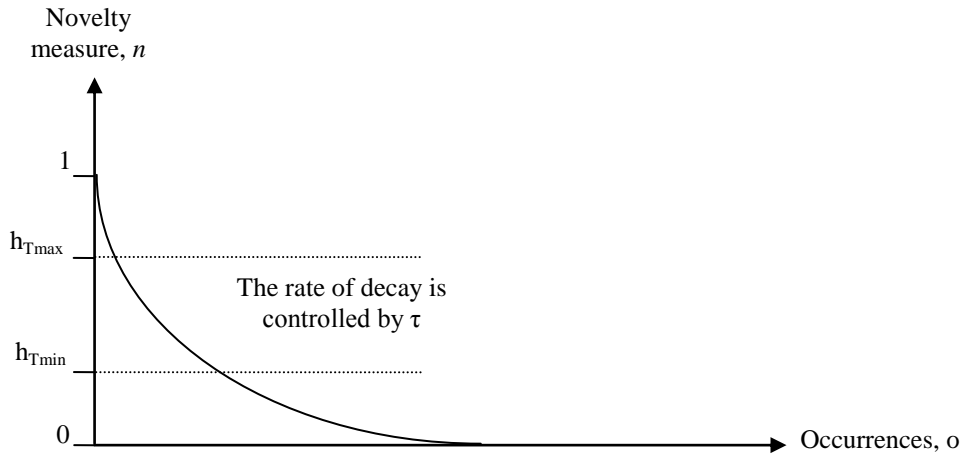


Figure 3.3: Decaying novelty function with thresholds.

The use of the maximum threshold, h_{Tmax} and minimum threshold, h_{Tmin} depicted in Figure 3.3 allows the habituation process to exhibit hysteresis. The hysteresis introduces a delay when changing states from normal to novel and vice versa. When a new region is created, the novelty measure is set to be equal to h_{Tmax} . The region remains novel until the value decreases below h_{Tmin} . After that, the region will remain normal until its novelty measure rises above h_{Tmax} . The state of the region

when its novelty measure is between h_{Tmin} and h_{Tmax} depends on the last threshold that it crossed. This effect is vital to avoid switching states (from novel to normal or vice versa) due to noisy inputs. A region will be deleted only if the novelty measure reaches 1.

Another added feature is the ability of the neural network to increase the size of its representation. New neurons should be created if the available neurons in the neural network cannot represent the changes in the environment. In this thesis, the Habituating Self Organizing Map (HSOM) was modified so that it can add a new neuron when there is a new perception. In practice, other methods such as the Grow When Required (GWR) network could also be employed to replace the HSOM.

Finally, preconditions are added to the expansion and mergence processes. Expansion is only for newly created regions and is not allowed for established regions. The reason is that there will be a conflict in determining the value of the novelty measure if a region is already established and the extended area is new. Another point regarding expansion involves separation of an old region and this should only be done after a new region has been fully expanded. For the mergence process, two neighboring regions with the same content could be merged only if both are habituated (where their novelty measures are below h_{Tmin}). The novelty measure of the merged region is the average of the novelty measures of the regions before they are merged.

3.3.2 Autonomous Mapping Algorithm

The algorithms for autonomous mapping are given here. The modification made to allow autonomous mapping in Algorithm 3.7 is highlighted as bold text.

Algorithm 3.7: Autonomous mapping using a flexible region map.

Notation:

BMU – best matching neuron

S_{BMU} – distance between BMU and sensor measurement

S_T – similarity threshold

```

Initialization:
Train HSOM using perception during the first few runs
in a new environment
Set  $V_i = 0$ 

Main process:
1:  Move_within_a_segment()
2:  While_in_segment()
3:    Get_pose()
4:    Get_sensor_measurement()
5:    Find_BMU()
6:    If ( $S_{BMU} > S_T$ )
7:      newHSOMneuron = current perception
8:    EndIf
9:    Create()
10:   Expand()
11:   Separate()
12:   Mark_visited_region()
13: EndWhile
14: Update_region_status()
15: Delete()
16: Merge()

```

Algorithm 3.8: Mark visited regions

```

Initialization:
is_region_i_visited = 0

1:  If (robot occupies region_i AND current
    perception matches region content)
2:    is_region_i_visited = 1
3:  EndIf

```

Algorithm 3.9: Update region status.

```

1:  For all regions
2:    If marked
3:      Increase its occurrences
4:    Else
5:      Decrease its occurrences
6:    EndIf
7:  EndFor

```

```

8:   is_region_i_visited = 0
9:   If (n==1)
10:       Delete region
11:   Else if (n>=hTmax)
12:       State of region i = novel
13:   Else if (hTmin <n<hTmax)
14:       State of region i = current state
15:   Else
16:       State of region i = normal
17:   EndIf

```

3.3.3 Mapping with Minimal Supervision

In critical applications such as a surveillance task, a human should be the arbiter when making any decisions. When a surveillance robot highlights a novelty, at some stage of the process a human expert (such as a security officer etc.) should be informed and he or she should then make the final decision on the appropriate action that should be taken by the robot. One of the actions that the robot could take is to adapt to the novelty and to consider it as part of the normal environment. In particular, the role of the human in the update process is to decide whether the new region represents a normal perception and whether the affected old region should be deleted or remain as it is. This could be done by having a human to monitor the sensor measurements and use the information to update the status of the regions given by line 14 in Algorithm 3.7.

3.4 Experiments

The experiments were conducted in an L-shaped room made of polystyrene blocks. For the setup of the ‘old’ environment, the room was empty. The room was changed to a ‘new’ environment by introducing a 100x800 mm² polystyrene block at the center of the room. The first experiment was conducted to:

1. Observe the results of region separation due to the creation of new regions.

2. Observe the value of novelty measure of a newly created region and separated regions during unsupervised update.
3. Test the performance of novelty detection using the updated flexible region map.

First the robot was made to perform wall following with the old environment settings from the start to the end points and this was repeated several times (see Figure 3.4). Then, the room was changed to the new setup and the learning process was repeated several more times. During wall following, the robot logged its laser measurements taken at every inspection step i.e. every 100mm along the path. The mapping and updating were done offline using the logged data. The flexible region map of the old environment was produced by following the standard procedure described in the previous chapter. The region tolerance of the flexible region map was set to a high value of 0.2 to create a reduced number of regions in the map. This was done to make observation of the results easier.

The only difference between a supervised and unsupervised update is in the way the status of a region is established. Other than the region separation process which was already tested during the experiments for the unsupervised update method, the performance of the supervised update method depends on the decisions of the human supervisor. For this reason, the experiment was conducted only to prove the feasibility of the unsupervised update method.

The results of the unsupervised update are as expected and are depicted in Figure 3.5. Figure 3.5 (a) shows the region created during inspection of the old environment while Figure 3.5 (b) shows the resulting regions due to the creation and separation of regions after a new object was introduced to the environment. Some of these regions (1, 2, 3 and 4) were deleted during the epoch when the new object was introduced. Other regions (8, 9 and 12) were deleted after they were dis-habituated while at the same time others (5, 6, 7, 10 and 11) were habituated.

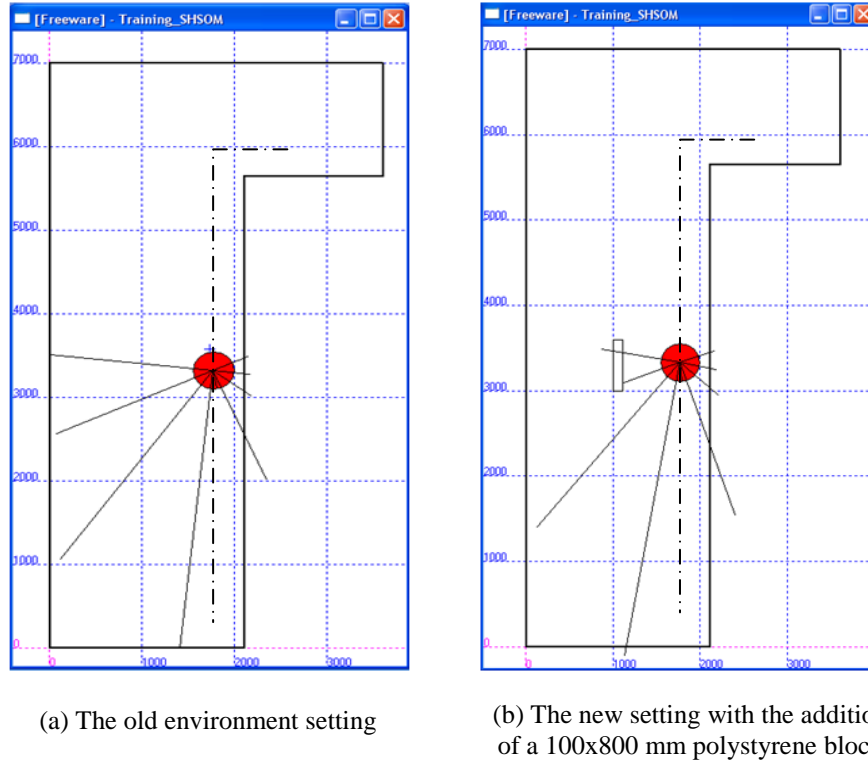


Figure 3.4: Environmental setup for the experiment. The lines coming out from the robots (the red circles) are the average laser measurements from 8 sector divisions of the 270° laser angular range.

A detail description of the experimental results is as follows. The robot traveled through the old environment during the first five epochs. A polystyrene block was introduced starting from epoch 6. During epoch 6, regions were created and separated. This is what happened during epoch 6. When the robot was near the polystyrene block, Region 2 was created. Then, Region 1 was separated into Regions 3, 4 and 5, based on the position and dimensions of Region 2. Later after several inspection steps, Region 6 was created. Region 6 partly coincided with Region 2, Region 4 and Region 3. As a result, these regions were separated into 6 other regions. Region 2 was separated into Regions 7 and 8. Region 4 was separated into Regions 9 and 10. Region 3 was separated into Regions 11 and 12. Regions 1, 2, 3 and 4 were immediately deleted after separation.

Figure 3.6 shows the novelty measure value of each region over the whole 15 epochs. As described in the algorithm, the initial value for a newly created region is

set to $h_{Tmax} = 0.9$. Depending on the decay rate, the novelty measure should become less than this value after a region is created the first time. This is why the starting value of the novelty measures in Figure 3.6 is approximately 0.81.

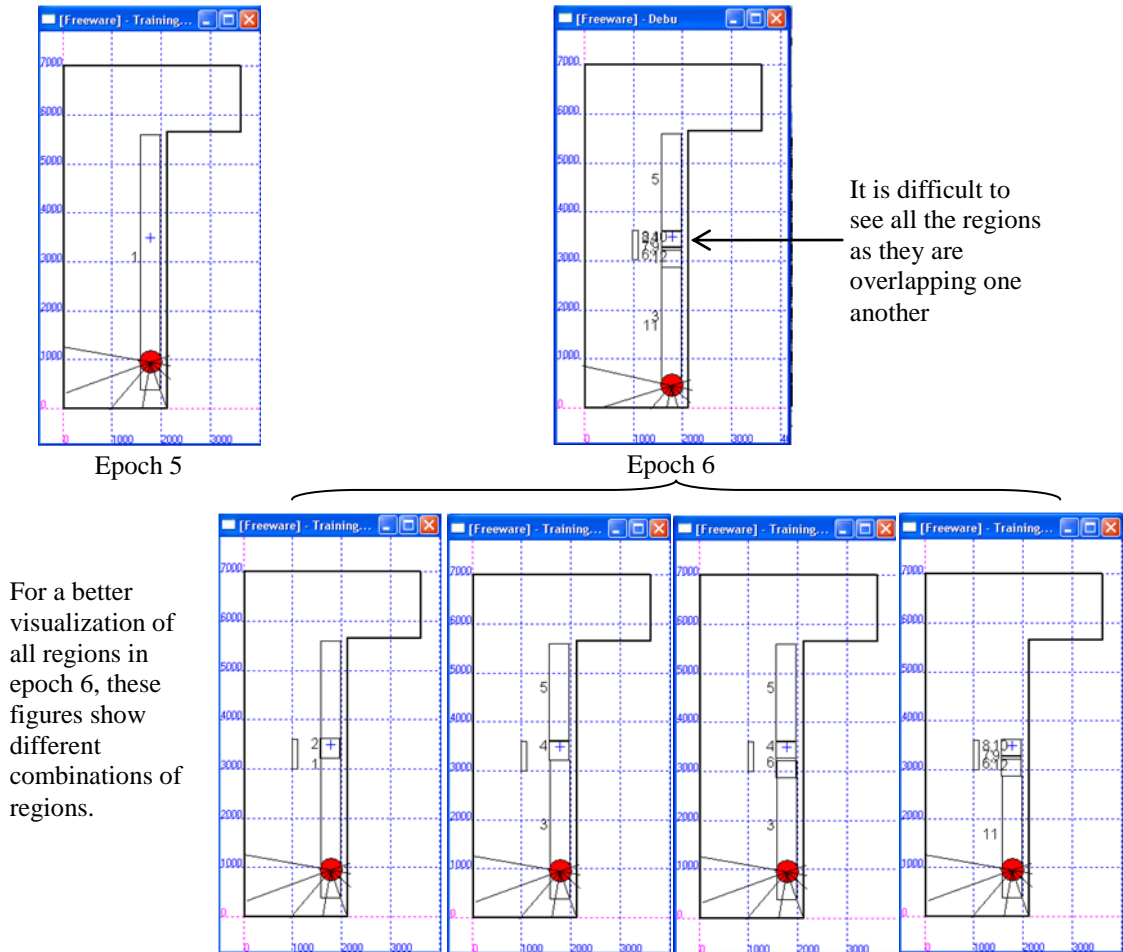


Figure 3.5: Results show new regions and the resulting separated regions during epoch 6 (displayed in several frames for better visualization). New region 2 separated region 1 into regions 3, 4 and 5. Region 6 separated three regions. Region 2 was separated into regions 7 and 8, region 4 into 9 and 10 and finally region 3 into 11 and 12.

The novelty measure of separated regions is copied from the novelty value of the original region during the epoch before separation. For example, in Figure 3.6 (see Figure 3.7 for a better visualization of overlapping lines), the novelty measure of R3, R4, R5, R11 and R12 are copied from R1's novelty measure, and thus they are the same. Although these regions are only created during epoch 6, as they are derived from R1, they still carry the history of R1. It can be seen that at locations covered by

two or more regions, regions with content that does not match the current perception will have their novelty measure increased. Eventually the value of their novelty measure becomes 1 and as a result, they are deleted (see R8, R9 and R12). In contrast, the novelty measure of regions with content that matches the current perception gradually decreases over several epochs. According to the algorithm, if the value falls below h_{Tmin} , the perceptions (sensor measurements or neurons) which are associated with the region are considered normal. Similarly, for increasing values of the novelty measure, when it rises above h_{Tmax} , the perceptions mapped onto the regions do not represent the normal environment anymore.

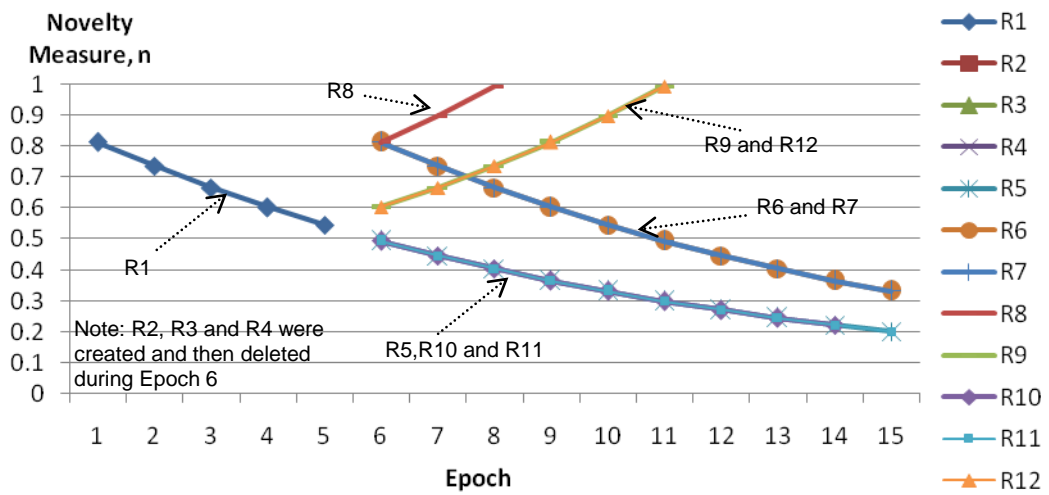


Figure 3.6: Values of novelty measures over 15 learning epochs. The discontinuation of old lines or the start of new lines is due to the deletion of regions or creation of new regions. When a new region is first created, its novelty measure is 0.81.

Figure 3.7 depicts individual graphs of each of the novelty measures shown in Figure 3.6 for easier visualization. It can be seen that R2 was deleted immediately after its creation. This occurs due to the creation of R6 which coincided partly with R2. As a result, R2 is separated into R7 and R8. Similarly, regions R3 and R4 were also deleted during the same epoch that they were separated from R1. Region R4 was separated into regions R9 and R10 whereas region R3 was separated into regions R11 and R12.

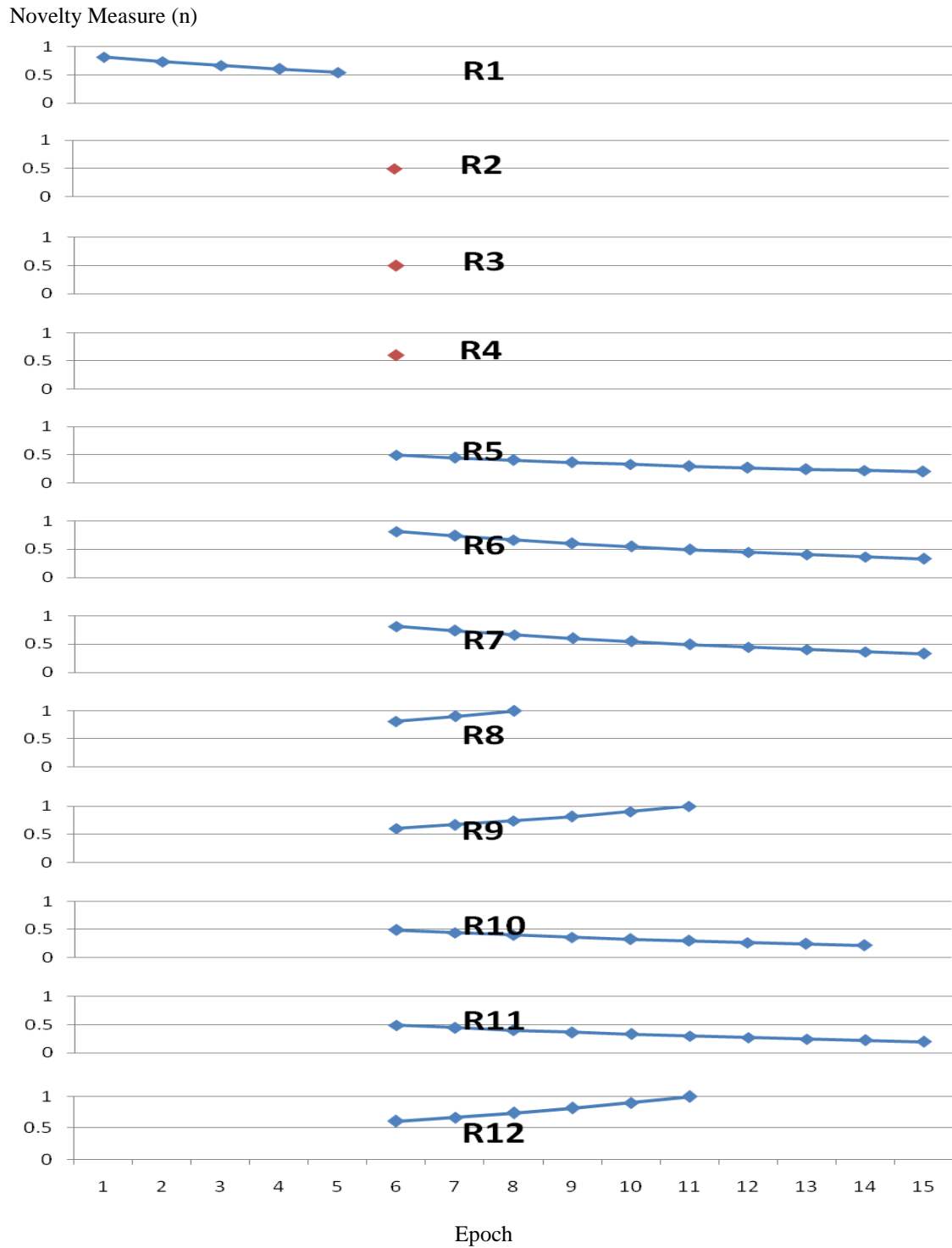


Figure 3.7: Individual graphs showing the novelty measure of all regions.

The main goal of the update procedure is to maintain good performance in the novelty detection system so that it can detect unusual conditions in a changed environment. For this reason, this experiment is designed to see the performance of

the novelty detection system, before and after the changes. The new environment was changed back to the old environment by removing the polystyrene block at the center of the room. Then the robot was made to perform inspection in the old environment by following the same route shown in Figure 3.4. This checks whether the robot was able to discard old information and adapt to a new situation. The experiment was conducted by using the repetitive observation strategy (ROS) described in Chapter 4. ROS is used to highlight the position of missing objects (object that are normally present) and unusual measurements caused by seeing the previously occluded wall. The performance of novelty detection using the updated map is shown in Figure 3.8. The anomaly event that occurred during the experiment was the removal of the polystyrene block from the middle of the room. By using the updated map, the robot was able to highlight this unusual condition. The position of the missing object is highlighted using the red dots and the unusual measurements are represented using the black dots.

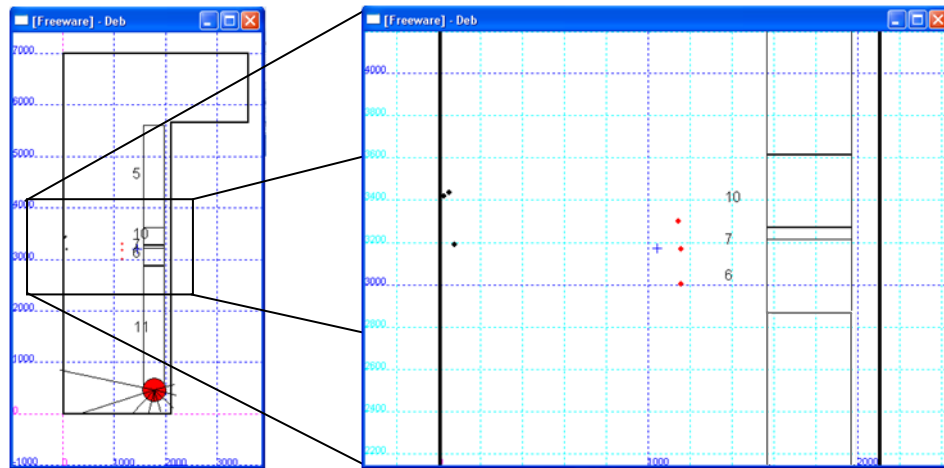


Figure 3.8: Results of novelty detection during epoch 15. The location of normal measurements (red dots where the block used to be) and unusual measurements (black dots indicating a portion of the wall that usually cannot be detected) are determined using the repetitive observation strategy described in Chapter 4.

A second experiment was conducted to see the result of the separation algorithm due to deviation of the robot from its original path. The deviation was caused by a blocked path which had prevented the robot from accessing and monitoring conditions in parts of an old region. As a result, the affected old region

was separated and the inaccessible region was dis-habituated or in other words the robot gradually forgot the condition of that area. This resembles an aspect of memory in biological systems.

The experiment was conducted using temperature data where values were not affected by the introduction of the object. This was done to make the visualization of the separation results more comprehensible. As can be seen from Figure 3.9, the robot was made to follow the wall of part of the environment for the first 5 epochs. Region 1 was created and its novelty measure was gradually decreasing. During epoch 6, a $300 \times 400 \text{ mm}^2$ object was placed in the robot's path, forcing the robot to deviate from its original path. Region 2 and 5 were created as the robot tried to navigate around the obstacle. This was an automatic decision by the robot as it was programmed to create regions when its heading changed to approximately 0° , 90° , 180° , or 270° . Immediately after the robot exited from region 1 on the original route, region 1 was separated into regions 3 and 4. Then when the robot entered into region 4 (now that region 1 no longer existed), region 4 was separated into regions 6 and 7. The position of the robot when it entered/exited the old region was used as the guideline for the separation.

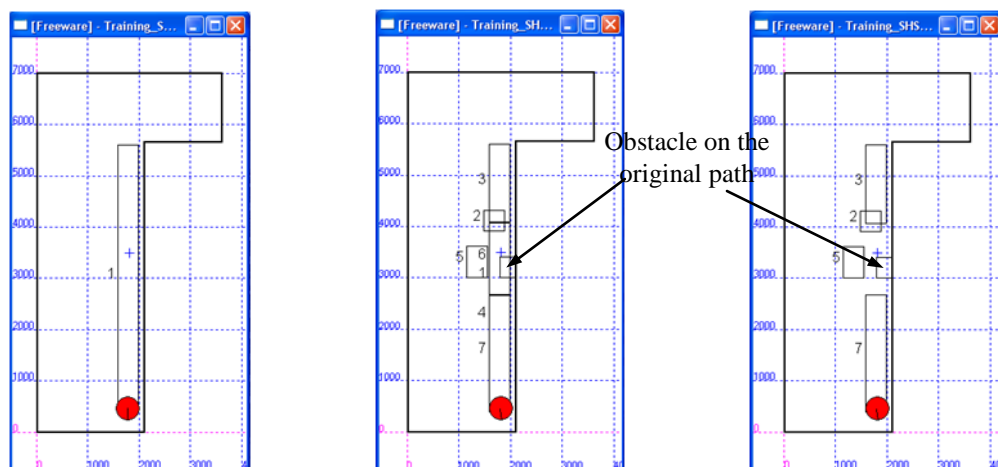


Figure 3.9: Results of autonomous mapping due to deviation from the original path. Temperature data is used to make the visualization of the regions easier.

After epoch 6, the robot was made to run for several more epochs. After every epoch, the inaccessible region i.e. region 6 became more and more novel. Eventually, the region was deleted after epoch 11 (see Figure 3.10).

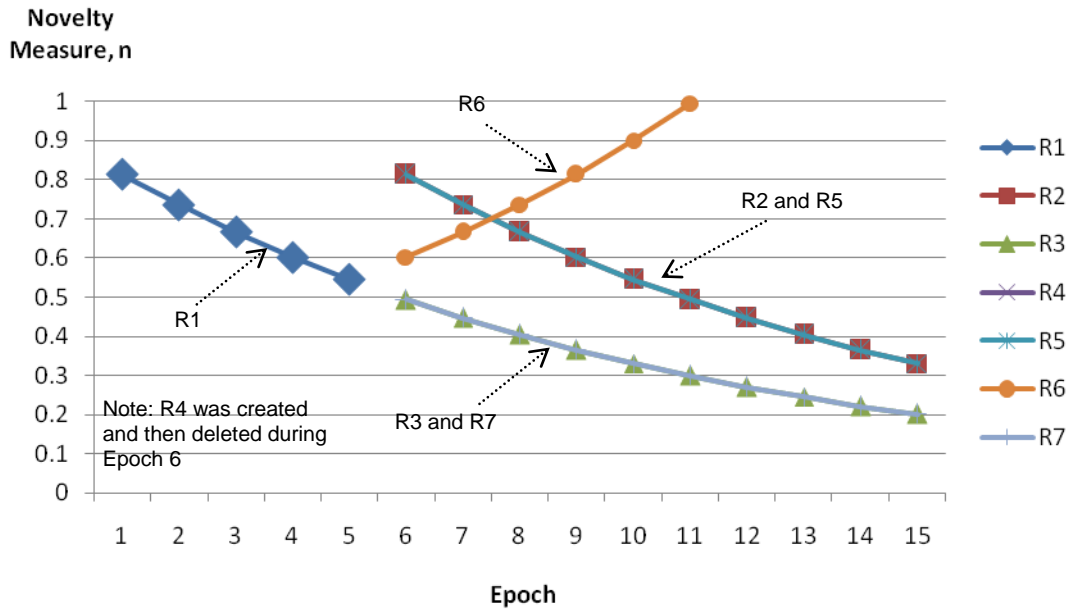


Figure 3.10: Values of novelty measures for 15 epochs. Region 6 is eventually deleted after it was inaccessible by the robot for several epochs.

3.5 Discussions and Conclusions

This chapter has presented one of the challenges in performing novelty detection using a mobile robot, which is how to maintain a representation of the true state of a changing environment. A solution to the problem of autonomous mapping of a flexible region map has been given. The results show that region separation makes changing part of an extended region possible. By associating each region with a novelty measure, it is possible to autonomously determine their status through an habituation process over several measurement epochs. As a result, the flexible region map was able to adapt to a new changed environment. A test using the repetitive observation strategy (ROS) demonstrated that the robot was able to unlearn an old representation and adapt to the new condition of the environment. The work in this

chapter shows that extra effort is needed (i.e. restructuring of regions) to update a flexible region map as compared to the common grid based map. However, examples from the experimental results highlight the ability of the flexible region map to accommodate to changes in the environment to change its size to the requirements of the data.

One possible application for the unsupervised update is that a region's novelty measure could be used to study or filter dynamic changes at specific locations in the environment. For example, a quantity that is commonly measured will have its region fully habituated. A quantity that is only observable at particular regular intervals will make its region's novelty measure produce a periodically fluctuating pattern. The level of a novelty measure itself indicates how common a perception is in an environment.

The following chapters will investigate how using a mobile robot which employs a novelty detection approach can benefit surveillance work.

Chapter 4

Repetitive Observation Strategy

This chapter presents the framework of the repetitive observation strategy. First a detail description of anomaly points (i.e. the estimated positions of the sources of novelty) is presented. This is followed by a description of the method used to cluster anomaly points. The chapter concludes with a discussion and conclusion.

4.1 Introduction

The repetitive observation strategy (ROS) is a method that gathers and groups observations of the sensed quantities from different sensor poses. Specific to this project, the term observation refers to determination of the position of the source of novelty. The term repetitive not only means that the observation is performed many times but also from different poses. This strategy uses the ability of a mobile robot to carry sensors to different positions, which makes it possible to observe the sensed quantities from different viewpoints.

The strategy is inspired by the natural behavior of animals when reacting to the perception of an anomaly. The first instance of an unusual perception using any sense such as vision, hearing or smell is usually followed by more attentive observations [66] using the same mode of sensing as well as others [67]. The observation is usually done from different viewing angles and positions to gather more information about the anomaly. For example, a bird's head movements in a novel situation (peering movements) are apparently due to the restricted field of vision of the birds. This results in the birds needing to move their heads in order to

permit a complete survey of their total surroundings [68]. Also, the findings of the work in [69] suggest that, when detecting novel objects, chickens investigate them by moving their head and looking at the objects with different parts of their eyes.

A higher level reaction to the detection of anomalies involves exploration and manipulation, which also allows animals to perceive an object from different angles and using different sensing modes. For example, a study presented in [70] has found that baboons react to spatial novelty by performing exploration in an unfamiliar or changed environment. In [71], it was found that a baboon's reaction to novel objects mainly involves manipulation by touching, grasping and transporting (apart from using other senses such as vision and hearing) where more familiar objects are investigated in a less detailed manner usually through looking or sniffing.

For some of these animals, the anomaly detection behavior saves them from being attacked in an ambush. At the same time, the repetitive observation strategy prevents unnecessary panic, and waste of energy in hiding or running from a false alarm i.e. a trade-off between conserving energy and avoiding predation [72]. When this behavior is adopted by an autonomous mobile robot surveillance system, it helps in reducing the number of false alarms, which in turn, saves the robot from wasting its limited energy performing further investigations of a false alarm.

In this project, measurements from different positions along the inspection route are considered as repetitive observation. In the initial stage, unlike the behavior of the animals, the robot does not purposely react to an anomaly, but merely performs inspection based on its original route. However, for sensors such as the laser range finder, by simply following the intended route, the robot can take measurements from different positions and headings as it moves past anomalous objects.

The contribution of this chapter comes from the investigation of two aspects of the repetitive observation strategy:

1. Estimating the position of the source of novelty and identifying factors that influence the distribution of anomaly points.

2. Processing data from repetitive observations (clustering algorithm).

The remainder of this chapter is organized as follows. Section 4.2 presents related work concerning the repetitive observation strategy. Then an overview of the system is given in Section 4.3. Section 4.4 discusses the approach used for estimating the position of the source of the novelty and detailed investigation of the distribution of the anomaly points. This is followed by Section 4.5 which describes the approach to clustering the observations. Finally the content of this chapter is discussed and conclusions given in Section 4.6.

4.2 Related work

To the best of the author's knowledge, there is no direct comparison in terms of functionality and working principal of the repetitive observation strategy with other work in the robotics field. However, there are many methods available which use repeated measurements to achieve their goals. Some of these which have some similarity with the work presented in this chapter are discussed in this section.

In 3-d scanning, measurements are performed repetitively often from different viewpoints to build a 3-d image of an object using techniques such as time-of-flight, triangulation (using laser stripers and a camera), photometry [73] and stereovision. These techniques use active sensors such as laser scanners and passive sensors such as stereo cameras. Data from these sensors are used to re-construct a 3-d representation of the object. Some example applications include rapid prototyping, geographic information system (GIS) mapping, quantity surveying etc. Unlike the situation with novelty detection, in these applications, the object position is known, so the human operator knows in advance where to position the scanner to get the best scanning angle.

The concept of triangulation has also been used to locate the position of the source of a gas leak [22]. Gas concentration sensors were distributed at known positions in a factory environment and communicated using a wireless sensor network. In the factory environment, gas leaks are assumed to spread evenly in all

direction from their source. By knowing the value of gas concentration (measured by the sensor) and the type of gas (from prior information), the source's distance from the sensors can be calculated using the gas diffusion equation. As measurements from at least three sensors are required to locate the source using triangulation, it can be said that this is a form of repetitive observation. However this solution is more suitable for static sensors and not for a single sensor that is mounted on a mobile platform.

Repetitive observation is also used as part of the search strategy used by a mobile robot to locate gas leaks by following the concentration of a chemical plume [74]. The robot is programmed to move toward positions that have a higher gas concentration. Its sensor reading is updated when it pauses during every inspection cycle. In this example, movement of the robot is only based on the current and the immediately previous measurement. However, for the strategy described in this chapter, the estimated position of the source of every positive detection of novelty is recorded and analyzed collectively.

A repeated observation is also used when updating information in a map like the status of occupancy of an occupancy-grid map [35, 44] and the covariance of landmark locations in a feature based map[37, 38]. This is to allow a robot to autonomously develop a navigational map from noisy and uncertain sensor measurement data. In terms of their objective, that is to determine the presence of obstacles and the position of a landmark using noisy sensor data, they are similar to the work presented in this chapter. However, its working principal is fundamentally different. The occupancy-grid map uses grid cells, and keeps track of the number of times an obstacle appears present or absent from the cell. Similarly for landmark location, repeated observation is used to make a statistical analysis on the position of the landmark. Unlike these two applications, in this thesis the repetitive observation strategy is used to examine the spatial distribution of the anomaly points. This means that the repeated measurements are not necessarily refer to the same location or cell but on different but neighboring positions in space.

In novelty detection applications which use mobile robots [11, 16, 51], repetitive observation is used to model the normal environment. This is done by habituating the neural network neurons which frequently match the input patterns that are observed in the environment. When training the neural network, the robot travels through the same environment repeatedly, until the neurons are habituated. In this particular work, repetitive observation is not implemented for training purposes. Rather, the method is used during inspection to gather spatial information about the detection of anomalies.

In summary, many of the implementations of repetitive observation in the work of others are fundamentally different in their working principal as well as their application compared to this work. However, they highlight some of the benefits of using a repetitive observation strategy i.e. to confirm the presence and position of an object as well to gather other related information.

4.3 System Overview

Figure 4.1 shows an overview of the system used for the repetitive observation strategy. The system consists of the autonomous mobile robot surveillance system described in Chapter 2 with an additional on-line clustering functional block. First, an autonomous mobile robot surveillance system is required to check for any unusual measurement. This is followed by estimation of the position of the source of novelty. The estimated positions of anomalous objects (anomaly points) are then clustered using an on-line clustering method.

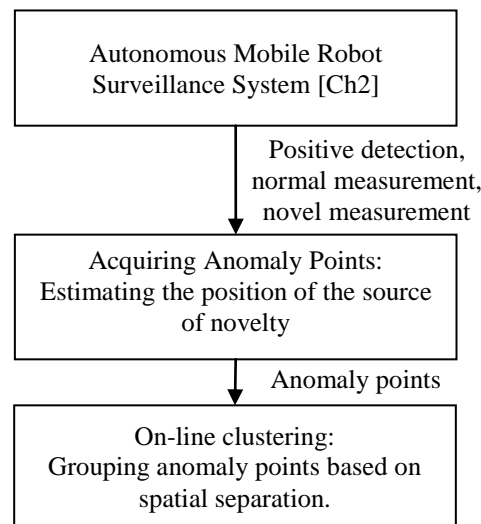


Figure 4.1: System overview.

4.4 Estimating the Position of the Source of Novelty

An anomaly point is an estimate of the position of an anomaly or the source of novelty using the results of novelty detection. This section describes how anomaly points are acquired from a laser range finder and other sensors.

4.4.1 Directional Sensors

Laser range finders are a good example of the type of sensor that can provide information about the position of an anomaly (anomaly point). To show that the method is robust, the laser range finder is down sampled by dividing its angular range into 8 sectors. This is to emulate other noisier range sensors with less dense angular resolution like an array of sonar or infra red sensors. Detailed discussion on this design consideration has been given in Chapter 2. With the limitation that is imposed on the laser range finder, it could not get a clear description of the anomaly just from a single scan, just like other type of range sensors that are arranged sparsely. Repetitive observations overcome this limitation by considering collective information from a number of scans instead of relying solely on a single scan.

In this project, the robot monitor changes by comparing (using the Euclidean dissimilarity measure) a current measurement with a normal measurement stored in the flexible region map. For the laser range finder, a measurement consists of a vector of the average of the laser measurements in the sectors (see Figure 4.2), where an average of a sector becomes a component of the vector. An anomaly is highlighted when the Euclidean distance value is higher than the region tolerance. In order to estimate the position of the source of the anomaly, first the robot finds which of the sectors causes the dissimilarity. This is done by performing individual comparisons of the vector components between the current and the normal measurements. The robot then determines which of them has value bigger than the region tolerance before estimating their position. As can be seen in Figure 4.2, the distance and direction from the anomaly to the sensor is represented by a vector \bar{d} where its magnitude, d is the average value of the laser measurements in the sector and its direction, β is the angle of the center of the sector with respect to the sensor's heading.

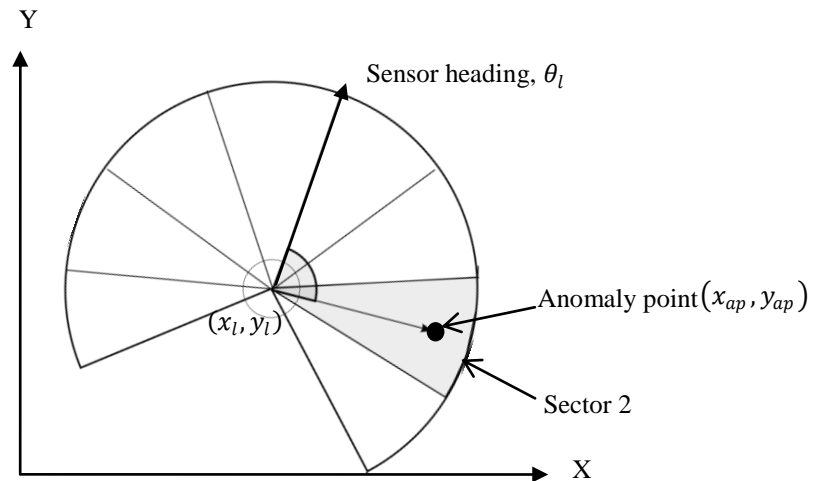


Figure 4.2: The laser angular range is divided into 8 sectors where the average value of laser measurements from Sector 2 is shown to have the highest dissimilarity. The vector \bar{d} carries the directional information and average distance value of the detected anomaly.

The magnitude of the distance, d from the sensor to the vicinity of the anomaly depends on whether the highlighted anomaly is due to a missing object or the appearance of an additional object. The actual distance measurement resulting

from a missing object is longer than the distance measurement of the normal neuron (see Figure 4.3). In contrast, the appearance of an additional object makes the actual distance measurement less than the distance in the normal neuron. Because of this, the estimated distance (d) to the anomaly can be determined by Equation (4.1). From the equation, d_i is the average laser distance of the sector which has the highest dissimilarity during novelty inspection and d_n is the average laser distance of the same sector if the laser measurement is taken during the normal condition.

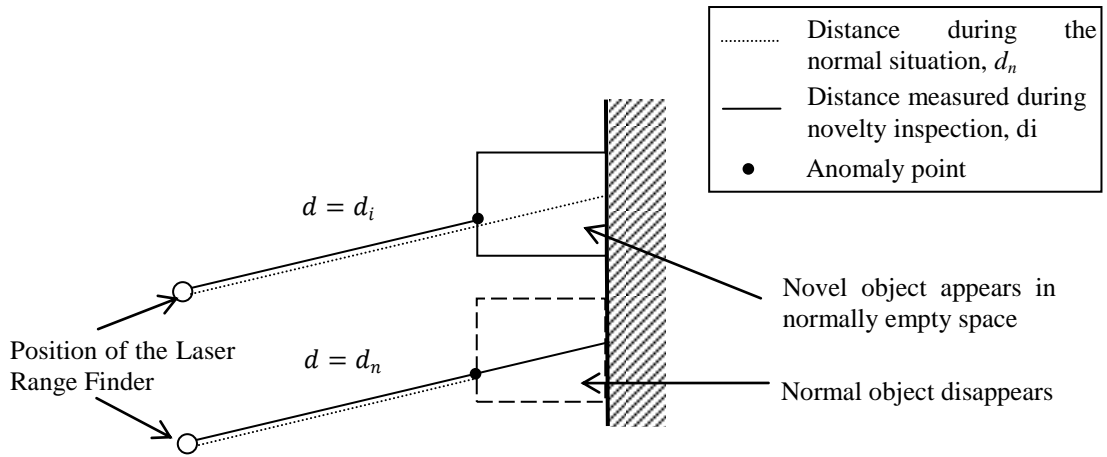


Figure 4.3: The magnitude of the vector \bar{d} , depends on the relation between the average value of the laser measurements taken during inspection d_i and during the normal situation, d_n .

$$d = \begin{cases} d_i, & d_i < d_n \\ d_n, & d_i > d_n \end{cases} \quad (4.1)$$

As mentioned before, the direction of the anomaly with respect to the sensor heading θ_l is denoted by β . By using the direction and distance to the anomaly, the anomaly point location (x_{ap}, y_{ap}) can be determined using Equation (4.2) and Equation (4.3) where (x_l, y_l) is the position of the laser range finder.

$$x_{ap} = x_l + d \sin(\beta) \quad (4.2)$$

$$y_{ap} = y_l + d \cos(\beta) \quad (4.3)$$

The Accuracy of the Anomaly Point

The accuracy of the anomaly point represents how close the estimated position of the object surface is to the actual surface. The accuracy is only as good as how well the average value represents the actual laser measurements in a sector. This is affected by the difference between the laser measurements changed by the anomaly and the value of the unaffected laser measurements. Another factor that affects its accuracy is the number of laser measurements in a sector that scan the surface of the anomalous object.

A test was conducted to investigate the relationship between measurements in a sector and the accuracy of the calculated anomaly point. An object was positioned so that half of the laser measurements in a sector were affected while the rest registered a fixed maximum range. The object's distance to the laser was varied so that the difference between the laser measurements of the object and the unaffected laser measurements also varied. The anomaly point is always assumed to be positioned in the center of the sector. The results in Figure 4.4 and Figure 4.5 show that when all the measurements in a sector are almost the same value, the average gives a fair representation of the actual distance. However, when the difference between them increases, the accuracy of the calculated anomaly point decreases.

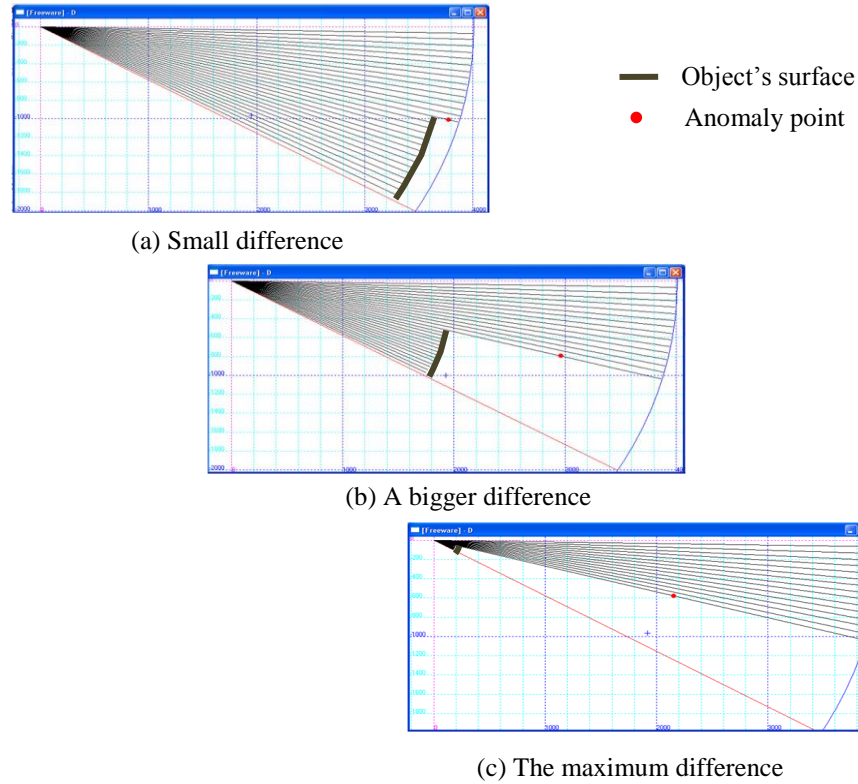


Figure 4.4: Examples of the resulting anomaly points as the position of the anomaly surface was varied.

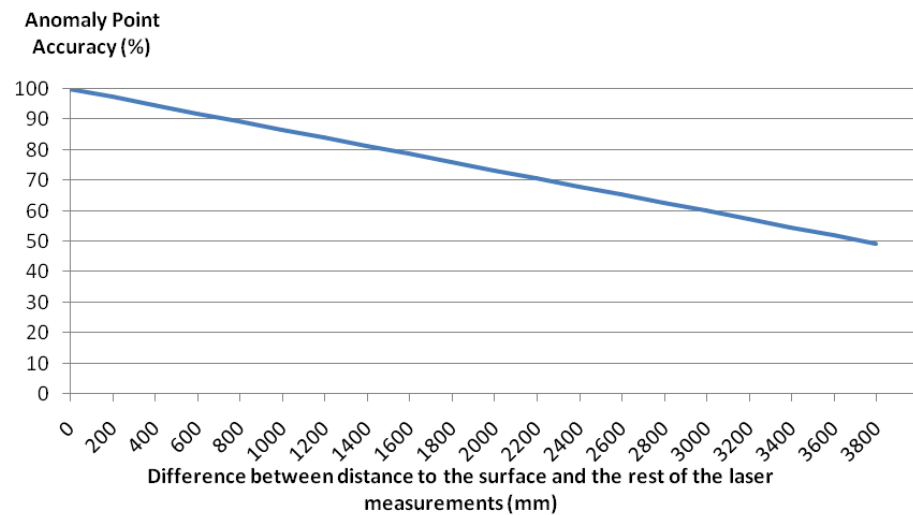


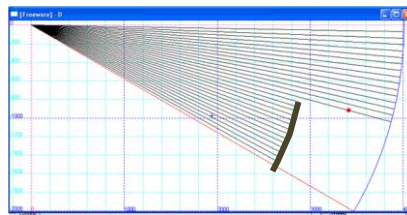
Figure 4.5: The accuracy of the anomaly point decreases when the difference between distance to the surface and the rest of the laser scan increases.

The accuracy of the anomaly point also depends on the number of affected laser scans in a sector. A test was conducted to see the effect of changing the number of affected laser measurements on the accuracy of the anomaly point. A surface was positioned at a fixed distance of 3000mm from the sensor. The number of affected laser scans was increased gradually from none to the total number of scans. The results are shown in Figure 4.6 and Figure 4.7. As expected, the accuracy of the anomaly point increases the higher the number of affected laser scans in a sector.

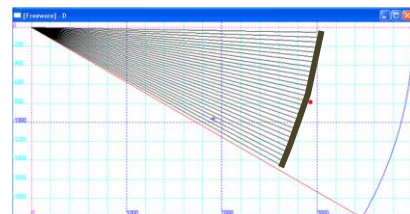
Several conclusions can be made from the results of the tests. One of them is that the positioning of the surface of the anomalous object in the sector influences the accuracy of the anomaly point. The best position would be when the surface affects all laser scans in a section. If this is not the case, then the accuracy is better if the difference between the distance to the surface and the laser scans that are not affected by the surface is minimized. One example of this kind of situation would be when the anomalous object is positioned near a permanent fixture such as wall.



(a) A few are affected



(b) Half the number affected



(c) All laser scans are affected

Figure 4.6: Examples of anomaly points when the number of laser scans affected by the object is varied.

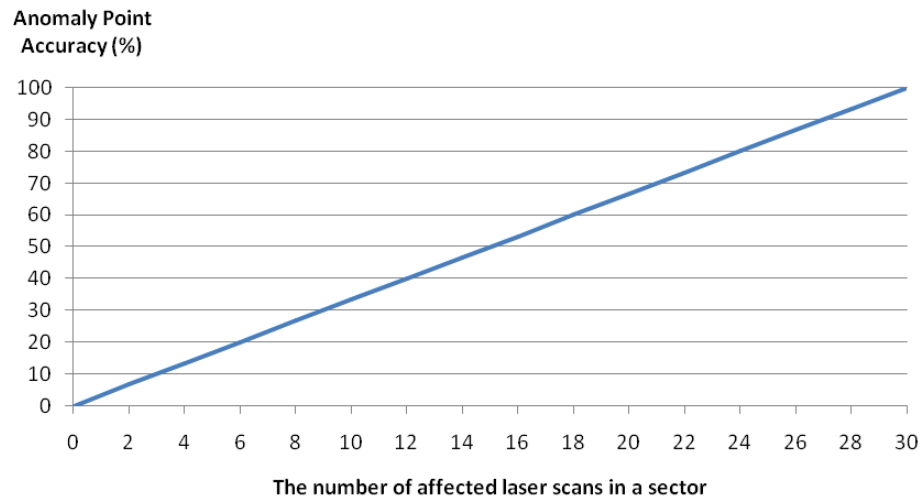


Figure 4.7: The accuracy of the estimated position of an anomaly point increases when the number of affected laser scans in a sector increases.

Anomaly Points During Actual Detection

The shape of the surface of an object also influences the outcome of the averaging. In practice, it is not possible to determine the shape of the anomalous object before it is detected. However, it can be generalized into three categories: concave, neutral or convex shapes. As depicted in Figure 4.8, the resulting anomaly point for a concave shape is positioned at the front of the object. In contrast, the anomaly point for a convex shape is positioned behind the object surface. The only case where the anomaly point coincides with the object surface is when the shape of the object is neutral which means its surface is parallel to the sector's arc. Out of the three shapes, most objects found in the man-made environment have a convex shape such as rectangular boxes and circular rubbish bins.

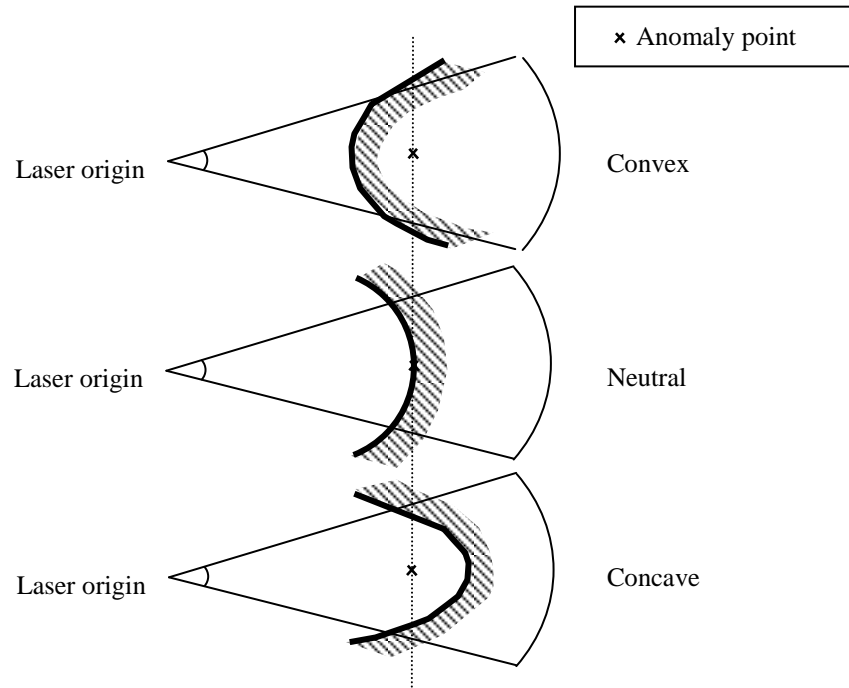


Figure 4.8: Convex, neutral and concave surfaces detected within a sector of a laser range finder scan.

Another practical aspect in determining the anomaly points is that the robot inspection route influences how an anomalous object is perceived. In most situations, it is assumed that the robot will move passed the object, with the opportunity to take measurement from different angles and distances. Note that by changing the sensor's perception angle, the accuracy of the anomaly points actually changes because of the variation of the number of affected laser scans and the difference in distance between the affected and unaffected laser scans in a sector. For this reason, in order to see the effect of the averaging of the laser measurements for a convex shape, an experiment was conducted in a simulated environment by placing a $400 \times 800 \text{ mm}^2$ rectangular shaped object at different positions along a 2400mm wide corridor (see Figure 4.9). The simulation then produced sensor measurements that would have resulted as the robot moved past the object. The objectives of the experiment were:

1. To see the relationship between the positioning of a convex object in a laser sector and the resulting average value of the laser measurement in the sector.

2. To see the relationship between the sensor's perception angle and the anomaly points.

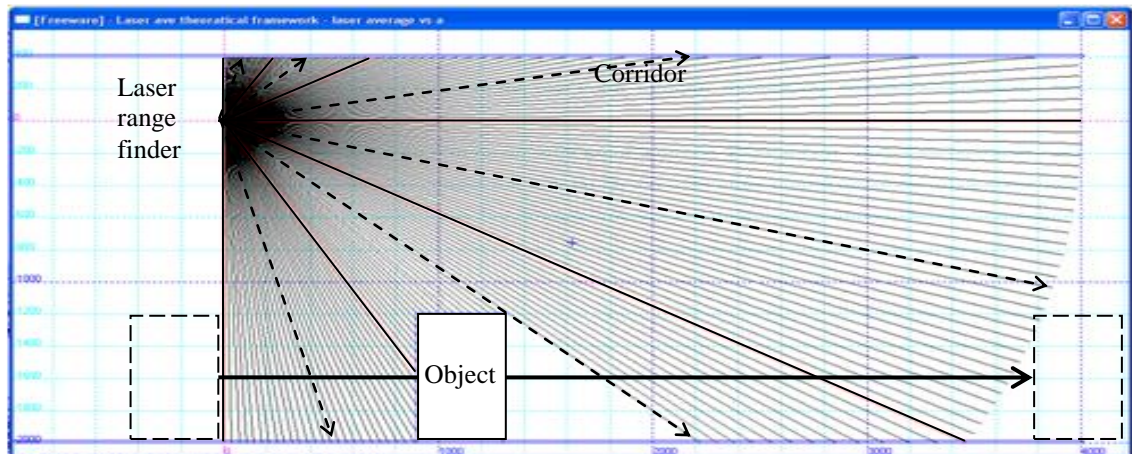


Figure 4.9: Test environment for investigating the difference between the average of laser measurements within a sector and the actual measurement at the center of the sector. A rectangular shaped object is shifted 10mm at a time along the bold line shown in the figure.

The average value of laser measurements in a sector is projected at the average angle of the laser beams in the sector (the center of the sector). This value is compared with the actual value of the laser measurement at the center of the sector. As depicted in Figure 4.10, the results show that the detection of the convex surface of a rectangular box produced an average laser measurement that was further than the actual distance. It can be seen that the average value of a sector is maximized when the object lies fully within the sector. With respect to the perception angle, the difference between the average and the actual distances depends on the angle of view of the laser and this ranges between 200 mm to 600 mm.

Figure 4.11 shows an example of the results of detection of a rectangle box. It can be seen how averaging of the laser measurements and the angle of perception affects the position of the anomaly point. As shown by the results, the detection of convex surfaces that are commonly found in a typical man-made environment produces anomaly points that are distributed beyond the surface of the object.

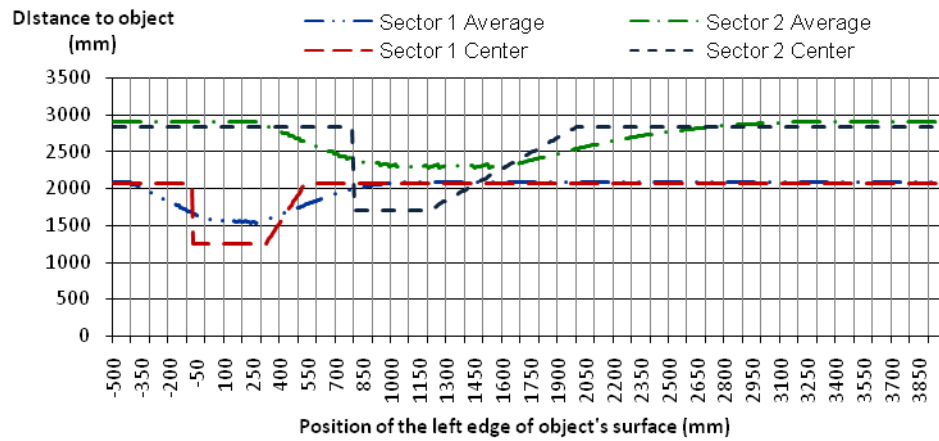


Figure 4.10: Comparison between the average laser measurement in two neighboring sectors and the actual laser measurement at the center of each sector.

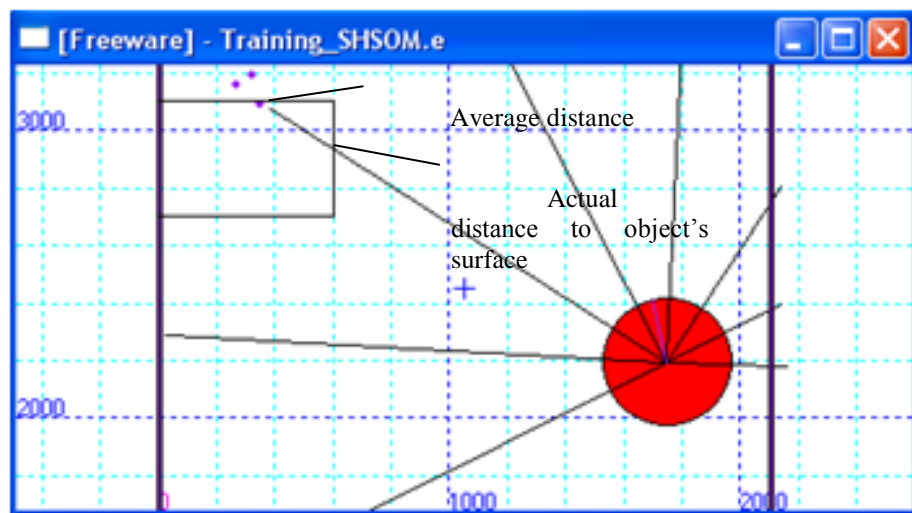


Figure 4.11: Results of anomaly detection from three inspection steps. The lines coming out from the robot show the average value of laser measurements within the respective sectors. The angle of each line is positioned at the center of each sector. The average distance is longer than the actual distance to the object.

4.4.2 Modeling the Distribution of Laser Range Finder Anomaly Points

Since the laser range finder provides a lot of useful information and because it is also the main sensor used in this project, it is important to study the distribution of anomaly points derived from the laser data. For this reason, a model of the distribution of anomaly points is described in this section. The model is developed to gain a thorough understanding of the distribution of anomaly points as well as its use for simulation work.

To predict the outcome of the detection of an unknown convex shaped object, the distribution of anomaly points is modeled using points on the perimeter of an ellipse. The reason why an ellipse was chosen is that its shape can approximate the shape of many typical objects found in the robot's environment such as rectangular boxes, indoor plants, circular bins and uneven shaped bags. The equations of the ellipse perimeter points are given by Equation (4.4) and Equation (4.5), where a and b are the semimajor and semiminor axes, μ denotes the mean of x , ν is the mean of y , θ is the major axis angle and α is restricted to the interval of $-\pi \leq \alpha \leq \pi$. The term ε_{ave} denotes the offset due to averaging.

$$x = \mu + a \cos(\alpha) \cos(\theta) - b \sin(\alpha) \sin(\theta) + \varepsilon_{ave} \quad (4.4)$$

$$y = \nu + b \sin(\alpha) \cos(\theta) + a \cos(\alpha) \sin(\theta) + \varepsilon_{ave} \quad (4.5)$$

To clarify the idea, if the robot observes the object from all sides, the resulting anomaly points will approximate the ellipse perimeter points shown in Figure 4.12. As can be seen from this figure, the mean of the ellipse points equates to the center of the anomalous object. The major and the minor axes are approximated using the length and the width of the object. If the object is observed only from a certain angle, only the corresponding ellipse points will be highlighted. The angle over which the object is observed is called the observation span, α .

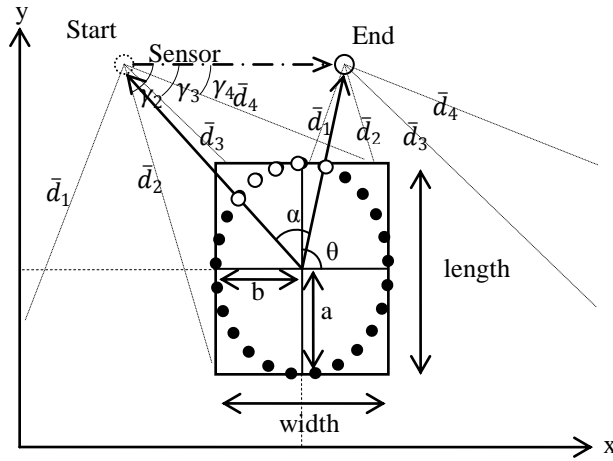


Figure 4.12: Anomaly point model of a rectangle shaped anomalous object.

Observation span, α is modeled as the angle between two vectors which have the same origin located at the center of the object (see Equation (4.6)). The first vector points to the position of the sensor location when the anomaly was first detected and the second vector points to the last position where the anomaly was detected. Only the points which are positioned within the span, $\varphi_A \leq \alpha \leq \varphi_B$ are considered as anomaly points (drawn as the hollow circles in Figure 4.12), where φ_A and φ_B are the angles of vectors A and B.

$$\alpha = \cos^{-1} \left(\frac{A \cdot B}{|A||B|} \right) \quad (4.6)$$

The last parameter for the model is the averaging error, ε_{ave} . The averaging error is the error resulting from averaging sensor measurements in a sector. As discussed earlier, the value of ε_{ave} depends on the shape of the object and the angle of perception of the sensor. Given that the difference between the average and the actual distance to the object surface is denoted by ε_{z_ave} , the averaging error in the x direction, ε_{x_ave} and the averaging error in the y direction, ε_{y_ave} are given by Equation (4.7) and Equation (4.8). The term γ is the angle of the projection of the vector, \vec{d} to the individual ellipse perimeter point or namely the perception angle.

The value of γ depends on the pose of the laser range finder with respect to the detected object. Given that we know the inspection route of the robot, the vector can be estimated (see Figure 4.12) from which the sector with the highest dissimilarity should be used to find γ . As an example, Figure 4.12 shows the position of the sensor at the start and the end of the robot inspection route. At the start and the end positions, the anomaly points should be determined from vector \bar{d}_3 and vector \bar{d}_1 respectively. In between the start and the end positions, the anomaly points should be determined from vector \bar{d}_2 .

$$\varepsilon_{x_ave} = \varepsilon_{z_ave} \cos \gamma \quad (4.7)$$

$$\varepsilon_{y_ave} = \varepsilon_{z_ave} \sin \gamma \quad (4.8)$$

Table 4.1 presents a guide for systematically determining the input parameters for estimating the value of the perception angle and the averaging effect for a given observation span. Similar to the example from Figure 4.12, the observation span is divided into smaller spans. Then in each smaller span, the perception angles that will affect the span are determined together with their respective averaging effects. The value of the averaging effect is approximated from the result of the test presented in the previous section, where a narrower perception angle should have smaller ε_{z_ave} . A span can be influenced by more than one perception angle. If this happens, the averaging effect should be distributed equally among the respective ellipse perimeter points within the span.

Table 4.1: A guide to determine the input parameter for estimating the distribution of the anomaly points.

Observation Span, α	Perception angle, γ	Averaging effect, ε_{z_ave}
angle_min < α < angle_a	Angle of \bar{d}_3	$\sim \bar{d}_{3_ave} - \bar{d}_{3_act} $
angle_a < α < angle_b	Angle of \bar{d}_2	$\sim \bar{d}_{2_ave} - \bar{d}_{2_act} $
angle_b < α < angle_max	Angle of \bar{d}_1	$\sim \bar{d}_{1_ave} - \bar{d}_{1_act} $

In order to validate the anomaly point distribution model, the results of repetitive observations from the actual environment (the same environment as the one shown in Figure 4.11) are compared with the prediction from the model. The covariance of the distribution of both anomaly points for three different observation angles is presented in Table 4.2. The results show that the model has similar statistical attributes when compared with the actual distribution.

Table 4.2: The comparison between the distribution of the anomaly points from the model and from the actual detection for 3 different cases of observation span.

	Anomaly points distribution					
	Case1: $330 < \alpha < 60$		Case2: $300 < \alpha < 60$		Case3: $290 < \alpha < 70$	
Robot motion	Upward direction		Downward direction		Bi direction	
Param.	Actual	Model	Actual	Model	Actual	Model
Mean x	381.2	361.8	355.1	360.0	383.0	338.8
Mean y	2999.2	2976.5	2840.0	2839.5	2933.6	2882.7
Std. dev x	57.8	36.6	42.4	38.5	61.8	48.2
Std. dev y	152.2	138.1	231.8	160.7	211.1	216.3
Corr xy	-0.75	-0.85	0.84	0.35	0.19	-0.315

As depicted in Figure 4.13, the ellipses produced using the distribution of both the actual and the model anomaly points have approximately the same shapes and orientations. This shows that the model can approximately represent the actual distribution of anomaly points.

Figure 4.13 shows that the distribution of anomaly points improves with increased observation span and more variation of the robot pose (robot perceives the anomaly while travelling in both upward and downward directions). However, the spread of the anomaly points from observation by the robot as it travels in both directions is similar to observation from one direction. This suggests that the latter strategy is sufficient when only information about the spread of the data is needed. These findings are vital for assisting the proposed path planning strategy for close range inspection since path planning relies on the distribution of anomaly points. It is

also important for determining the appropriate threshold value for clustering the anomaly points.

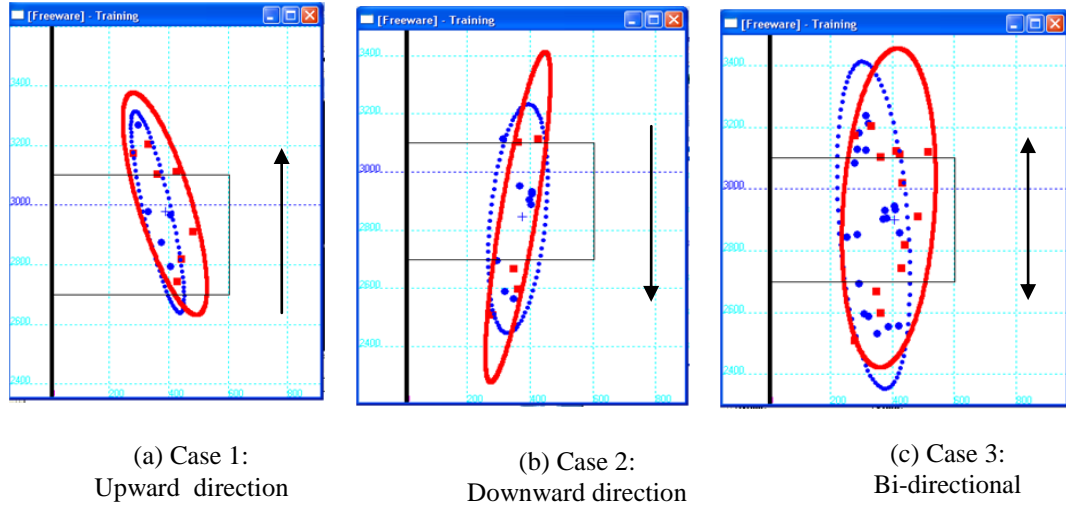


Figure 4.13: Comparison of ellipses generated using the model and actual distributions when the robot is moving in different directions. The model data is presented using the blue circular dots and dashed ellipses. Experimental data is indicated with red dots and solid red ellipses.

4.4.3 Anomaly Points using Data from Other Types of Sensors

For directional sensors such as the laser range finder described in the previous section, it is obvious that the anomaly points refer to the position of the detected anomaly. However for many ambient quantities being measured such as temperature and air velocity, the measurements do not return any direction information that can be used to identify the position of the source of the novelty. In these cases, one of the approaches that will benefit from repetitive observation is to identify the position of the sensor itself when it detects anomalous measurements. Thus for these types of sensors, their anomaly points are the position of the sensor when it detects anomalous measurements. Since the position of all sensors that belong to this category can be assumed to be at the center of the robot, the sensor position is the same as the robot position.

4.5 Clustering Anomaly Points

Clustering is the process of partitioning a dataset into subsets or groups without having a prior knowledge of the appropriate way of grouping the samples in the dataset [60]. In this project, clustering is used to group estimated anomaly detection points based on their spatial separation. The discussion in this section focuses on the clustering of anomaly points resulting from novelty detection using laser range finders.

Each anomaly point is detected during a different inspection cycle i.e. at a different time and robot pose. If an anomalous object is static, the robot should observe it positioned at approximately the same location, during successive inspection cycles, as long as the anomaly is within the detection range of the sensor. The following are the characteristics of the anomaly points derived from laser measurement data that are being considered. Their characteristics affect the design of the clustering method:

1. Clustering needs to be applied while the surveillance task is performed as the robot might need to take immediate action on the detected anomaly. This means that it needs to be done even before all anomaly points are present. This implies that the clustering must be done on-line. The method must allow the creation of new clusters if the data warrants it.
2. An anomaly point represents the estimated position of the surface of a detected object. Thus the distribution of anomaly points depends on the shape of the surface of the object (see Figure 4.14).

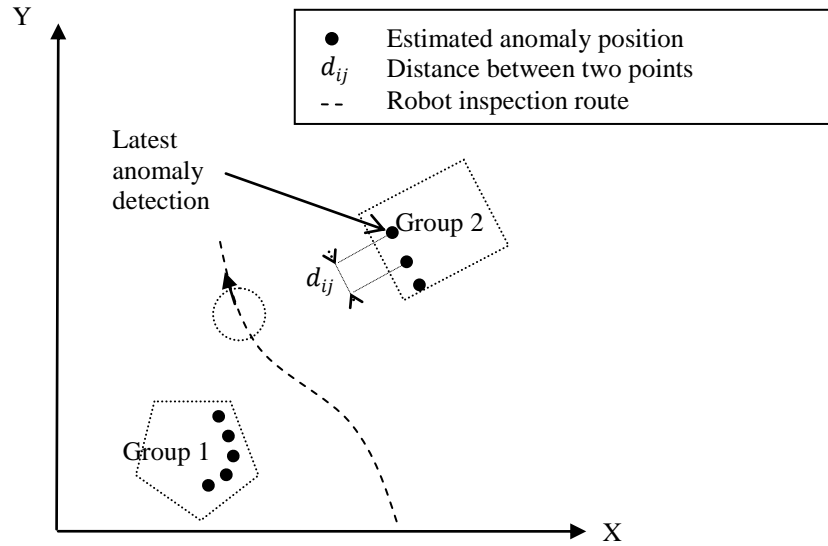


Figure 4.14: The robot observes anomalies from different positions on its route using a laser range finder. The distribution of the anomaly points approximates the shape of the surface of the object.

4.5.1 Similarity Measures

This section describes the approach to partitioning a set of samples into clusters. As mentioned before, the distribution of anomaly points depends upon the shape of the surface of the object. For this reason, an on-line clustering technique to group anomaly points based on the distance from the latest point to any existing group member d_{ij} (see Figure 4.14) was developed. The minimum neighbor distance parameter, d_{max} determines the maximum allowable distance between group members. The choice of d_{max} is very important. If the value is too small all anomaly points will be allocated to isolated clusters. If the value is too large, all points will be grouped into a single cluster.

The minimum value of d_{max} could be based on the robot inspection step size. This is especially true for sensors where anomaly points are based on the sensor or the robot position. For anomaly points generated by the laser range finder, assuming that the surface of the object has no sudden changes in depth, then the distance between neighboring anomaly points should be of the same order as the inspection

robot step size. However, in practice anomaly point observation from different perception angles can result in uneven distribution. This means that the distance between the neighboring anomaly points could be larger than the robot inspection step size.

The distance between the anomaly points is measured using the Euclidean distance. The choice of Euclidean distance as a similarity measure is appropriate as the feature space (x and y dimension) is isotropic and data are expected to spread evenly in all directions. The Euclidean distance measure is given by Equation (4.9) where x_i, y_i and x_j, y_j are two anomaly points in a 2-d Cartesian space and d_{ij} is the Euclidean distance between them.

$$d_{ij} = \sqrt{(x_i - x_j)^2 + (y_i - y_j)^2} \quad (4.9)$$

Algorithm 4.1 summarizes the clustering procedure.

Algorithm 4.1: Clustering algorithm.

Notation:

d_{ij_new} - Spatial distance between a new anomaly point and an anomaly point in existing groups

d_{max} - Maximum allowable spatial distance between anomaly points in the same group

Initialization:

Membership = 0

Procedure:

```

1:   Get new anomaly point
2:   For all groups
3:     For all anomaly points in the group
4:       If (  $d_{ij\_new} < d_{max}$  )
5:         Join group (new anomaly point)
6:         Membership = 1
7:         Break

```

```

8:      EndIf
9:      EndFor
10: EndFor
11: If ( Membership = 0 )
12:     Create_new_group (latest_detection_position)
13: End

```

4.5.2 Challenges of On-line Clustering

The on-line clustering technique uses a threshold i.e. the minimum neighbor distance parameter, d_{max} for the creation of a new cluster. The drawback of this approach is that it depends on the order of data presentation. There is a possibility that a new cluster is created based on an anomaly point that eventually turns out to be near to a point in an available cluster (see the example illustrated in Figure 4.15).

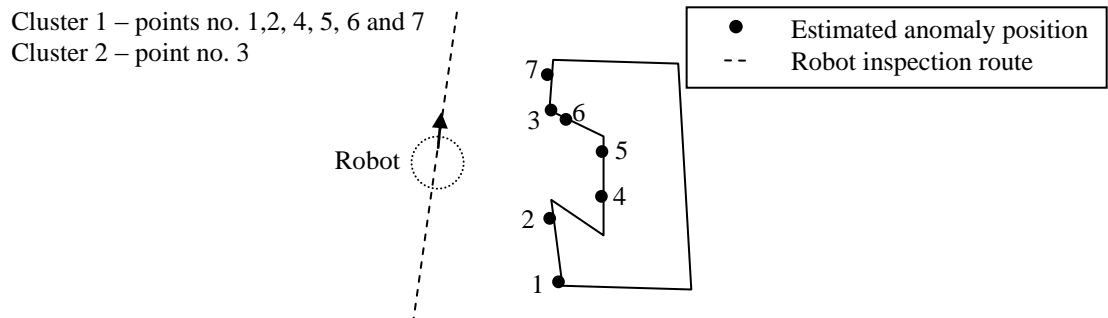


Figure 4.15: An example of the drawback of using the distance threshold for creation of a new cluster. Ideally, point no. 3 should be grouped into the first cluster. The numbering represents the order of data presentation.

One solution to this problem is that during each iteration, the algorithm merges two clusters if the distance between an anomaly point in one cluster and another anomaly point in another cluster is below the threshold as given by Algorithm 4.2.

Algorithm 4.2: Combining nearby groups.

Notation:

d_{max} - Maximum allowable spatial distance between anomaly points in the same group

d_{ij_group} - Spatial distance between an anomaly point in one group and another anomaly point in a different group

Procedure:

```

1:   For all groups
2:       For_all_anomaly_points_in_a_group
3:           If (  $d_{ij\_group} < d_{max}$  )
4:               Combine_groups (groups which the two
                    anomaly points belong to)
5:           EndIf
6:       EndFor
7:   EndFor

```

Algorithm 4.2 involves exhaustive search which is not an ideal solution especially if the size of the dataset is large. Fortunately, in the discussion in the following chapters, it can be seen that based on experience, the effect of the dependency on order of data presentation on on-line clustering is negligible especially for the specific applications developed for this project. For this reason, the above algorithm is not an absolute necessity. However, the improvement of the method would still be worthwhile.

4.6 Discussion and Conclusions

This chapter draws together the key considerations involved in the quantification of anomaly point distribution especially for the laser range finder. The anomaly point distribution model is presented to identify parameters which affect the distribution of the anomaly points. The anomaly point model takes the form of points on the perimeter of an ellipse so they could represent the surface of common 2D shapes in the environment. An on-line clustering method is also introduced together with important implementation issues relating to the appropriate clustering threshold and the order of data presentation. Clustering is used to group together anomaly points based on their distance to each other. The next chapters ventures into the application

of the repetitive observation strategy in filtering false positives and in providing information to perform close range inspection.

Chapter 5

False Positive Filter

This chapter examines the task of reducing the number of false positives in the novelty detection results. First an overview of related work in the field is given followed by an overall description of the proposed system. Then a detail description of the false positive filter and experimental results are presented followed by some discussion and conclusions.

5.1 Introduction

Novelty detection procedures can suffer from two kinds of errors: missed detection when novelty is not highlighted and when measurements are erroneously considered novel when a situation is normal. The work described in this chapter tries to overcome the latter problem, which is also called false positive detection.

False positives could create unnecessary alarm and waste energy and time. For an autonomous surveillance mobile robot, this could mean wasting its own resources by performing further investigation of a false alarm. Also, by focusing its attention towards the false alarm, the time that should be spent covering other areas is sacrificed and hence this reduces the productivity of the surveillance robot. The robot would also send a false alarm to its human controllers and thus waste their time also. To make the situation worse, if the false alarm occurs too often, the warning message would lose its urgency and when a true alarm is received, the human controller would delay in taking the necessary action.

Motivated by this, the work in this chapter is dedicated to reducing the number of false positives in novelty detection performed by autonomous mobile surveillance robots. The method benefits from the ability of the surveillance system to move and make repeated observations from different locations. The positions of the detected anomalies are identified and the distribution of these positions is used to identify false positives.

The rest of this chapter is organized as follows. Section 5.2 describes related work which is followed by an overview of the system in Section 5.3. The criteria used to filter false positive detections are discussed in Section 5.4. Section 5.5 gives experimental results. The chapter closes with the discussions and conclusions given in Section 5.6.

5.2 Related Work

Other researchers have investigated ways to reduce false positive detection. Usually, the problem is tackled at the machine learning level [2, 11, 75-78]. One of the common approaches is applied during detection. Performance of the novelty detection process is optimized by tuning the threshold (i.e. the sensitivity) used to classify the input pattern. The tradeoff between having high and low sensitivity is as follows. If the system's sensitivity is low, it will have difficulty detecting anomalies but if the system is too sensitive, it will make a lot of false positive detections.

For this reason an external filter has the advantage that it can improve the performance of the novelty detection mechanism regardless of its sensitivity settings. External filters work by further analyzing the results of the novelty detection to identify false detection. In [79] the residual optic flow measure was used to remove false positive detection of an anomalous person using data from a camera on a moving mobile robot. Sequences of images of a moving human have a higher value of residual optic flow measure than stationary objects (due to local optic flow caused by the limbs which move somewhat independently of the rest of the human body). Thus objects which were miss-identified as a person were filtered out based on their

low optic flow error rate. Similarly, in a fiber detection application in medical imaging [80], additional tests were applied to detected fibers to reduce the false positive rate. The tests use unique characteristics of the fibers to identify them. In these examples, the target object to be detected is known (i.e. a moving human and a tissue fiber) thus their characteristics could be identified in advanced.

In a slightly different application [81, 82], a filter was used not to reduce false positives but to remove corrupted laser measurements caused by dynamic objects when performing Markov localization. Since the work uses a similar sensor to the one used in this project (i.e. the laser range finder), it is appropriate to mention the work here. The robot filters out moving objects by categorizing sensor readings into two groups; one which contains readings that are assumed to originate from people (corrupted), and one which is assumed to correspond to static obstacles in the map (authentic). Given the robot pose, the robot uses a novelty detection mechanism to identify which of the laser readings do not match the expected values of the laser measurements at that pose.

In conclusion, as suggested in [57], the most suitable approach to reducing false positives for any system very much depends on the particular application. For example, for the work described here, the target object to be detected is unknown and thus this limits the characteristics that can be used to identify a true detection. Also the strategy proposed in this chapter requires active observation from different viewpoints and thus needs the ability to move sensors to different positions. Mobile robots have this capability hence making the strategy suitable for mobile robot applications.

5.3 System Overview

Figure 5.1 shows an overview of the false positive filter. The repetitive observation strategy provides information of the size of each anomaly point group. False positive filtering then uses this information to filter the false positive detections based on the number of anomaly points that each group contains.

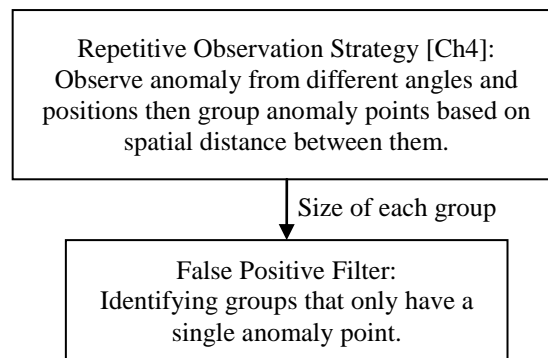


Figure 5.1: The system for filtering false positives.

5.4 Filtering false positive detections

Attributes of false positive detections

The nature of the application in hand (i.e. novelty detection) makes it unlikely to have any prior knowledge of the anomalies to be detected. Thus for the external filter to work it needs to make use of general properties that are common for most anomalies. In this case, the problem of anomaly detection is confined to the problem of detecting static sources of novelty. An attribute that is true for any static source of novelty is that repeated observations of the anomaly should point to approximately the same location in space.

In contrast, false positive detections should point to random locations. Thus over repeated observations, the distribution of the estimated position of the source of novelty (anomaly points) for false positives should be low in number and the anomaly points should be positioned in isolation. This is especially true if the false positive is caused by random errors which are due to random and inherently unpredictable fluctuations in the measurement apparatus or the system being studied.

This characteristic is the determining factor used by the false positive filter introduced in this chapter. Figure 5.2 shows an example of the expected results of novelty detection using a laser range finder. The robot pauses at regular intervals on its inspection route to scan and compare the input measurements with the

prerecorded normal measurements. As can be seen, it is expected that the presence of an anomalous object would result in several anomaly points positioned close to each other unlike a single anomaly point caused by false positive detection.

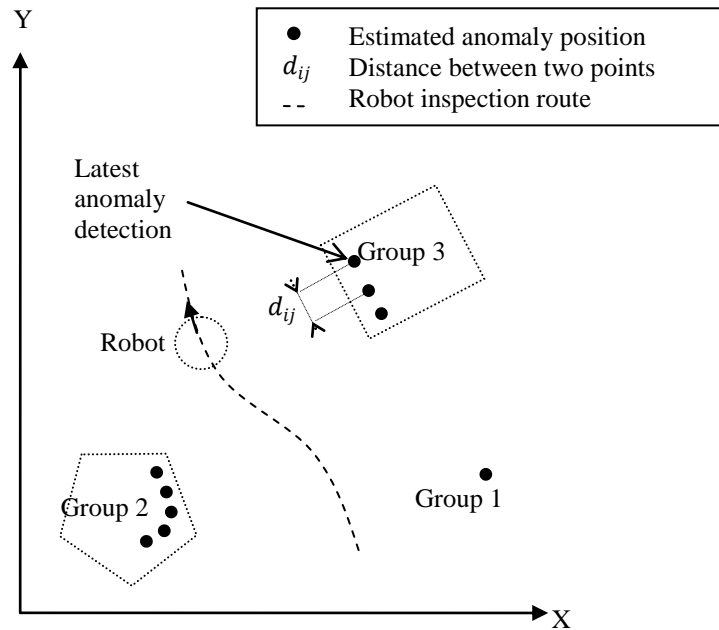


Figure 5.2: The robot observes anomalies from different positions on its route using a laser range finder. The single anomaly point that forms Group 1 is from a false positive detection.

Filtering Process

As depicted in Figure 5.1, the process of false positive filtering begins with repetitive observation by a mobile robot. The robot moves on its inspection route and pauses at regular intervals to take sensor measurements. Novelty detection is performed where the sensor measurements are compared with the prerecorded normal measurements. In this project, the robot employs the Habituating Self Organizing Map novelty filter and maps normal sensor measurements using the flexible region map. However, as the false positive filter works externally, in practice any type of novelty detection mechanism or mapping technique could work with the filter. Then, for any detected anomalies, the estimated position (i.e. anomaly point) is determined if possible. If it is not possible to locate the anomaly point then the position of the sensor, which is usually the same as the robot position, is used instead. On-line clustering is used to group the anomaly points based on their distance to their nearest neighbor.

The repetitive observation strategy (ROS) is followed by the false positive filter. This filter uses information regarding the size of each cluster provided by ROS. Based on the assumption that anomaly points caused by false positive detections are positioned in isolation, any singleton cluster is then filtered out and is regarded as a false positive. It can be seen in the results of experiments presented in the following section that clusters which have 2 or less and 3 or less members could also indicate a false detection, depending of the threshold used to cluster the anomaly points.

Consideration for On-line Clustering

Basically, if a group contains only one anomaly point (i.e. a singleton cluster) then it is labeled as a false positive detection. During inspection the robot makes repetitive observations by following its planned route and taking measurement at regular intervals. However, as the clustering is performed on-line, the size of a group also changes over time. Any group will naturally start having one member and will eventually grow to its final size. In order to avoid these groups being filtered out before they get to their final size, filtering is only applicable to areas which are already beyond the working range of the sensor as shown in Figure 5.3.

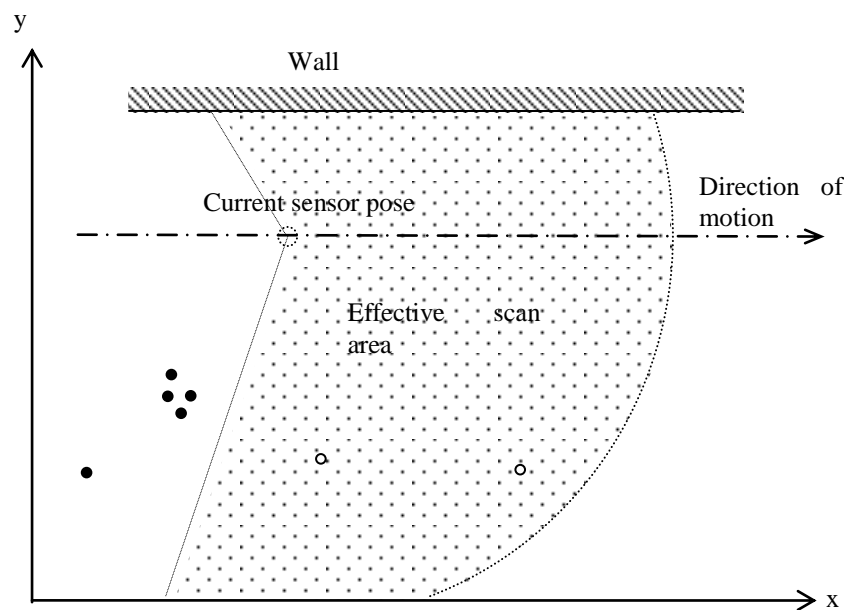


Figure 5.3: The filter is only applicable to groups of anomaly points that are already out of the working range of the laser range finder (shown using the black dots). The white dots are anomaly points which are still within the working range of the sensor.

5.5 Experiments

Objectives

The experiments were conducted in a corridor environment in Building 36, Monash University (Clayton campus). During the training and inspection period, the robot navigated using a wall following behavior and corrected its position using particle filter localization. A real corridor environment was used to challenge the robot with real world data so that a significant number of false positives detections would be detected.

The objectives of the experiments were:

1. To visually observe the result of repetitive observation and singleton cluster filtering.
2. To compare the performance of novelty detection when using and not using the singleton cluster filter.
3. To compare the performance of the singleton cluster filter with filters that are based on clusters with up to 2 and up to 3 members.
4. To see the effect of changing the maximum neighbor distance parameter, d_{max} on the performance of novelty detection with the singleton cluster filter.
5. To observe the results of novelty detection with singleton cluster filtering when using other types of sensors.

Procedures

Firstly, the robot was trained to learn normal sensor measurements in its environment. The sensor measurements were the 8 values of the average distance

measurement from the laser range finder as describe in Chapter 4 as well as measurements from other sensors including an anemometer and an ambient light sensor. As depicted in Figure 5.4, the robot navigated autonomously from point A to point B using a wall following algorithm. While travelling between the two points, it took distance measurements using its laser range finder and recorded its heading and current position at each 100mm step. All of the measurements were logged. The process was repeated five times during the period that the environment was considered to be in its normal state. The process was also repeated several times while part of the environment was changed and therefore unusual. The environment settings during the normal and unusual situations are summarized in Table 5.1.

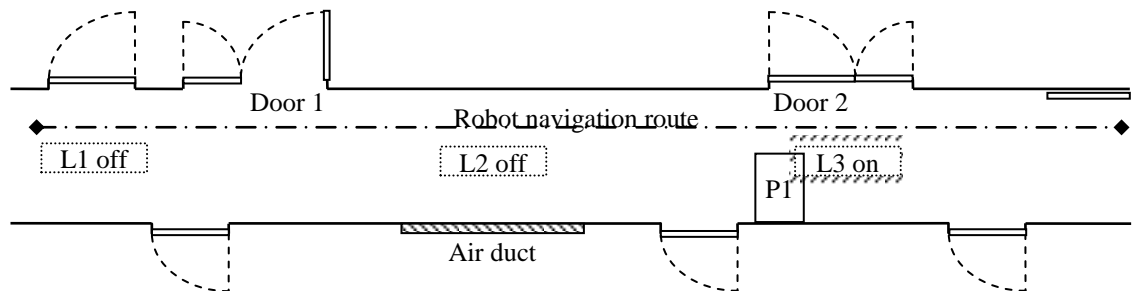


Figure 5.4: State of the robot's environment in its normal state. Door D1 was normally both closed and open while door D2 was always closed. Rectangular box labeled P1 represents the approximate position of the rubbish bin which was introduced during the experiment.

Table 5.1: Environmental settings during the experiments.

		Situation	
		Normal	Unusual
States	Object		
	Door 1, D1	Closed or Open	Open
	Door 2, D2	Closed	Open
	Rubbish bin	Missing	At P1
	Lighting	L1, L2 = off, L3 = on	L1, L2 = on, L3 = off
	Air ventilation	Off	On

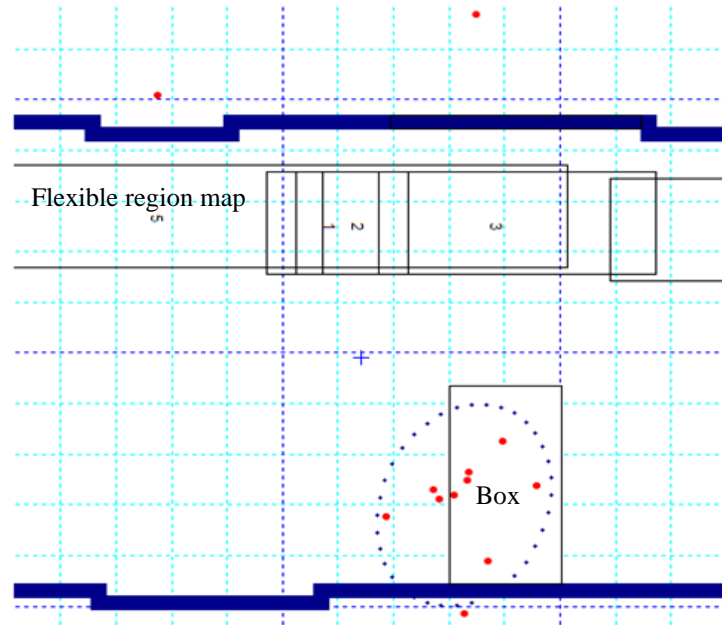
The logged training data gathered from the normal environment was used to train the HSOM network offline by following the training process described in

Chapter 2. Then, the anomaly estimation algorithm was tested using the logged data from the changed environment which represented environmental settings that were either normal or unusual. For easy visualization, the distributions of anomaly points are represented using covariance ellipses. The number of anomaly points that are highlighted as a true anomaly or a false positive was counted for the different situations listed in Table 5.1. Then the true positive rate, TPR , the false positive rate, FPR and the false negative rate, FNR were calculated using the method describe in Section Chapter 2.

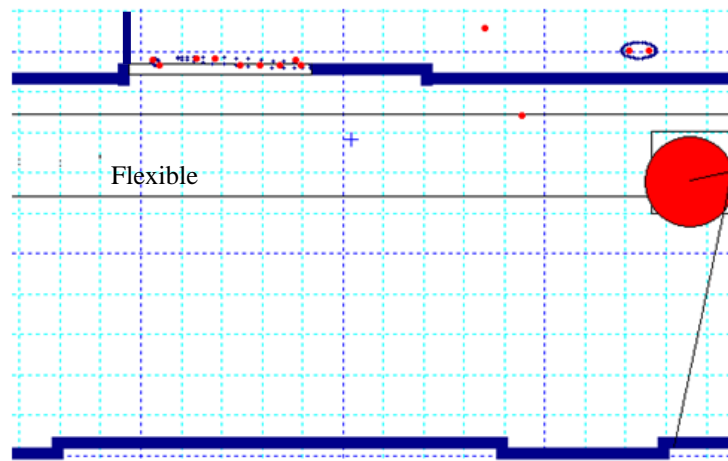
The experiments were repeated with different values of maximum neighbor distance parameter d_{max} (see Chapter 4) and different sensitivity settings for the novelty detection mechanism which was achieved by changing the similarity threshold value, S_T . The maximum distance parameter determines the size of a cluster. The performance of the novelty detection mechanism is analyzed using Receiver Operating Characteristic (ROC) analysis [83].

Visual observations

As can be seen in Figure 5.5, the estimated anomaly points that are enclosed by an ellipse are assumed to represent a true anomaly, based on the singleton cluster filter. Singleton clusters (anomaly points which have no neighbors) are categorized as false anomalies. In Figure 5.5 (b), a group consisting of 2 anomaly points was created. They are false positive detections but were recognized as true anomalies.



(a) A normally empty space is occupied by a box.



(b) A normally closed door is open during inspection.

Figure 5.5: Examples of detection results using the Singleton Cluster Filter. The clustering process groups nearby estimated anomaly points (the red dots) and represents the groups visually using ellipses. Note that in (a), some of the estimated anomaly points appear to be on the far side of the wall and others inside the box. This is mainly due to the fact that the laser measurements are taken as average readings.

Receiver Operating Characteristic Curve

An ROC graph depicts the tradeoff between detecting true positives and false positives when changing the sensitivity settings of the system [83]. Sensitivity is defined as the number of true positives over the total number of true positives and false negatives. The sensitivity of a novelty detection mechanism can be tuned by changing the value of the similarity threshold, S_T . The similarity threshold determines the maximum allowable distance (i.e. in terms of measure of similarity) between two patterns (sensor measurements) that belong in the same category. By reducing S_T , the sensitivity will increase as the system leaves no room for false negatives (not highlighting an actual threat). However, at the same time, the number of false positives will also be increased.

Particularly for laser range measurements, due to averaging error as discussed in Chapter 4, the anomaly points that represent a true source of novelty will not be positioned exactly on the surface of the object. For this reason, in the experiments, anomaly points that are closer to the surface of the anomalous object by a distance of less than 200mm are considered as true detections. This value is chosen after considering the size of the object, its distance from the robot and the size of the laser measurements sector as described in Chapter 4. When any of the anomaly points that represent a true detection is filtered out, they are counted as a false negative detection. On the other hand, those that are not filtered out are counted as true positives. Similarly, anomaly points that are positioned more than 200mm from the surface of the anomalous object are considered as false detections. If anomaly points that represent false detections are filtered out, they are counted as true negatives but if they are not, they are counted as false positives.

The ROC curve was constructed by plotting the false positive and the true positive rate of novelty detection using different values of similarity threshold, S_T . The maximum neighbor distance, d_{max} was set to a fixed value of 200mm. For easy reference, the novelty detection mechanism is given the acronym of RHSOM which stands for Regional Habituating Self Organizing Map and the Singleton Cluster Filter

is given the acronym SCF. Figure 5.6 shows the comparison of the ROC curve between RHSOM and RHSOM with SCF.

As can be seen, at the highest sensitivity setting, the SCF reduces the false positive detection by more than 20%. The result is very desirable since this allows the novelty detection mechanism to be set to a higher sensitivity setting without having to suffer a high false positive rate. By using the Singleton Cluster Filter (SCF), there is a possibility that RHSOM would not achieve a higher true positive rate because of the problem of the dependency on the ordering of data presentation when performing on-line clustering. In the experiment, an anomaly point referring to the box was first observed in isolation. Its neighboring anomaly points were produced only after several further observations and they were grouped into a different cluster. Thus the first anomaly point remained in a singleton cluster. However, in practice, as can be seen from the example of novelty detection results in Figure 5.7(c), repetitive observation produces many anomaly points that highlight the position of the novel box. Missing a few of the anomaly points that refers to the box will not affect the overall performance of the novelty detection system.

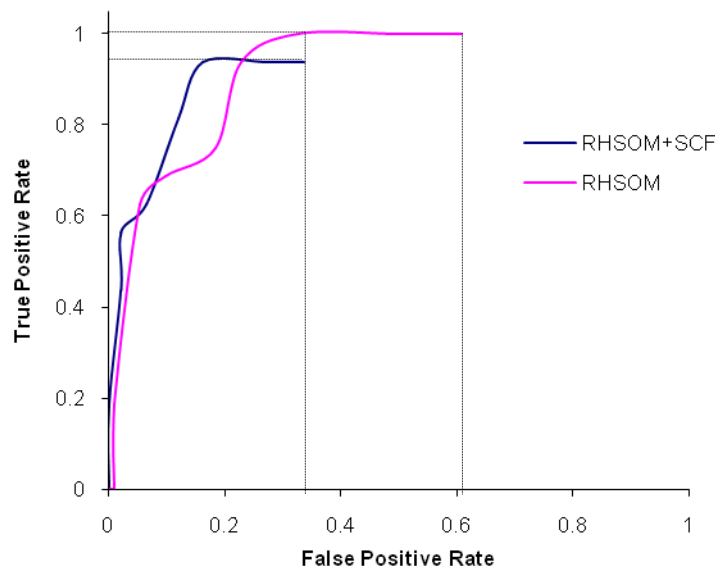


Figure 5.6: Comparison of ROC curves for RHSOM and RHSOM with SCF.

Figure 5.7 shows how the results of novelty detection change with different sensitivity settings. When using the singleton cluster filter, at lower sensitivity settings, fewer false positives are detected. However, when the sensitivity is increased, more false positives together with true positives are produced. A few of the false positives are near each other and are grouped into clusters of 2 members. Since only singleton clusters were filtered these remain as false positives.

Beyond Singleton Clusters

A comparison was made to determine the effect of filtering beyond singleton clusters. This means that clusters that have 2 or less members and clusters that have 3 or less members were also filtered out. A receiver operating characteristic curve was plotted for RHSOM with SCF, RHSOM with 2CF (2 or less member cluster filter) and RHSOM with 3CF (3 or less member cluster filter).

The results show that when compared to the singleton filter, the false positive rate improves by 20% when filtering is done on all clusters with 2 or less members. A better result is achieved by filtering clusters with 3 or less members and in this case there were no false positives at all. However, the true positive rates for both filters were reduced by about 25% compared with the singleton cluster filter. Nevertheless, as can be seen in Figure 5.9, the anomalous object was detected successfully as a result of the many observations made during the inspection.

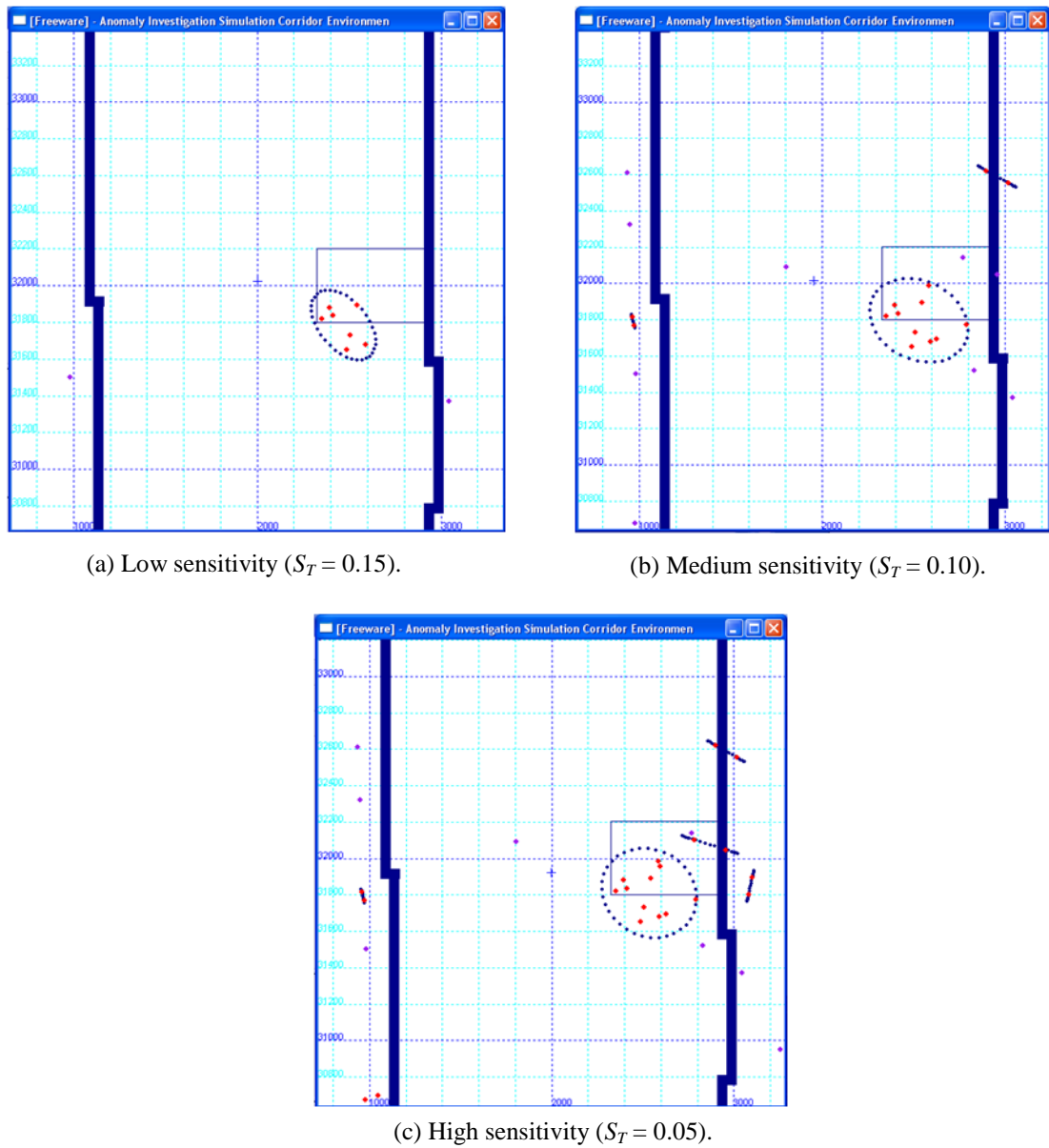


Figure 5.7: Results of different sensitivity tuning. The anomaly points are represented by the red dots while the purple dots represent singleton clusters. The ellipses created near the rubbish bin indicated by the box are considered to represent true positive detection.

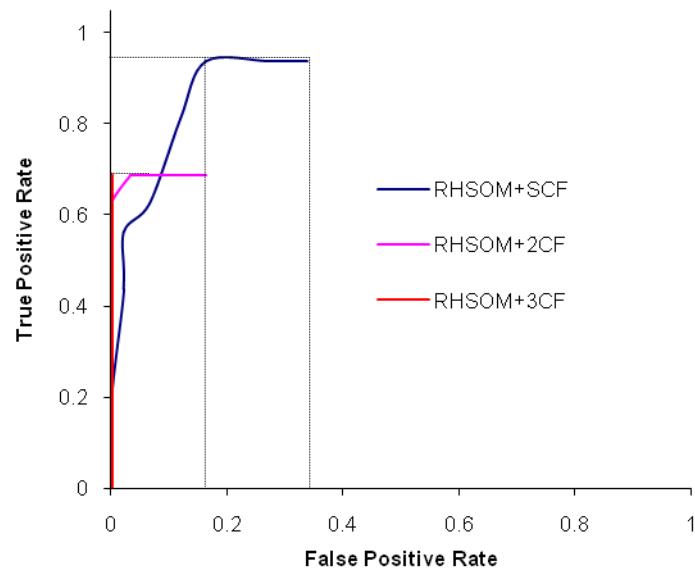


Figure 5.8: Comparison of ROC curves for RHSOM with SCF, RHSOM with 2CF and RHSOM with 3CF.

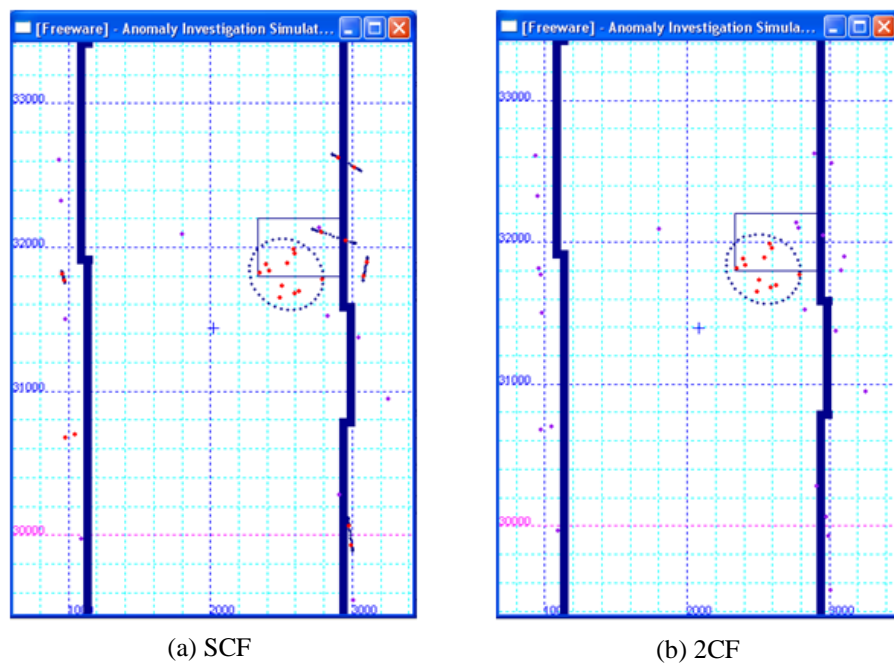


Figure 5.9: Filtering using SCF and 2CF. By filtering clusters with 2 or less anomaly points, a lower false positive rate was achieved but the true positive rate was also reduced. Although the true positive rate was reduced, as a result of many observations the anomalous object was still highlighted.

Changing the Clustering Threshold

An investigation was performed to see the effect of changing the clustering threshold i.e. the maximum neighbor distance parameter d_{\max} . Using the same sensitivity setting ($S_T = 0.05$), d_{\max} was set to 4 different values (see Figure 5.10). From the results it can be seen that the higher the value of the maximum neighbor distance, the larger the groups become. It is seen that, almost all anomaly points resulting from the anomalous object were successfully clustered into non-singleton clusters when d_{\max} was set to be equal and higher than the robot inspection step size (which was 100mm for this experiment).

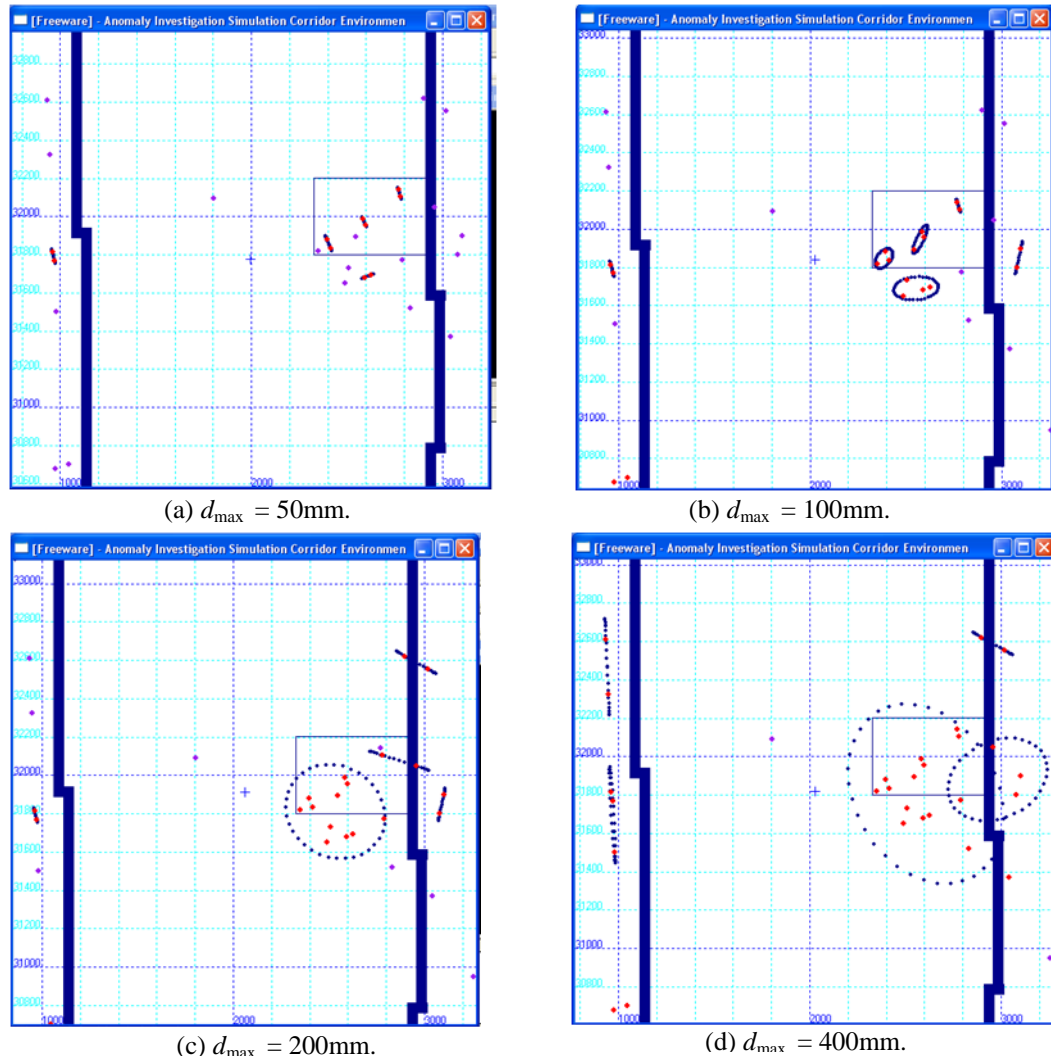


Figure 5.10: The maximum neighbor distance parameter d_{\max} affects the size of the groups formed.

A receiver operating characteristic was used to see the effect of different values of d_{\max} on the performance of the filter. With reference to Figure 5.11, as observed previously, the best value for d_{\max} is approximately equal to the robot inspection step size which is 100mm.

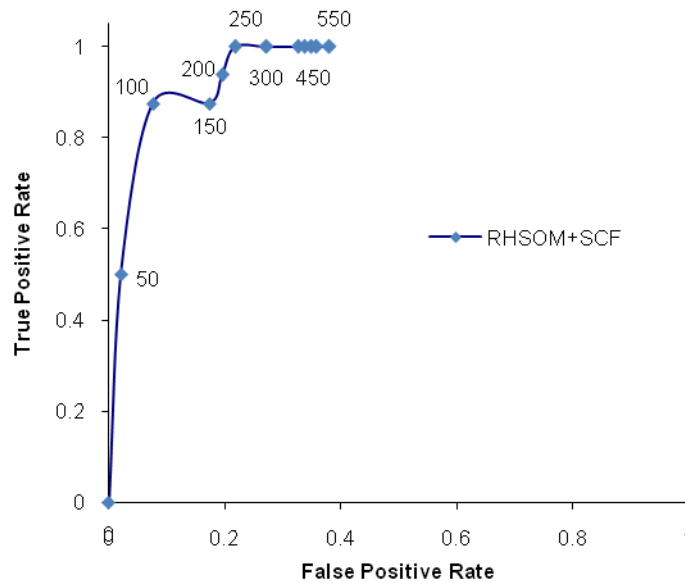


Figure 5.11: ROC curves for the RHSOM with SCF when using different values for d_{\max} (value indicated by the numbers near the markers).

Results for other types of sensors

Another sensed value that is more likely to suffer from fluctuation in its measurements and thus causes many false positives is air flow velocity. Figure 5.12 shows the results of singleton cluster filtering of novelty detection applied to airflow velocity measurements in the corridor. The anomaly points are based on the position of the sensor when it detected the anomalous measurement.

presence of true anomalies. Isolated anomaly points, indicated by clusters which have small size are filtered out.

The experimental results show that the filter improved the overall performance of novelty detection using Regional Habituating Self Organizing Maps (RHSOM) for a range of sensitivity settings. The advantage of the filter is that it allows a novelty detection system to be tuned to a higher sensitivity. This means that the novelty detection system is able to detect a true anomaly while maintaining a low false alarm rate. Since the filter works externally, it can be coupled with any novelty detection approach.

One of the drawbacks of using the filter is that it adds another parameter to the system that must be adjusted i.e. the maximum neighbor distance parameter d_{\max} . However, with correct tuning as described earlier, the filter should increase the overall performance of novelty detection.

Currently the robot does not actively observe detected anomalies. Instead, it just takes measurements by following its programmed navigation route. Nevertheless, the angle and position of the sensor still changes with respect to the detected anomalous object position as required for the repetitive observation strategy. In the next chapter, the inspection strategy will be further developed to actively observe detected anomalous objects by performing actions based on the results of repetitive observation and false positive filtering.

Chapter 6

Close Range Inspection Strategy

This chapter presents a strategy for performing a further investigation of an anomalous object based on the output of the novelty detection system that has been described thus far. The chapter starts with an introduction and discussion of related work. Next there is an outline of the overall system followed by a detailed description of the close range inspection strategy. The section finishes with experimental results followed by a discussion and conclusion.

6.1 Introduction

In surveillance tasks, using sensors on a mobile robot has many advantages over using static sensors alone. One of the advantages is that the robot could bring the sensors closer to the target area, effectively increasing their sensitivity and resolution. In contrast, since static sensors are positioned at fixed locations, a vast number of the sensors would be required to cover the whole surveillance area [22]. This makes it impractical to use the type of sensors which have a very limited working range [20, 21, 24] as this would require too many of the sensors. They also would need to be placed at inconvenient locations because of their short sensing range.

All sensors including those which have a large work range would benefit from being closer to the target object as this would increase their sensitivity. For example, chemical concentration is more diluted the further it travels from the source. The same dependency can be found with other measured quantities such as radiation level, magnetic field or ambient light. Even with images from a camera, a

close range snapshot will provide information of more detailed features like the texture of the object.

Another benefit of mobility is that it provides an opportunity to investigate the source of the sensed quantities from different angles. A camera would certainly benefit from this, as many objects look different from different angles. In situations where air flow carries a chemical plume in a specific direction, bringing the sensor to different points around the source object will increase the chances of detecting the chemical.

Motivated by these benefits, a novel approach to planning a close range inspection operation using a mobile robot and range sensor data was developed. The strategy utilizes information from the repetitive observation strategy and false positive filter which was presented in previous chapters. Close range inspection is performed only when an anomaly is detected using sensors which have a larger work range and can provide position information.

The rest of the chapter is organized as follows. Section 6.2 outlines related work. An overview of the system is presented in Section 6.3. The method is described in Section 6.4. Section 6.5 discusses the results of the experiments. A demonstration of close range inspection using sensors with limited working range is presented in Section 6.6. The chapter is concluded in Section 6.7.

6.2 Related work

The scope of the work described in this chapter is focused on how a mobile novelty detection system that has been described thus far could fully utilize its capabilities and overcome its limitations in order to perform a close range inspection. These make the work in this chapter unique. Thus far, the robot is capable of performing novelty detection on extended areas, identifying the location of the source of novelty using the repetitive observation strategy and filtering noise using the false positive filter. On the other hand, the system also has some limitation. As it is designed for mobile robots or standalone novelty detection systems with limited capabilities, it is

expected that the robot will use non-sophisticated and noisy sensors that don't require too much processing power, use a small amount of storage and are not expensive. As mention before, this is one of the reasons why the laser range finder that is used in this thesis is down sampled in order to emulate these more limited sensors. The discussion in this section will be based on these capabilities and limitations, as well as the nature of the task which is close range inspection.

Close range inspection requires a navigation strategy. One of the simplest navigation methods is the bug algorithm and its variants [84-90]. A primary advantage of the bug algorithm is that minimum information is needed, that is a start and a goal position and sensor measurements for obstacle avoidance. A more advanced navigation approaches involves planning of the path. Some of the popular approaches for path planning includes visibility graph (e.g. A*[91] and the Dijkstra algorithm [92]), grid based (e.g. distance transform [93]), potential fields [94] and sampling based. These methods require additional information that is the position of the robot and details of the space that it occupies (i.e. configuration space). Unlike the algorithms in the bug family [95], path planning requires prior knowledge of the obstacles before the robot can move toward a goal.

Traditionally the objective of path planning is to determine the best path to use between start and goal points. Focus is usually given to finding the lowest cost path from the robot's start state to the goal state. Cost can be in terms of the distance travelled, energy spent etc. However, unlike the common objective of path planning, the objective of close range inspection is to maximize the inspection coverage. The objective of the coverage path planning [96] is closer to the problem at hand because it gives more attention to the layout of the path itself. This type of path planning places emphasis on the space swept out by the robot. Examples of robotic applications that benefit from coverage path planning are lawn mowing [97], harvesting[98], mine hunting [99] and floor cleaning [100]. In order to accomplish their task, they must cover all reachable points in the environment. Coverage path planning usually involves breaking down the target region into cells through a process called decomposition. The problem is then simplified to visiting all cells

within the target region [101, 102]. This is done to provide some form of guarantee or measurable proof of either the completeness or optimality of the coverage.

Close range inspection is unique in its objectives and in the challenges that arise in achieving them. First, unlike any path planning strategy, the aim is to travel as close to and to cover as much of the perimeter of the anomalous object as possible. Secondly, there is no prior information available for performing the navigation, including the start and goal position. Thus, for whatever navigation approach that is employed by the close range inspection strategy, the robot needs to autonomously determine the start and goal position. By using novelty detection and the repetitive observation strategy, some information could be acquired about the approximate position of the object. Assuming that no other prior information is available, a reactive algorithm similar to the bug navigation method is the best option. However, some modification is needed to achieve the objective of close range inspection, which is fundamentally different from the standard bug algorithm.

6.3 System Overview

Figure 6.1 shows an overview of the system for implementing the close range inspection strategy. The strategy uses information from the repetitive observation strategy and the false positive filter.

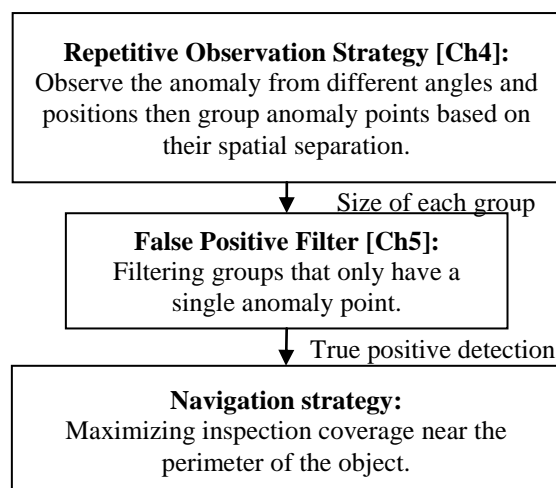


Figure 6.1: Overall close range inspection strategy.

6.4 Close Range Inspection

6.4.1 Problem Definition

As mention in Chapter 4, when using range sensors, the anomaly could be the appearance of novel objects or the disappearance of normally seen objects in the environment. First the situation when a novel object is detected is discussed. When a novel object appears, the object could be fully or partially accessible. Close range inspection is defined as the problem of maximizing the inspection coverage of an autonomous mobile robot near the accessible perimeter of an anomalous object. Accessible perimeter is the area near the perimeter of an object which could be access by a robot taking into account the size of the robot and the safety distance between the robot and the inspected object in order to avoid collisions. Inspection coverage is the proportion of the accessible perimeter that is visited when performing the close range inspection. It is assumed that the amount of coverage is proportional to the chances of gathering new information. For this reason, the performance of the close range inspection strategy or the coverage could be indicated by measuring the perimeter covered, $p_{covered}$, and dividing by the maximum accessible perimeter of the object, $p_{accessible}$, as given by Equation (6.1).

$$Coverage = \frac{p_{covered}}{p_{accessible}} \times 100\% \quad (6.1)$$

For the situation where a normally seen object disappears, the coverage could still be defined by using Equation (6.1). However, since a missing object has no physical boundary, $p_{accessible}$ is simplified to be a straight line between the nearest and the furthest anomaly points. An example application of close range inspection of a missing object is the detection of clues such as chemical residue left by a thief. In this project, all the situations described here i.e. fully accessible, partially accessible and missing object will be tackled by the same general algorithm.

6.4.2 Navigation Strategy

The easiest strategy to get close to the inspected object is by having the robot moves as close as possible to a point near the surface of the object. However, if this is the total strategy inspection coverage is limited to a single point on the perimeter of the object. If the size of the object is bigger than the working range of some of the robot's sensors, this simple approach is not enough to ensure a thorough inspection.

The inspection coverage could be increased by having the robot circumnavigate the object of interest. As can be seen from Figure 6.2, the aim of the inspection is to visit all positions along the accessible perimeter of the object. The path is offset from the actual surface of the object to allow a minimum safety distance, D_s between the robot and the object.

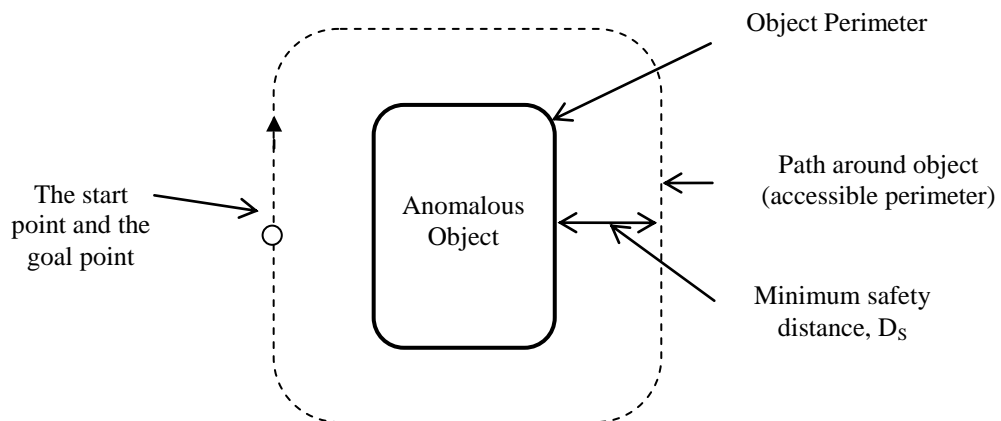


Figure 6.2: Coverage is defined using the length of the accessible perimeter path. 100% coverage is achieved if the robot encircles the whole object by following the path.

The accessible perimeter of an object could be constrained by the layout of surrounding objects as well as the physical size of the robot. As can be seen from the example in Figure 6.3, the path around the object is reduced because the object is positioned near a wall. Although there is a gap between the object and the wall, it is too small for the robot to go through. Thus the robot could only perform close range inspection on part of the perimeter of the object.

For navigating around the object to perform close range inspection, the robot needs to know the size and the position of the object in order to define the boundary of the target area and to identify a start and a goal position. Since the nature of the task at hand is to perform a further investigation of an unknown object, acquiring information regarding the size and layout of the object is not a trivial task. One solution is to use feature extraction to differentiate the object from its environment as in [103]. However, since the features of the anomalous object are unknown, this option is not applicable.

This is where the distribution of the estimated positions of the sources of novelty (anomaly points) becomes useful. By using the repetitive observation strategy, the position and the size of the source of the novelty can be approximated. The repetitive observation strategy will especially benefit range sensors which do not produce dense data. With enough observations, the distribution of the anomaly points can represent the position and the size of the perimeter of an anomalous object or at least part of the object. By using the anomaly points as a guide, it is assumed that during close range inspection, the robot would cover at least the part of the object which was observed when it performed novelty detection on its original inspection route (see Figure 6.4). The problem of navigation for close range inspection is then simplified to the problem of finding appropriate start and goal points from the anomaly point distribution and ensuring the robot remains close to the perimeter of the object while traveling between the two points.

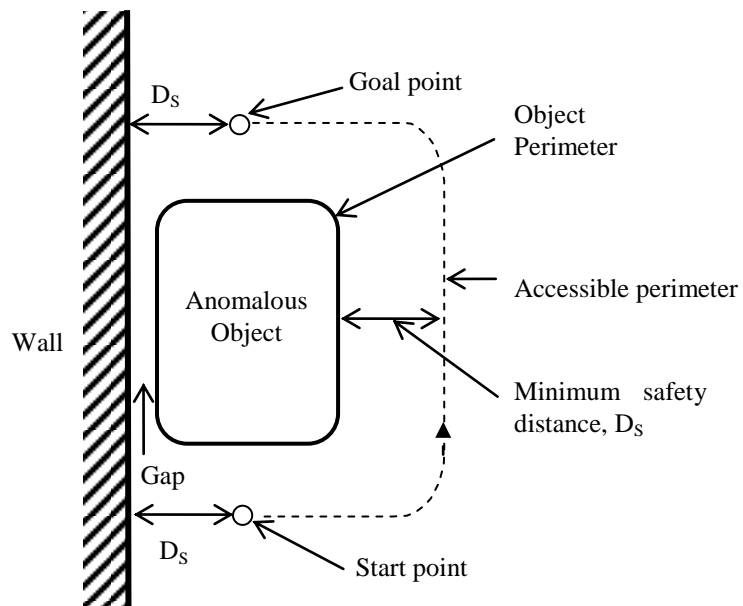


Figure 6.3: The accessible perimeter of an object could be constrained by an adjacent wall and the minimum safety distance to objects.

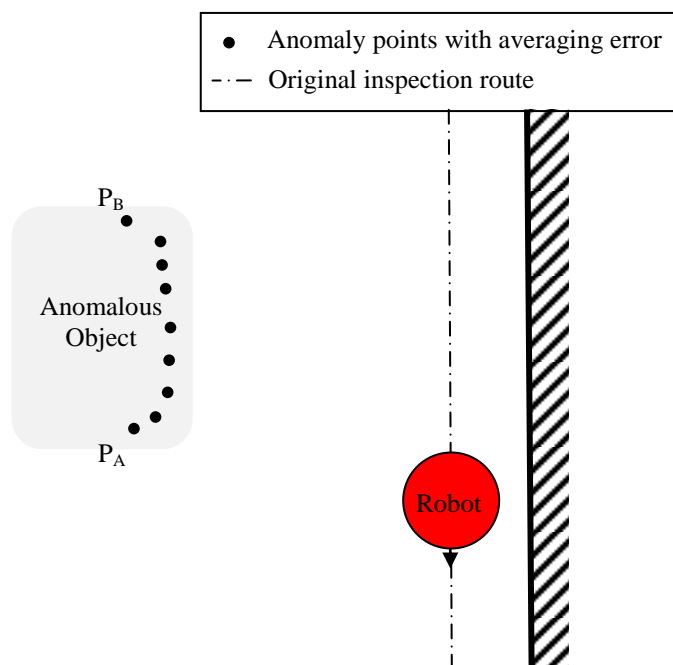


Figure 6.4: The anomaly points represent part of the perimeter of an anomalous object.

For navigating between the two points, the robot should move straight between the start and goal position while avoiding any obstacles in between. This strategy will cover the problem of close range inspection of missing object as well as for appearing novel object. If a novel object exists, it becomes like an obstacle for the robot to avoid. By using a wall following behavior for obstacle avoidance, the distance between the robot and the novel object is maintained at a close distance. In order to ensure that the robot maximized its inspection coverage, the robot is programmed to return to its starting position once it has reached its goal position. While travelling along its close-range inspection path, the robot could operate its close-range sensors.

6.4.3 Practical Consideration for Terminating Navigation at a Goal Point

From the discussion in the previous section, P_A and P_B are represented as points in 2-d space and the robot task is to move between these two points. However, this is not practical in a real world scenario because the anomaly points could be positioned inside an object. In addition, the robot positioning accuracy is not 100%, the robot size is bigger than a point and the robot is restricted to move within a safety distance from the object. For this reason a distance threshold, D_T is introduced so navigation could be terminated when a robot is within a certain radius from the points.

There are two scenarios where D_T is not ideal for ensuring termination. First the robot could not be within the required radius from the goal point if D_T is smaller than the nearest position that the robot could physically navigate to. Secondly, if D_T is set too big then there is a possibility that robot does not achieved 100% coverage as the inspection is terminated some distance before it reaches the goal point. To avoid facing these problems, another termination criterion is introduced where the distance between robot's starting position and the goal position, D_{RG} is used. Navigation is terminated if the distance covered by the robot (as it travels towards the goal position) is more than D_{RG} plus a threshold D_E . D_E is required as the robot needs to travel a longer distance to move pass the goal position when it circumnavigates an anomalous object.

In a practical scenario, there is a possibility that the robot moves away from its goal position when it reacts to obstacles. For example, consider what would happen if there is a wall on the left side of the object in Figure 6.5. When the robot moves from P_B to P_A , avoiding obstacles (the wall) this will make the robot move away from P_A . To solve this problem, navigation is terminated if the robot moves away from the goal position by the same distance as D_E . This is necessary to guarantee termination of the close range inspection. In short, D_E is the threshold distance for terminating navigation as the robot moves *past* or *away* from the goal.

6.4.4 Algorithm for Close Range Inspection

Algorithm 6.1 describes the close range inspection algorithm. The following are the conditions which are used in the algorithm (see notation in Algorithm 6.1 for the description of the notation (*note: D_{RG} indicates distance between robot and goal. Goal, G could be point A or point B*)):

1. $D_{RG} > D_{RG} + D_E$ indicates that the robot is moving further away from its target destination.
2. $D_{Travel} > D_{RG} + D_E$ indicates that robot has move past its target destination.
3. $D_{RG} < D_T$ indicates that robot has arrived at its target destination.

Algorithm 6.1: Close Range Inspection (see illustration in Figure 6.5):

Notations:

- P_C - Position where the robot confirms the presence of a true anomaly and starts close range inspection.
- P_G - Goal position
- P_A - Nearest anomaly point position from P_C .
- P_B - Furthest anomaly point position from P_C .
- P_R - Current robot position.
- D_{AB} - Distance between P_A and P_B .
- D_{LDA} - Distance travel since robot last detected an anomaly point which belongs to a confirmed detection.

D_{FPF} - Threshold distance for confirming a true positive detection. This is to increase the observation span and helps in confirming the presence of a true anomaly (see Chapter 5).
 D_{RG} - Distance between P_R to P_G
 $D_{RG'}$ - Current distance between P_R to P_G
 D_{RA} - Initial distance between P_R and P_A .
 $D_{RA'}$ - Current distance between P_R and P_A .
 D_{RB} - Initial distance between P_R and P_B .
 $D_{RB'}$ - Current distance between P_R and P_B .
 D_{RO} - Current distance between P_R and object.
 D_{Travel} - Robot's distance travel.
 D_E - Threshold distance for stopping the robot as it moves past or further away from the goal.
 D_T - Threshold to indicate that robot has reached the target position.
 D_S - Minimum safety distance between P_R and object.
Reach goal - $D_{RG'} < D_T$
Pass goal - $D_{Travel} > D_{RG} + D_E$
Move away from goal - $D_{RG'} > D_{RG} + D_E$
Safe - $D_{RO} > D_S$

Parameter values (note: distance to target position is measured from the center of robot):

$D_E = 500\text{mm}.$
 $D_T = 300\text{mm}.$
 $D_S = 600\text{mm}.$

```

Main()
1:   While Perform common (non close range) inspection
2:       If ( $D_{LDA} > D_{FPF}$ )
3:            $P_C = P_R$ 
4:           Close Range Inspection()
5:           Move to  $P_C$ 
6:       EndIf
7:   EndWhile

```

```

Navigate( $G=A/B, W=\text{left/right}$ )
1:   Set  $D_{RG} = D_{RG'}$ . Reset  $D_{Travel} = 0$ .
2:   Turn to  $P_G$ 
3:   While (Not Past goal AND Not Move away from goal)
4:       If (obstacles)
5:           Follow  $W$  wall
6:       Else
7:           Move straight to  $P_G$ 
8:       EndIf
9:       Operate close range sensor

```

10: EndWhile

Close Range Inspection()

1: Find P_A and P_B .

2: While (Safe AND Not Reached goal)

3: Navigate(A, left)

4: EndWhile

5: Navigate(B, left)

6: If (Past goal)

7: Navigate(A, left)

8: If (Past goal)

9: Terminate CRI

10: Else (i.e. Moved away from goal)

11: Navigate(A, right)

12: If (Past goal OR Moved away from goal)

13: Terminate CRI

14: EndIf

15: EndIf

16: Else (i.e. Moved away from goal)

17: Navigate(B, right)

18: If (Past goal)

19: Navigate (A, right)

20: If (Past goal OR Moved away from goal)

21: Terminate CRI

22: EndIf

23: Else (i.e. Moved away from goal)

24: Terminate CRI

25: EndIf

26: EndIf

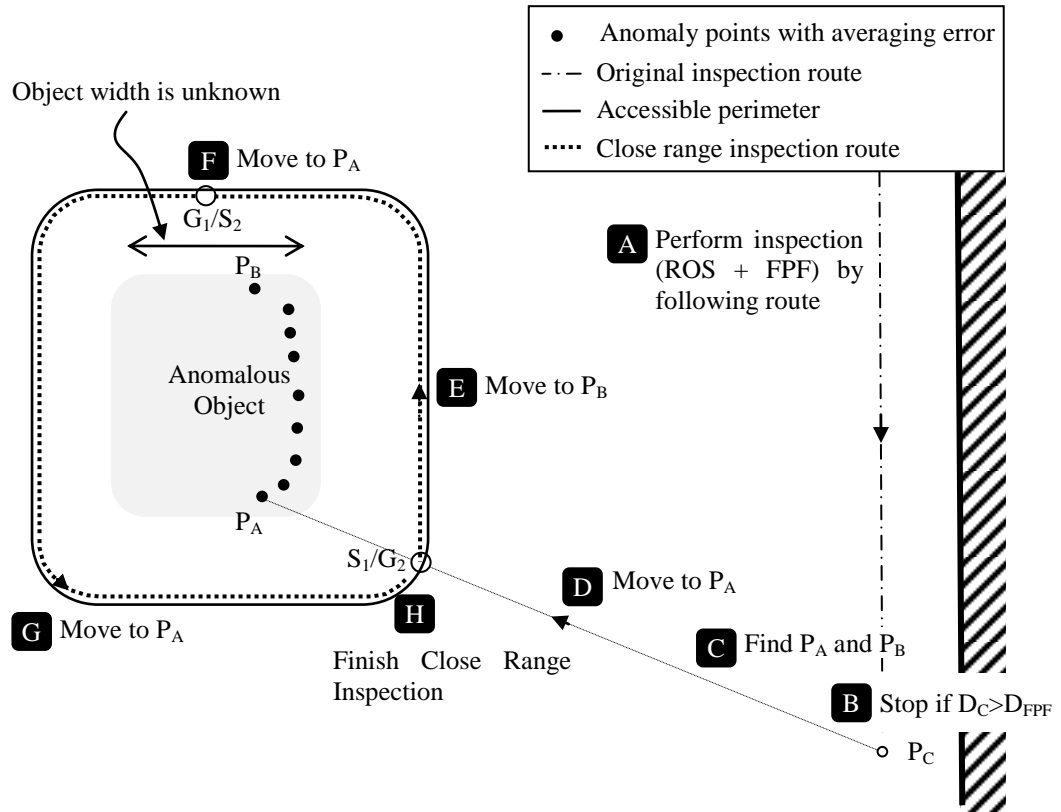


Figure 6.5: Illustration of the close range inspection algorithm.

6.5 Experiments

This section describes a robotic experiment investigating the close range inspection of an anomalous object. The experiment was designed to demonstrate that the proposed algorithm can be used to perform close range inspection of anomalous objects. The objective of the experiment is to examine the route generated by the algorithm.

Procedures

The robot explored the L-shape environment described in Chapter 2 using a wall following behavior. An Habituating Self Organizing Map was used to build a model of the perceptions that it received from the environment and mapped it to a flexible region map. The robot localized itself using a particle filter localization method. After the map had been established, anomalous objects were introduced into or a

normal object was removed from the environment (see Figure 6.6). The robot was then made to perform surveillance in the environment by following the original inspection route. The robot was expected to autonomously perform close range inspection on any foreign or missing object. The performance of the close range inspection is measured using Equation (6.1). The length of the accessible perimeter, $p_{accessible}$ is measured taking into account a safety distance of 400mm from the robot center to the object or the wall.

Results

In the following figures, different colors are used to represent the robot inspection trails in order to clarify the trails when the robot was moving in different directions. Figure 6.7 shows the results of the close range inspection algorithm when investigating an object with limited accessible perimeter. After considering the physical size of the robot and safety distance of 400mm from walls and objects, the length of the accessible perimeter was determined to be approximately 2200mm and is shown using the dashed line. By using the close range inspection strategy, the robot managed to visit 100% of the accessible perimeter of the object.

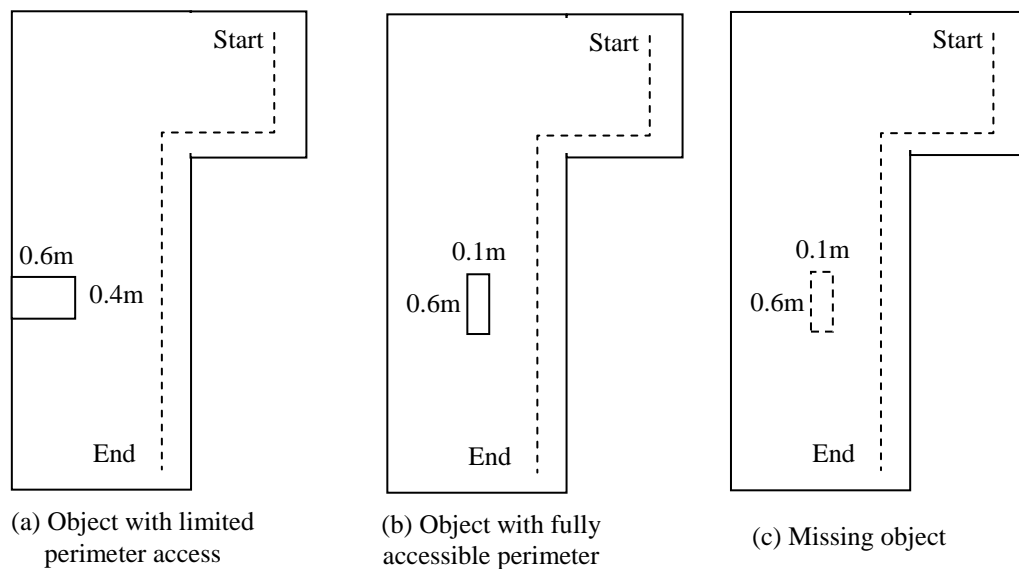


Figure 6.6: Positions of the anomalous object introduced into or missing from the environment.

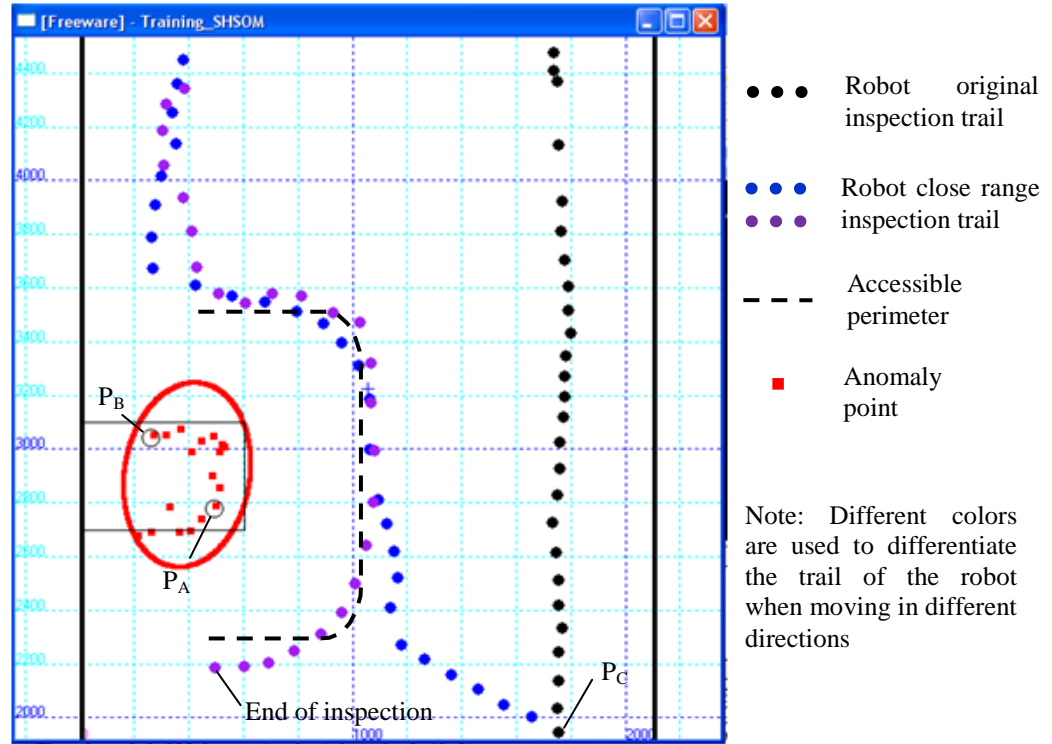


Figure 6.7: The resulting inspection path when the anomalous object is on the wall. The circled red dots indicate inspection starting and termination points.

Figure 6.8 shows the results of close range inspection of an object which is fully accessible. The robot successfully achieved 100% coverage. Figure 6.9 shows the result of close range inspection of a missing object. For the last experiment, result from the autonomous mapping from Chapter 3 was used as the normal model of the environment. As can be seen, the robot achieved 100% coverage of the area vacated by the missing object but it overly inspected the nearby area. This happened because it uses the same value of the stopping threshold, D_E as in the two previous experiments. It can be seen that there is a tradeoff in choosing a high or low value of D_E . A higher D_E value guarantees total coverage but the robot might over inspect. On the other hand a lower D_E value ensures that the robot navigates only near the vicinity of the anomalous object at the expense of the possibility of not achieving 100% coverage.

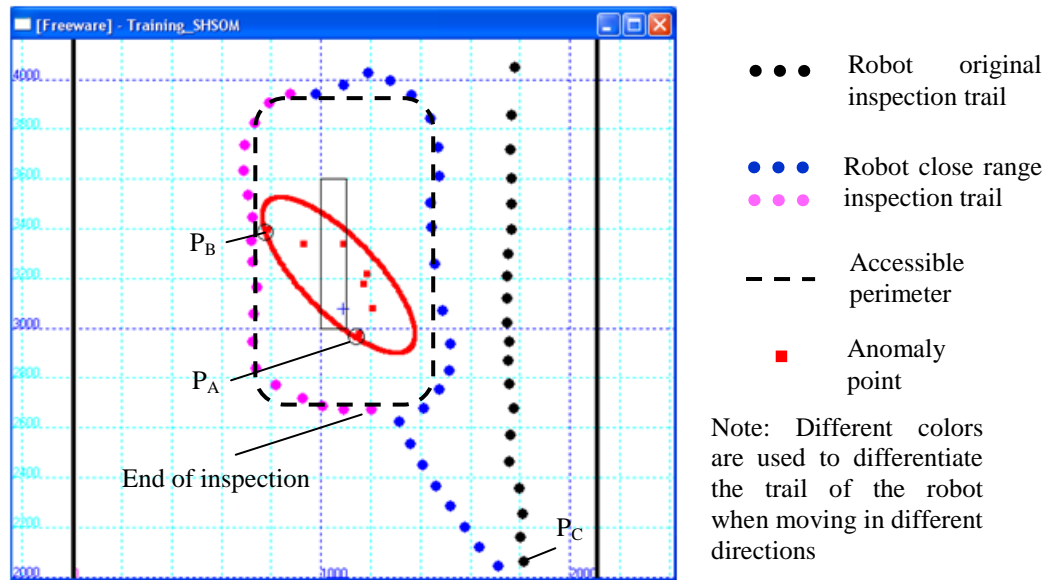


Figure 6.8: The resulting inspection path when the object is fully accessible. The circled red dots indicate inspection starting and termination points.

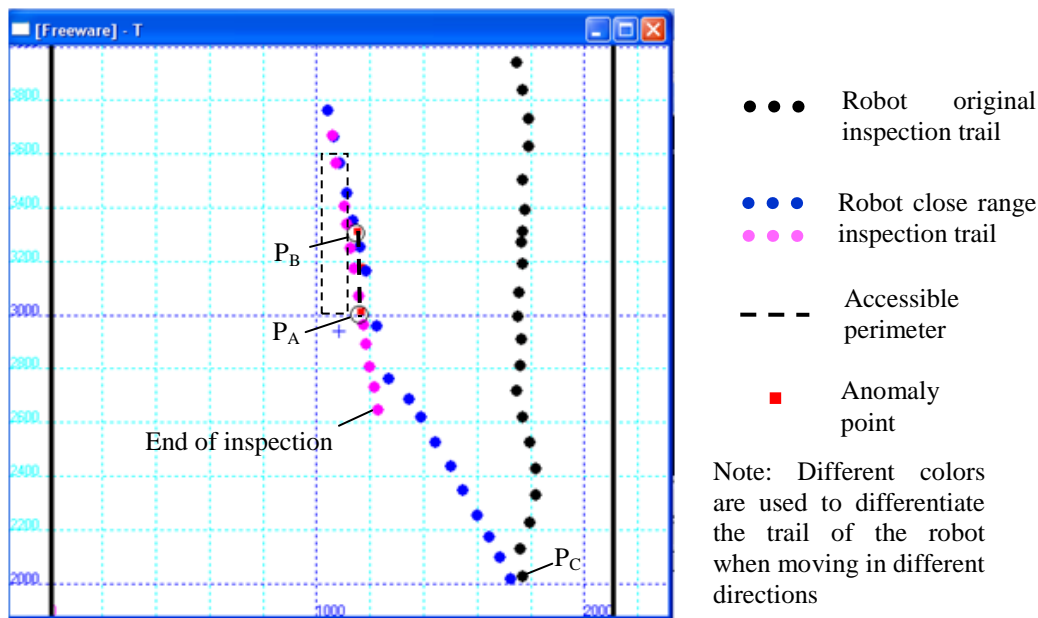


Figure 6.9: The resulting inspection path when performing close range inspection on a missing object.

6.6 Demonstration of using Sensors with Limited Work Range

In order to demonstrate the functionality of the complete close range inspection system, sensors with limited work range were mounted on the robot. In an actual surveillance/inspection scenario, examples of close range sensors that are commonly used are ion mobility spectrometers and X-ray machines [104]. For this project, because of cost and safety issues, it was decided to use less expensive and safer to operate sensors. For this reason, a novel electromagnetic radiation (EMR) sensor was developed (see Figure 6.10). The sensor can detect working electronics inside a package. A lot of dangerous packages such as explosive devices or devices designed to release dangerous chemicals are controlled by electronics.

Apart from being a practical choice for demonstration purposes with this project, the EMR sensor in itself is a useful development. While it is easy to develop countermeasures against an inspection system that uses a single type of sensor, it would be much more difficult to avoid detection by many different types of sensors. As the EMR sensor is not expensive, is safe to use and could sense operating electronics, it is ideal to be among the range of sensors that could be used by an inspection robot.

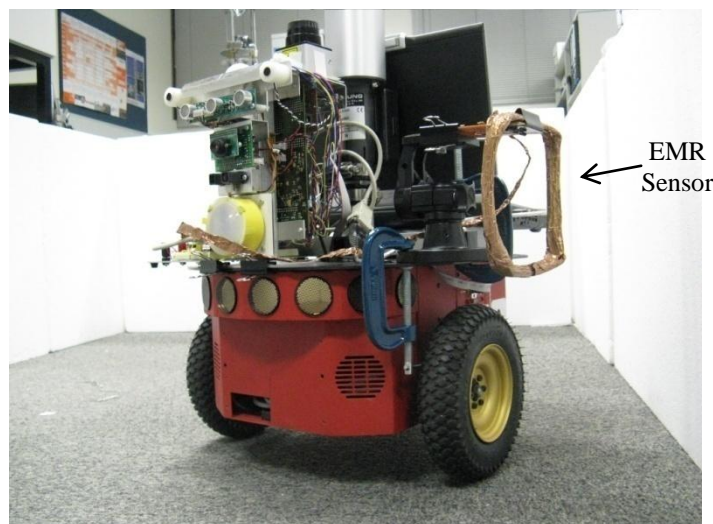


Figure 6.10: Electromagnetic radiation sensor mounted on the mobile robot.

The electromagnetic radiation (EMR) sensor system is depicted in Figure 6.11. The EMR sensors works by recognizing wave patterns of the amplified and rectified electromagnetic radiation emitted by operating electronic circuits. Circuits in electronic devices such as mobile phones and electronic timers produce periodic electromagnetic waveforms that are usually unique to the type of circuit. The sensor uses a loop aerial to receive the electromagnetic waves from the electronic devices. The aerial needs to be as close as 20cm from the devices to receive the electromagnetic radiation. The received waveform is analyzed using a number of algorithms and scores are given to the results that indicate the presence of operating electronic circuits. The development of the EMR sensor is described in detail in Appendix A.

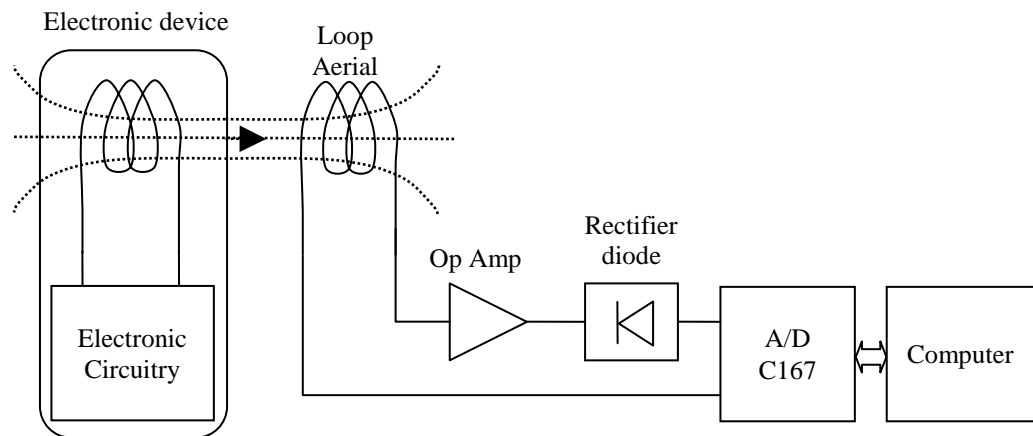


Figure 6.11: The EMR sensor system.

The close range inspection strategy demonstrates the synergy between different types of sensors particularly:

1. Between sensors with long working range and short working range.
2. Between sensors with low and high latency.
3. Between sensors that measure different quantities.

The inspection strategy uses a few selective sensors which work relatively fast and could cover a wider area during the robot's normal inspection mode such as range sensors. Then only during the close range inspection mode does the robot use

other sensors which work at close range and that have a high latency. The EMR sensor is an example of such sensors. Apart from being short range, the EMR sensor also takes time to operate as it needs to take samples of measurements for an extended period of time. It takes more than a minute for the sensor to take enough samples to extract signatures from the waveforms. In this chapter, the demonstration particularly highlights how a laser range finder complements the shortcomings of the EMR sensor.

In order to demonstrate a close range inspection activity using an actual close range sensor, the same setup as in the previous experiment was used. During inspection, two objects were introduced; a box and a polystyrene block with a pocket file (see Figure 6.12). A hand phone (Nokia N93i) on standby mode was placed inside the pocket file. The robot was expected to detect the box and the polystyrene block, perform close range inspection on them and highlight the object that contained the hand phone. The sensor was also expected to detect and highlight the signal from the laptop that the robot was carrying, if signal from the hand phone or any other operating electronic devices was not detected. As the sensor was placed on the left side of the robot, it was used only when the inspected object to the left of the robot. In short, the sensor was turned on only when the robot perform close range inspection while navigating using left wall following.

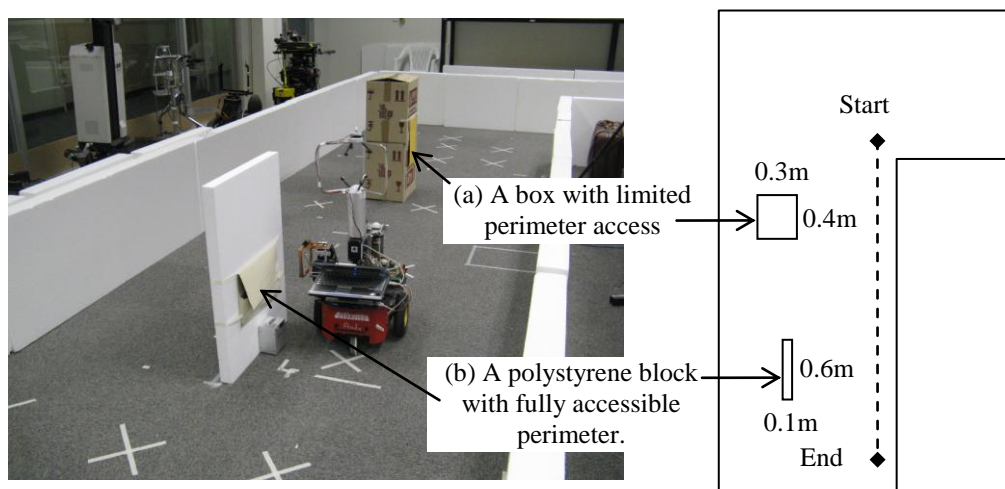


Figure 6.12: Positioning of the anomalous objects introduced into the environment.

angular resolution. This chapter demonstrates how the repetitive observation strategy and false positive filter described in the previous chapters could overcome this hardware limitation. Experimental results show that the algorithm successfully brought the robot close to the perimeter of the anomalous object and the vicinity of the missing object. The results show that the robot achieved 100% coverage in all the tests. The demonstration with the electromagnetic radiation (EMR) sensor that has a limited work range highlights the benefit of close range inspection.

There are many advantages of using the close range inspection strategy. Firstly, this strategy opens up the possibility of using other types of sensors which were previously neglected for surveillance tasks because of their limited working range. Secondly, as the approach is robust and require minimal information, any range sensors including less expensive but noisier sensors with coarse angular resolution could be used.

The close range inspection algorithm has room for improvement. Currently a threshold D_E is used as a termination condition. However, the threshold does not guarantee total coverage. If it is set too high, the robot might inspect too much of the unrelated surrounding area. However if it set too low, the strategy might not achieved 100% coverage. A better approach for terminating close range inspection is still open for investigation.

Other than for surveillance, the close range inspection strategy could also be useful for autonomous learning. The robot could gather data about new objects using many of its sensors at close range. The robot could inspect new objects from different viewpoints by following the close range inspection route. Direction for future work include the possibility of using sensors other than range sensors to estimate the anomaly position and to perform further close range inspection.

Chapter 7

Discussion and Conclusion

This concluding chapter provides a review of the thesis and suggests areas of work that could be developed further. Finally, the conclusion of the thesis is given.

7.1 An Overview of the Thesis

Monitoring changes using a novelty detection approach has many potential applications for many different kind of robots. However, until now very few mobile robots have actually employed novelty detection. To date, the use of rigid map structures to map normal data of the environment makes it difficult to adapt to new and unknown environments. Current techniques also consume much of a robot's valuable resources such as data storage and processing capacity, which in turn will put a limitation on the robot design.

The flexible region map described in Chapter 2, addresses these problems. Its flexible structure adjusts to the distribution of the normal measured quantities in the environment and hence effectively reduces the storage requirement. It is also data driven, which means that the map structure need not be predefined. In addition to that, an autonomous mapping method that is presented in Chapter 3 allows the flexible region map to autonomously adapt to the normal condition in new or changed environments.

In addition to proposing a flexible region map system and a method of autonomous mapping, this thesis also made contributions in making the results of

novelty detection of practical use for a mobile robot. The repetitive observation strategy and false positive filter discussed in Chapter 4 and Chapter 5 reduce the number of false detections and estimate the position of the source of any anomaly. The close range inspection strategy presented in Chapter 6 uses this information to guide the robot for performing close range inspection of anomalous objects. These methods were proven to work with relatively low resolution and noisy data as has been demonstrated using data from the down sampled laser scans.

7.2 What is New in this Thesis

The following list gives some of the main original ideas and contributions of this thesis:

1. A novelty detection map which uses a flexible region structure.
2. Investigation of using a number of different sensors when mapping and performing novelty detection with a flexible region map. The sensors include a laser range finder, an anemometer, an ambient light sensor, an olfaction sensor and a chemical concentration sensor.
3. A novelty detection map with flexible region structure that quantifies the novelty of a region using the habituation principal.
4. The first system that can autonomously produce a spatial mapping of normal sensor measurements in the environment for novelty detection purposes.
5. A false positives filter based on the spatial distribution of the estimated positions of the sources of the anomaly.
6. A navigation strategy for performing further close range investigation of any detected anomaly using a laser range finder.
7. A new sensor for detecting operating electronic devices that are hidden inside any package.

7.3 Limitations and Future Work

This section discusses some of the possibilities for further development of the work in this thesis in order to overcome some of the limitations and to improve the capabilities of the current system.

7.3.1 A More Flexible Region Structure

Currently, the regions in the flexible region map are limited to expand in 4 different directions (0° , 90° , 180° and 270°). As a result, the robot could only map and perform novelty detection when it is orientated to one of these four headings. In the future, the resolution of the heading could be increased so that the robot could map sensor measurements in more unstructured environments. In order to do this, the equations to represent and to restructure (expand, merge and separate) the regions would need to be made more general.

7.3.2 Multi-sensor Synergy

Having sensors that measure different entity that complements each other is an interesting idea. As fusion at measurement level is not possible for these sensors, novelty detection provides a way to associate information from these sensors. This has been demonstrated in Chapter 6, but there are plenty of room for improvement in this area. One of the possibilities is introducing a set of general rules that when two or more sensors produce novel measurements at the same time, the robot should react to them sequentially one after another based on the amount and the type of information content that they provide. In other words, priority should be given to measurements by sensors that have more information or to those that require urgent attention.

7.3.3 Extracting Information from Sensors

In Chapters 4 and 5, estimating the position of the anomaly using novelty detection results of a laser range finder has been discussed. It is possible that other sensors could also be used for this purpose. For example, the level of chemical concentration gives an indication of the distance between an olfaction sensor and the source of a gas leak. If the robot could take measurements from different positions as suggested by the repetitive observation strategy, it could perhaps estimate the position of the source of the gas leak by using triangulation. Similarly, quantities like sound, light and others are also more intense when they are measured closer to the source. Although this naive approach has been considered by others, novelty detection mechanism makes the idea unique as it provides normal measurements information, which could be used to find the position of missing normal measurements such as missing objects (as presented in Chapter 6), missing light, missing sound of a broken machine etc.

7.3.4 Commercialization: Novelty Detection Standalone Module

The system could ultimately be use in the form of standalone novelty detection modules which could be mounted on new or existing mobile robots, functioning as a supporting sub-system. This is made possible by the fact that the mapping system described in Chapter 2 and 3 is designed to work with the limited data storage and processing capacity associated with an inexpensive system. A more interesting application would be to mount these novelty detection modules on systems other than robots such as animals, motor vehicles or mobile devices such as mobile phones, provided that they could estimate their position in space. Nowadays, this could easily be done with the existing global positioning systems (GPS) in motor vehicles and even in mobile phones. They could then be used as part of an inspection or surveillance system or for other applications.

7.4 Conclusion

The aim of this thesis has been to investigate the challenges and benefits of using novelty detection for mobile robots. Firstly, an autonomous flexible region mapping methods has been developed to map novelty detection data at different locations in the environment. These techniques were tested in an L-shaped environment as well as in a real corridor environment and proved capable of significantly reduce the storage size when compared to conventional mapping systems. The results also show that it could autonomously update the normality status of its perception of its environment. All this was achieved while maintaining a low false positive and a low false negative rate for the novelty detection results.

Next the benefit of using a mobile robot was highlighted by utilizing the mobility of the robot to achieve a lower false positive rate and to perform a further inspection action on the detected anomalies. The receiver operating characteristics (ROC) curves created using the novelty detection results show that the repetitive observation strategy together with the false positive filter was able to reduce false positive rate. The output of the filtering process was used for the close range inspection strategy. Experiments in the L-shaped environment show that by using the laser range finder novelty detection results, the robot was able to increase its inspection coverage near the vicinity of the source of the anomaly.

These results lead to the conclusion that the autonomous mobile novelty detection system proposed in this thesis has solved some of the main challenges of performing novelty detection using a mobile robot, particularly the problem of mapping normal data of the environment. The results also highlighted the benefits of using a mobile system for novelty detection including to reduce false positives and to perform further investigations using close range inspection.

Finally, the system offers many advantages including requiring relatively little data storage for the map, being able to autonomously adapt to new or changing environments and having a low false positive rate even with noisy sensors. These advantages can ultimately be exploited by developing a small and inexpensive

standalone commercialized unit for deployment on new robots, pre-existing robots or other mobile systems.

Appendix A

Electromagnetic Radiation Sensor

A.1 Introduction

This section reports the development of a system to capture electromagnetic radiation (EMR) from electronic devices and algorithms that were developed for recognizing the sources of the EMR. Common methods used to trigger explosive devices electronically include mobile phones, remote controls, electronic timers and intelligent controls which will trigger in response to a particular set of conditions. Since any operating electronic devices including electronic triggering devices produced EMR, the main idea behind the explosion detection mechanism described in this work is to detect the EMR produce by these triggering devices.

In the circuitry of electronic devices, current that flows induces some magnetic field. The flow of current depends on the state of the circuit and the magnetic field changes proportionally to the current. Depending on the activity of the circuit, the change in the pattern of the flow of current is repetitive hence producing a unique periodic waveform. Different attributes such as frequency and other patterns can be extracted from a periodic waveform generated by the EMR. These attributes form a signature that could uniquely represent each type of device, providing a robust and efficient method to differentiate between them.

Several works using similar sensors has been reported. In [105, 106], mobile robots navigate by following dipole magnetic field signals produced by a transmitter and beacons. In other work [107] a similar approach is reported but using radio frequency identification transponders (RFID). The use of a magnetic field sensor on a mobile robot to monitor and locate the source of EMR in the environment has been described in [108]. In [109], a magnetic field sensor sheet was used to detect a

moving tunneling robot. In another application [110], an electromagnetic sensor is used for meteorite search by looking for their unique signature. Of all these work, none use the sensor to recognize objects that produced the EMR particularly coming from explosive triggering devices.

The following sections discuss in detail the design and operating principal of the EMR sensor. First the method of capturing the EMR signal using a loop antenna is described. Then the algorithms that were developed to identify the source of the signal are presented.

A.2 Sensor Design

The use of loop antenna is most appropriate to capture the signals since EMR produced by electronic devices is mainly due to inductive coupling [110]. A loop antenna is chosen over other types of antenna in some other works [105-113] as well as for this project because of its directional property and because of its design simplicity. Being sensitive to direction of the electromagnetic field is useful for helping to locate the source of the magnetic field. At the optimum alignment between the loop aerial and the source of signal, the induced voltage E_s is given by Equation (A.1) where e is the field strength in $\mu\text{V}/\text{meter}$, N is the number of turns, A is the area of the loop in square meters and λ is the wavelength of the signal in meters.

$$E_s = \frac{2\pi e N A}{\lambda} \quad (\text{A.1})$$

The signal captured by the loop aerial is amplified using a wide bandwidth op amp. It is then rectified and fed into a 10 bit A/D converter of the Infineon C167CS - LM processor. A computer is connected by serial link to the processor, and is used for signal processing. The sampling rate of the Infineon C167CS-LM is about $15\mu\text{sec}$, limiting the system to only process signals below 66 kHz. Figure A.1 shows a schematic diagram of the sensor.

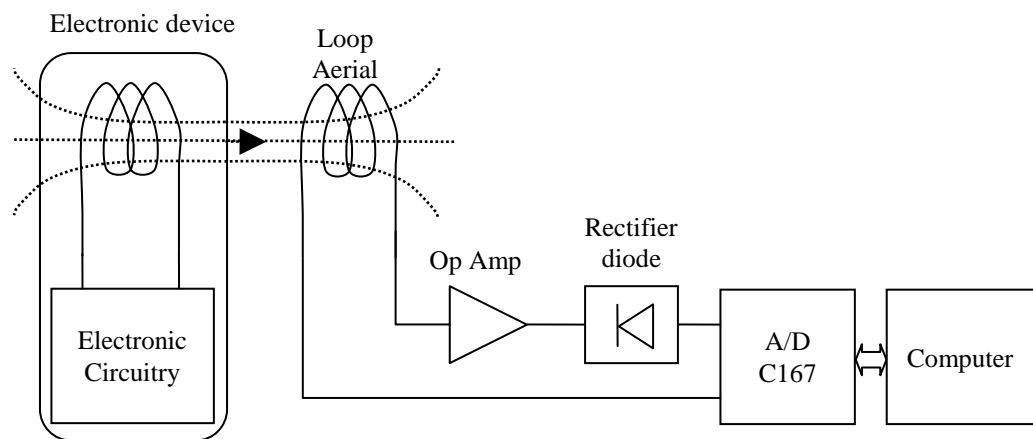


Figure A.1: The EMR signature sensor system, the electronic device and the inductively coupled magnetic field between them.

As the sensor is used on a mobile robot and requires the use of a laptop, the positioning of the sensor on the robot needs to be considered. In [110] it has been reported that EMR that comes from the laptop and the mobile robot contributed significantly to the ambient magnetic field. For this reasons, the loop antenna is positioned as far as possible from the electronics of the robot and the laptop.

A.3 Data Processing

Data processing is performed to extract the signature of the signals that are detected by the loop antenna. These signatures are used for recognizing different devices that are the source of the magnetic field. Several signatures were developed to recognize different electronic devices. For a more individual device specific signature, the number of peaks in the detected waveform and time between peaks are used. For a more general signature, the maximum and minimum time between peaks as well as a histogram of the time between peaks is used. Combinations of these signatures are used to recognize different devices.

Observations of the EMR waveforms generated by a CD player and a mobile phone (HP1) were made using a digital oscilloscope (see Figure A.2) to assess the types of signatures that could be use to identify these devices. It can be seen that the

CD player produces a higher frequency signal than HP1 while the HP1 produced distinct peaks every 250 ms. A closer look at the mobile phone's waveform in Figure A.2 shows that a peak actually consists of two separate peaks separated by 3.75 ms (see Figure A.3).

There is a possibility that a single EMR waveform could produce a combination of low and high frequency signals. For this reason, the sampling rate must be high and the window period must be sufficient to avoid loss of information. Simple statistics were extracted from the waveform 'on the fly'. This is to avoid the need to store a full set of data over a certain amount of time considering the large amount of data involved.

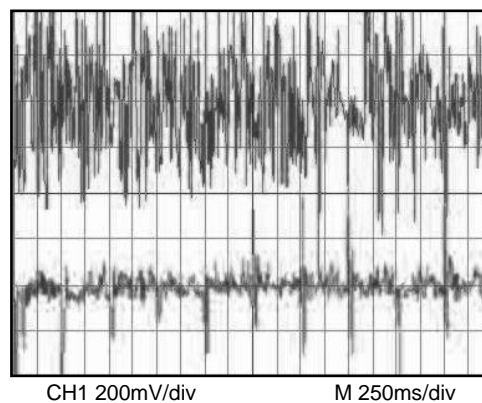


Figure A.2: The waveform of the CD player (top) and the mobile phone (bottom) EMR.

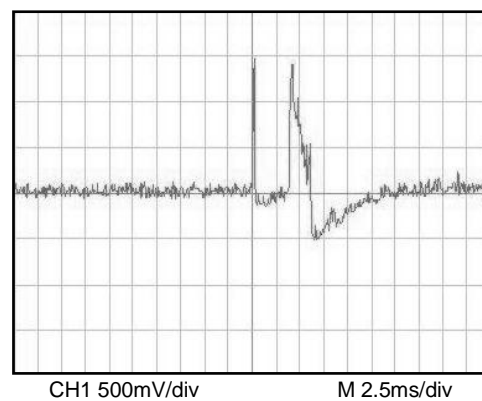


Figure A.3: A close up look at the mobile phone's waveform.

There are four algorithms that were developed to extract different signatures from the EMR waveforms: 1. Time between peaks (TBP) (see Algorithm A.1), 2. Number of peaks (see Algorithm A.2), 3. Minimum and maximum time between successive peaks (see Algorithm A.3) and 4. Time between peaks histogram (see Algorithm A.4).

For the time between peaks, the system detects peaks in the EMR waveform and calculates the timing between them. The peak detection is independent of sensing range since the threshold is based on a certain percentage (80%) of the maximum amplitude, E_{Smax} . However, if the maximum amplitude is below a minimum threshold level, T_{min} , then they are ignored.

The second algorithm is a measure of the number of peaks over a certain period of time. The third algorithm measures the maximum and the minimum time between successive peaks. Last but not least, the histogram of the time between peaks tabulates the frequency of the TBP over a certain period of time.

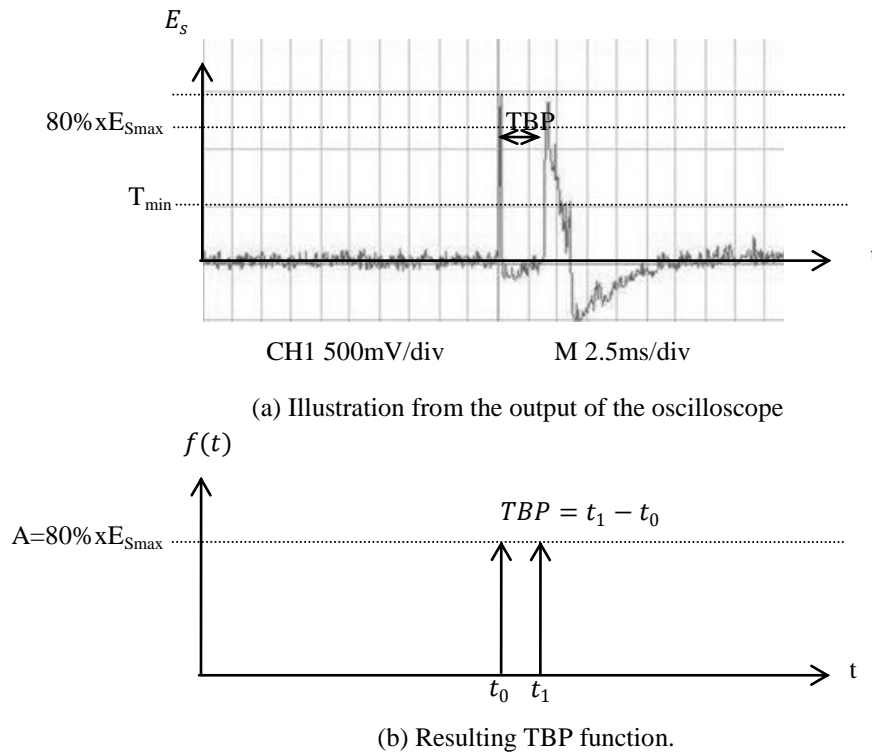


Figure A.4: The illustration of the time between peak algorithm.

The TBP algorithm produces the below function:

$$f(t) = \begin{cases} A, & t \in t_{i-1}, t_i, \dots, t_{n-1}, t_n \\ 0, & \text{otherwise} \end{cases} \quad (\text{A.2})$$

where

$$tbp = t_i - t_{i-1} \quad (\text{A.3})$$

$$a = 80\%E_{S_{\max}}$$

n = the number of times that the time between peaks was observed.

Algorithm A.1: Time between peaks (TBP).

- 1: Determine the maximum amplitude, $E_{S_{\max}}$ from the first x ms captured from a signal, E_s . (In the experiments x was set to be 1000ms).
 - 2: Wait for any E_s above the minimum threshold level, T_{\min} .
 - 3: If $\text{signal} > 80\% \times E_{S_{\max}}$, start timer.
 - 4: Signal will rise to maximum and fall below threshold. Continue timer until E_s rise above $80\% \times E_{S_{\max}}$.
 - 5: If $\text{signal} > 80\% \times E_{S_{\max}}$ again, stop timer. $TBP1 = \text{timer}$.
 - 6: Start timer for the next TBP. Repeat 3-4 for y successive peaks. (In the experiments $y = 40$).
-
-

Algorithm A.2: Number of Peaks.

- 1: For a fix period of time, count number of signals going above the minimum threshold level.
-
-

Algorithm A.3: Minimum and Maximum Time between successive peaks.

- 1: Capture the time between n successive peaks.
- 2: Record the minimum and maximum amount of time between peaks among the n samples.

Algorithm A.4: Time between peaks histogram

- 1: Measure time between n successive peaks.
 - 2: Set the appropriate time range to cover high and low frequency signals. Subdivide range into several bins.
 - 3: Allocate all n samples into bins (produce a histogram).
-
-

A.4 Performance

In order to investigate the possibility of using the signatures to recognize electronic devices signatures were determined from a CD player, and two different hand phone, HP1 and HP2. The signatures were measurements of the number of peaks, the time between peaks and the minimum and maximum time between peaks. Histograms of 40 samples of successive time between peaks were also produced.

As depicted in Table A.1, the number of peaks varies due to the strength of the signal. The minimum and maximum time between peaks of the EMR from the devices is not significantly different. So it might be not practical to use minimum and maximum time between peaks to differentiate between these devices. The most reliable signature appeared to be the time between peaks of the devices. Each device produces more than one unique time between peaks which provides the EMR sensor with more signatures to recognize different signal sources.

The performance of time between peaks was tested by performing EMR signal recognition of a CD player, HP1 and a digital oscilloscope. 40 measurements were taken from each device while they were operating. Only signatures of the CD player and HP1 were known. Measurements that matched these signatures were labeled as either CD player or HP1 while those that did not match any signatures

were labeled as an unknown device. Table A.2 shows the results of the experiment. As can be seen, 95% out of 40 attempts, HP1 was correctly identified while 87.5% out of 40 attempts, the CD player was correctly recognized. It was expected that the digital oscilloscope would be identified as an unknown device, but that only occurred 50% out of the 40 measurements.

Table A.1: The signature of devices used in the experiments recorded over 60 seconds.

Actual signal source	Number of peaks	Min and max time between peaks (ms)	Time between peaks (ms)*
CD Player	50 – 650	Min = 0.1 Max = 500	0.6, 14.4
HP 1	20 – 150	Min = 0.1 Max = 450	3.75, 154, 250,450
HP 2	5 – 100	Min = 0.1 Max = 800	400, 800

*There are many recorded time between peaks for each devices. However, the values listed were among highest occurrence of time between peaks among other observations

Table A.2: Results of 40 measurements to recognize different devices using the time between peak signatures.

Signal sources	System interpretation		
	HP 1	CD player	Unknown
HP 1	38	1	1
CD Player	0	35	5
Digital Oscilloscope	12	8	20

Since a single device has several significant *time between peaks* which occur repetitively, a histogram of the distribution of the time between peaks can provide another signature of the device. This signature is an overview of the time between peaks signatures as it is a result of an analysis of the distribution of time between peaks. The histogram was created by using 40 successive measurements of the time between peaks of the devices. Two histograms were produced, one with bins of 50ms intervals, and one with 5ms intervals.

Figure A.5 and Figure A.6 show the resulting histograms. In Figure A.5, it can be seen that the CD player produced time between peaks of less than 50 ms while both hand phones have a more even distribution with more than 15 occurrences below 50ms and two small rises in between 200 ms to 250 ms and between 350 ms to 400 ms. The second histogram shown in Figure A.6 was created because most of the time between peaks were within the lower range of the first histogram i.e. between 0 ms to 50 ms. As can be seen from both histograms, the similarity between the hand phones is that both have time between peaks that are distributed from 0 to 400ms. The CD player's time between peaks are 150ms and below with many actually below 5ms.

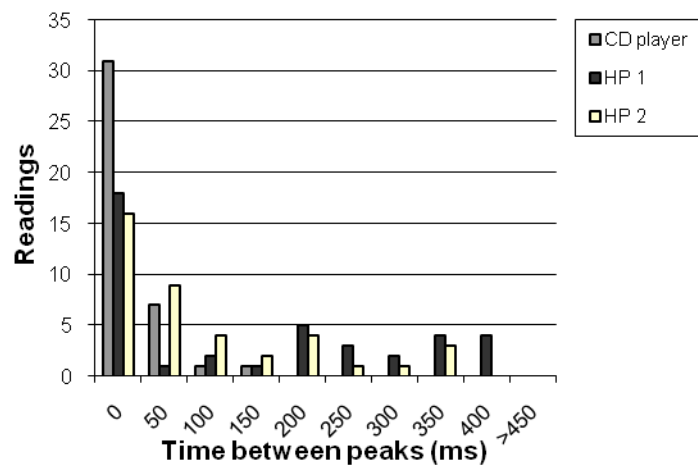


Figure A.5: The histogram of time between peaks from 0 to more than 450 ms.

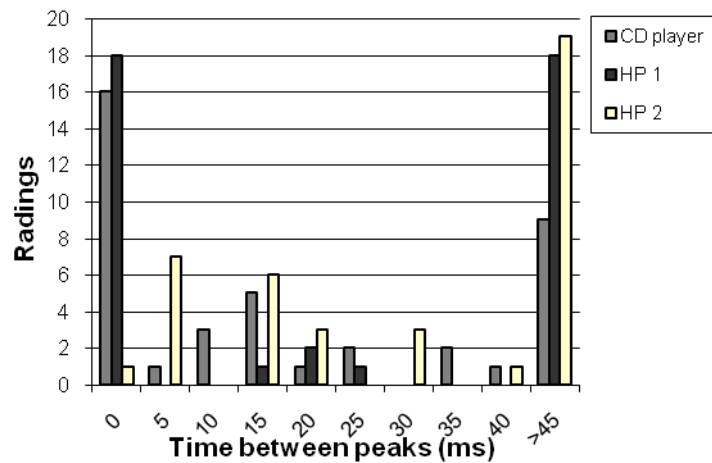


Figure A.6: The histogram of time between peaks from 0 to more than 45 ms.

The distribution of time between peaks differs from one device to another because of the way different devices operate. For example, it was expected that both hand phones produce quite similar histogram distributions because of the similar processing involve in the electronics of these two devices. Thus it can be concluded that the histogram of time between peaks provides a general signature of the type of electronic device.

Since the sensor was intended for used on a mobile robot, an experiment was conducted to demonstrate the feasibility of using the sensor when it was carried on a mobile robot. The time between peaks and its histogram were used to detect and recognize different electronic devices; HP1, CD player and HP2. Although the signatures of all these devices were known from the previous experiments, the signature of HP2 was not registered in the look up table for recognition purposes. It was assumed that the result of the detection of HP2 would either belong to *unknown device* category, or to HP1 since both HP2 and HP1 have similar signatures especially with their histogram of time between peaks.

To simulate the actual inspection scenario, the devices were placed inside cardboard boxes (see Figure A.7). From the figure, box A contained HP 1, box B contained a CD player, box C was empty and box D contained HP 2. During the experiment, the robot was programmed to move past the boxes while pausing every

50mm to take sensor measurements. During each pause, the measurement was taken for a period of 1200ms.

In this particular experiment, the time between peaks histogram in Figure A.5 was used to recognize the objects inside the boxes. In the explosive detection application, the type of device the sensor tries to detect is known. Particularly in this example, the target device that could be used for triggering an explosive is the hand phone. Based on this, a simple scoring scheme of the searched for device was used to decide whether one was detected. A device received a higher score if more attributes of the signature were detected. For experimental purposes, the signature of the CD player was also presented to see if the device was recognizable. During the experiment, HP2 was introduced as an unknown device to see if the signature of similar device (hand phone) could be generalized. Table A.3 shows the attributes that were used as the scoring points.

Table A.3: Examples of the attributes used for the signature and the scoring scheme of the CD player and HP1 based on the histogram in Figure A.5.

	Device	Attributes: TBP (ms)	
		0 – 50	200 - 450
Score	CD player	+1	-1
	HP 1	+0.5	+1

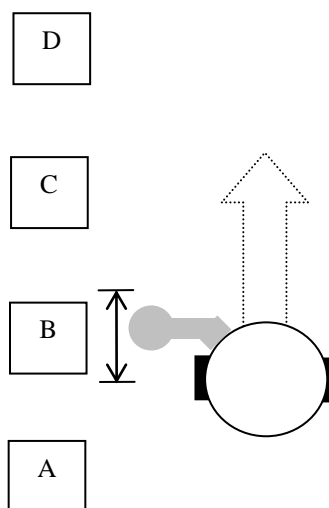


Figure A.7: The mobile robot with the sensor attached is moved past several boxes that contain different electronic devices. Box A contains HP1 and box B contains a CD player. Box C is empty while box D contains HP2.

Table 4 shows the results of 10 experimental runs. The system correctly detected HP 1 in box A 7 times. It mistakenly sensed a CD player in the same box 3 times. The system correctly detected the presence of the CD player inside box B 8 times. It mistakenly sensed HP 1 2 times. This is probably due to the similarity between the histograms of both devices at the lower time between peaks.

As expected the system detected no electronic devices in box C. Interestingly, the system detected HP 2 in box D and recognized it as HP 1. As can be seen from the histogram in Figure A.5, both devices have a very similar signature and therefore this result is not surprising.

Table A.4: Result of 10 measurements to recognize different devices using the time between peak signature and the histogram.

Boxes	System interpretation			
	HP 1	CD player	No Signal	Unknown
A	7	3	0	0
B	2	8	0	0
C	0	0	10	0
D	10	0	0	0

A.5 Discussion about the EMR sensor

The experimental results show that when operating, different electronic devices could be recognized based on their EMR signature. Although from the results, misclassification occurred between a CD player and HP1, it is believed that more signatures could be used in order to be more specific in determining the type of electronic devices. In addition, in a real scenario, it will be unusual for any electronic devices to be left while they are still operating inside an unattended bags or boxes. So in practice, the detection of a strong EMR signal from an unusual object in an environment is already a strong indication of a possible explosive threat.

The EMR sensor provides complementary information for the robot which would help to confirm the identity of some suspicious items. It provides a unique identification of features of electronic devices, which no other sensor can provide. However, due to noise from the environment that comes from known and unknown

sources, signature that depends on the amplitude of the signal will not be adequate as EMR signals from different sources are combined. On top of that, the field strength of many of the targeted electronic devices such as the timers is too weak when compared to ambient noise making them difficult to be detected, unless the sensor is very close to the devices. However, with further development the sensitivity and noise rejection of the EMR sensor could be improved.

Appendix B

List of Publications

- [1] M. F. Miskon and R. A. Russell, "A novel electromagnetic signature sensor for mobile robots," in *IASTED International Conference on Robotics and Application*, Weurzberg, Germany, 2007.
- [2] M. F. Miskon and R. A. Russell, "A Repetitive Observation Strategy for Recognizing a True Anomaly and Estimating its Position," in *Australasia Conference on Robotics and Automation* Canberra, 2008.
- [3] M. F. Miskon and R. A. Russell, "Mapping Normal Sensor Measurement Using Regions," in *IEEE International Conference of Industrial Technology* Melbourne, Australia, 2009.
- [4] M. F. Miskon and R. A. Russell, "Autonomous mapping of Flexible Region Map for Novelty Detection," accepted to *Second International Conference on Intelligent Robotics and Applications*, Singapore, 16 - 18 December, 2009.
- [5] M. F. Miskon and R. A. Russell, "Close Range Inspection Using Novelty Detection Results," accepted to *Second International Conference on Intelligent Robotics and Applications*, Singapore, 16 - 18 December, 2009.

References

- [1] "Meriam-Webster's Online Dictionary," 2009. <http://www.merriam-webster.com/dictionary/novel> (11 August 2009).
- [2] D. Dipanker and S. Forrest, "Novelty detection in time series data using ideas from immunology," in *Proceedings of the 5th International Conference on Intelligent Systems*, Reno, Nevada, 1996.
- [3] D. Dasgupta and F. Nino, "A comparison of negative and positive selection algorithms in novel pattern detection," in *Proceedings of the IEEE International Conference on Systems, Man, and Cybernetics*, Nashville, TN, 2000, pp. 125–130.
- [4] L. Tarassenko, "Novelty detection for the identification of masses in mammograms," in *Proceedings of the 4th IEE International Conference on Artificial Neural Networks*, Cambridge, UK, 1995, pp. 442–447.
- [5] C. Manikopoulos and S. Papavassiliou, "Network intrusion and fault detection: a statistical anomaly approach," in *IEEE Comm. Mag.* vol. 40, October 2002.
- [6] D. Fox, W. Burgard, S. Thrun, and A. Cremers, "A hybrid collision avoidance method for mobile robots," in *In Proceedings of the IEEE International Conference on Robotics and Automation.*, 1998.
- [7] M. J. Quinlan, S. K. Chalup, and R. H. Middleton, "Application of SVMs for Colour Classification and Collision Detection with AIBO Robots.," *Neural Information Processing Systems (NIPS)*. 2003.
- [8] M. J. Quinlan, S. K. Chalup, and R. H. Middleton, "Techniques for Improving Vision and Locomotion on the Sony AIBO Robot. ," 2003.
- [9] M. J. Denham and S. L. McCabe, "Biological temporal sequence processing and its application in robot control," in *UKACC International Conference on Control 1996*, 1996, pp. 1266-1271.
- [10] S. Lenser and M. Veloso, "Automatic Detection and Response to Environmental Change," in *Proceedings of the 2003 IEEE International Conference on Robotics and Automation*, Taipei, Taiwan, 2003, pp. 1416-1421.

-
- [11] P. Crook and G. Hayes, "A robot implementation of a biologically inspired method for novelty detection," in *Proc. Towards Intelligent Mobile Robot Conference*, Manchester, 2001.
 - [12] S. Marsland, U. Nehmzow, and J. Saphiro, "Novelty detection for robot neotaxis," in *Proceedings of 2nd International ICSC Symposium on Neural Computation*, Berlin, 2000, pp. 554-559.
 - [13] S. Marsland, "On-line novelty detection through self-organization, with application to inspection robotics," PhD thesis, University of Manchester, 2001.
 - [14] U. Nehmzow and H. V. Neto, "Novelty-based visual inspection using mobile robots," in *In Towards Autonomous Robotic Systems: Proceedings of the 5th British Conference on Mobile Robotics (TAROS'04)*, Colchester, UK, 2004.
 - [15] H. V. Neto, "Real-time Automated Visual Inspection using Mobile Robots " *Journal of Intelligent and Robotic Systems*, vol. 49, pp. 293-307, 2007.
 - [16] S. Marsland, U. Nehmzow, and J. Saphiro, "On-line novelty detection for autonomous mobile robots," *Journal of Robotics and Autonomous Systems*, vol. 51, pp. 191-206, 2005.
 - [17] P. Chakravarty, A. M. Zhang, R. Jarvis, and L. Kleeman, "Anomaly Detection and Tracking for a Patrolling Robot," in *Australasian Conference on Robotics and Automation (ACRA)* Brisbane, Australia, 2007.
 - [18] R. Brooks, "A robust layered control system for a mobile robot," *IEEE Journal of Robotics and Automation*, vol. 2, pp. 14-23, 1986.
 - [19] John L. Anderson, Antonio A. Cantu, Andrea W. Chow, and Paul S. Fussell, *Existing and Potential Standoff Explosives Detection Techniques*. Washington D.C: The National Academic Press, 2004.
 - [20] M. F. Miskon and R. A. Russell, "A novel electromagnetic signature sensor for mobile robots," in *IASTED International Conference on Robotics and Application*, Weurzburg, Germany, 2007.
 - [21] A. Lilienthal, A. Zell, M. Wandel, and U. Weimar, "Experiences Using Gas Sensors on an Autonomous Mobile Robot," in *Proceedings of EUROBOT 2001, 4th European Workshop on Advanced Mobile Robots.*, Lund, Sweden, 2001, pp. 1-8.
 - [22] A. Saidi, S. Chiricescu, J. M. Norris, and M. A. Schuette, "Method and System for Gas Leak Detection and Localization." vol. US 2008/0168826 A1, U. S. P. A. Publication, Ed. United State of America: Motorola, Inc., 2008.
-

-
- [23] P. Chakravarty, D. Rawlinson, and R. Jarvis, "Person Tracking, Pursuit and Interception by Mobile Robot," in *Australasian Conference on Robotics and Automation (ACRA)*, Auckland, New Zealand, 2006.
- [24] John. L. Anderson, Antonoi A. Cantu, Andrea W. Chow, Paul S. Fussell, Ralph G. Nuzzo, John E. Parmeter, Gary S. Sayler, Jean'ne M. Shreeve, Richart E. Slusher, Michael Story, William Trogler, Vennkat Vekatasubramanan, Lance A. Waller, Jonathan Young, and C. F. Zukoski, *Existing and Potential Standoff Explosives Detection Techniques*. Washington D.C.: The national Academic Press, 2004.
- [25] B. B. Petchenik, "From Place to Space: The Psychological Achievement in Thematic Mapping," *American Cartographer*, vol. 1, 1979.
- [26] A. Tapus and R. Siegwart, "Incremental Robot Mapping with Fingerprints of Places," in *IEEE/RSJ International Conference on Intelligent Robots and Systems (IROS 2005)* Alberta, Canada, 2005.
- [27] B. D. Dent, *Cartography: Thematic Map Design*. Boston: William C Brown, 1999.
- [28] K. Sahr, D. White, and A. J. Kimerling, "Geodesic Discrete Global Grid Systems," *Cartography and Geographic Information Science*, vol. 30, pp. 121-134, 2003.
- [29] H. Samet, "An Overview of Quadtrees, Octrees, and Related Hierarchical Data Structures," *NATO ASI Series*, vol. F40, 1988.
- [30] H. Samet, "Neighbor Finding Techniques for Images Represented by Quadtrees," *Computer Graphics and Image Processing*, vol. 18, pp. 37-57, 1982.
- [31] A. Guttman, "R-Trees: A Dynamic Index Structure for Spatial Searching," in *Proc. 1984 ACM SIGMOD International Conference on Management of Data*, 1984, pp. 47-57.
- [32] N. Beckmann, H.-N. Beckmann, H.-P. Kriegel, R. Schneider, and B. S. ., "The R*-Tree: An Efficient and Robust Access Method for Points and Rectangles," in *SIGMOD Conference*, 1990, pp. 322-331.
- [33] S. T. Leutenegger, J. M. Edgington, and M. A. Lopez, "STR: A Simple and Efficient Algorithm for R-Tree Packing," Report, Institute for Computer Applications in Science and Engineering, Mail Stop 403, NASA Langley Research Center, Hampton, VA 23681-0001, 1997.
- [34] S. Thrun, "Robotic mapping: A survey," Tech. Rep. CMU-CS-02-111, School Computer Science, Carnegie Mellon University, Pittsburgh, PA 15213, Feb 2002.
-

-
- [35] A. Elfes, "Using occupancy grids for mobile robot perception and navigation," in *Computer*, vol. 22, 1989, pp. 46-57.
 - [36] H. P. Moravec, "Sensor fusion in certainty grids for mobile robots," *AI Magazine*, vol. 9, pp. 61-74, 1988.
 - [37] R. Smith, M. Self, and P. Cheeseman, "Estimating uncertain spatial relationships in robotics," in *Autonomous Robot Vehicles*, I. J. Cox and G. T. Wilfong, Eds.: Springer-Verlag, 1990, pp. 167-193.
 - [38] R. C. Smith and P. Cheeseman, "On the representation and estimation of spatial uncertainty," Technical Report TR 4760 & 7239, SRI, 1985.
 - [39] F. Lu and E. Milios, "Globally consistent range scan alignment for environment mapping," *Autonomous Robots*, vol. 4, pp. 333-349, 1997.
 - [40] S. Thrun, D. Fox, and W. Burgard, "A probabilistic approach to concurrent mapping and localization for mobile robots," *Machine Learning*, vol. 31, pp. 29-53, 1998.
 - [41] R. Chatila and J.-P. Laumond, "Position referencing and consistent world modeling for mobile robots," in *Proceedings of the 1985 IEEE International Conference on Robotics and Automation*, 1985.
 - [42] N. Ho and R. Jarvis, "Large Scale 3D Environmental Modelling for Stereoscopic Walk-Through Visualisation," in *3DTV Conference* Kos Island, Greece, 2007.
 - [43] A. Yahja, A. T. Stentz, S. Singh, and B. Brummit, "Framed-Quadtree Path Planning for Mobile Robots Operating in Sparse Environments," in *Proceedings of IEEE Conference on Robotics and Automation, (ICRA)*, May, 1998.
 - [44] W. Burgard, D. Fox, D. Hennig, and T. Schmidt, "Estimating the absolute position of a mobile robot using position probability grids," in *Proceedings of the National Conference on Artificial Intelligence*, Portland, OR, USA, 1996, pp. 896-901.
 - [45] N. Tomatis, I. Nourbakhsh, and R. Siegwart, "Combining Topological and Metric: A Natural Integration for Simultaneous Localization and Map Building," in *Proceedings of the Fourth European Workshop on Advanced Mobile Robots (Eurobot 2001)*, 2001.
 - [46] G. Ferri, M. V. Jakuba, E. Caselli, V. A. Mattoli, B. A. Mazzolai, D. R. A. Yoerger, and P. A. Dario, "Localizing multiple gas/odor sources in an indoor environment using bayesian occupancy grid mapping," in *IEEE/RSJ International Conference on Intelligent Robots and Systems 2007*, pp. 566-571.
-

-
- [47] D. Fox, W. Burgard, and S. Thrun, "Markov Localization for Mobile Robots in Dynamic Environments," *Journal of Artificial Intelligence Research*, vol. 11, pp. 391-427, 1999.
- [48] N. Ho and R. Jarvis, "Vision Based Global Localisation Using a 3D Environmental Model Created by a Laser Range Scanner," in *IEEE/RSJ International Conference on Intelligent Robots and Systems (IROS)* Nice, France., Sep 2008.
- [49] F. Tungadi and L. Kleeman, "Multiple Laser Polar Scan Matching with Application to SLAM," in *Australasian Conference on Robotics and Automation (ACRA)* Brisbane, Australia, Dec 2007.
- [50] S. Marsland, J. Saphiro, and U. Nehmzow, "A real-time novelty detector for a mobile robot," in *Proceedings of European Advanced Robotic Systems Conference*, Salford, 2000.
- [51] S. Marsland, U. Nehmzow, and J. Saphiro, "A model of habituation applied to mobile robot," in *Proceedings of Toward Intelligent Mobile Robots*, Bristol, 1999.
- [52] S. Marsland, U. Nehmzow, and J. Saphiro, "Environment-specific novelty detection," in *Proceeding of 7th International Conference on Simulation of Adaptive Behavior*, Edinburgh, 2002.
- [53] D. R. Caldwell, "Unlocking the Mysteries of the Bounding Box," *Coordinates: Online Journal of the Map and Geography Round Table*, American Library Association, Ser. A, No. 2, 2005. <http://purl.oclc.org/coordinates/a2.htm> (June 11, 2009).
- [54] S. Fazli and L. Kleeman, "Wall Following and Obstacle Avoidance Results from a Multi-DSP Sonar Ring on a Mobile Robot," in *Proceedings of the IEEE International Conference on Mechatronics & Automation*, Niagara Falls, Canada, 2005.
- [55] I. M. Rekleitis, "A Particle Filter Tutorial for Mobile Robot Localization," Technical Report TR-CIM-04-02, Centre for Intelligent Machines, McGill University, Canada., 2004.
- [56] M. Markou and S. Singh, "Novelty detection: A review - Part 1: Statistical approaches," *Signal Processing*, vol. 83, pp. 2481-2497, 2003.
- [57] M. Markou and S. Singh, "Novelty detection: A review - Part 2: Neural network based approaches," *Signal Processing*, vol. 83, pp. 2499-2521, 2003.
- [58] S. Marsland, "Novelty detection in learning system," *Neural Computing Surveys*, vol. 3, pp. 157-195, 2003.
- [59] T. Kohonen, *Self organising maps*: Springer, 2001.
-

-
- [60] R. O. Duda, P. E. Hart, and D. G. Stork, *Pattern Classification*, 2nd ed. New York: John Wiley & Sons, INC., 2001.
- [61] J. C. Stanley, "Computer simulation of a model of habituation," *Nature*, vol. 261, pp. 146-148, 1976.
- [62] P. M. Groves and R. F. Thompson, "Habituation: A dual-process theory," *Psychological Review*, vol. 77, pp. 419-450, 1970.
- [63] D. Wang and M. A. Arbib, "Complex temporal Sequence Learning Based on Short-term Memory," 1990.
- [64] M. F. Miskon and R. A. Russell, "A Repetitive Observation Strategy for Recognizing a True Anomaly and Estimating its Position," in *Australasia Conference on Robotics and Automation* Canberra, 2008.
- [65] M. F. Miskon and R. A. Russell, "Mapping Normal Sensor Measurement Using Regions," in *IEEE International Conference of Industrial Technology* Melbourne, Australia, 2009.
- [66] D. LaBerge, *Attentional processing: The brain's art of mindfulness*. Cambridge: Harvard University Press, 1995.
- [67] D. B. Dusenbery, *Sensor Ecology: How Organisms Acquire and Respond to Information*. New York: W. H. Freeman And Co., 1992.
- [68] K. Dunlap and O. H. Mowrer, "Head movements and eye functions of birds," *Journal of Computational Psychics*, vol. 11, pp. 99-113, 1930.
- [69] M. S. Dawkins, "What are birds looking at? Head movements and eye use in chickens," *Animal Behaviour*, vol. 63, pp. 991-998, 2002.
- [70] S. Gouteux, J. Vauclair, and C. Thinus-Blanc, "Reaction to spatial novelty and exploratory strategies in baboons," *Animal Learning & Behavior*, vol. 27, pp. 323-332, 1999.
- [71] A. Joubert and J. Vauclair, "Reaction to Novel Objects in a Troop of Guinea Baboons: Approach and Manipulation," *Behaviour*, vol. 96, pp. 92-104, 1986.
- [72] A. I. Houston, J. M. McNamara, and J. M. C. Hutchinson, "Trade-Off between Gaining Energy and Avoiding Predation," *Philosophical Transactions: Biological Sciences*, vol. 341, pp. 375-397, 1993.
- [73] R. J. Woodham, "Photometric method for determining surface orientation from multiple images," *Optical Engineerings*, vol. 19, pp. 139-144, 1980.
- [74] R. A. Russell, "Robotic Location of Underground Chemical Sources," *Robotica*, vol. 22, pp. 109-115, 2003.
-

-
- [75] H. V. Neto and U. Nehmzow, "Incremental PCA: An alternative approach for novelty detection," in *In Towards Autonomous Robotic Systems: Proceedings of the 6th British Conference on Mobile Robotics (TAROS'05)*, London, UK, 2005.
- [76] S. Singh and M. Markou, "An Approach to Novelty Detection Applied to the Classification of Image Regions," *IEEE Transactions on Knowledge and Data Engineering*, vol. 16, pp. 396-407, 2004.
- [77] G. Fumera, F. Roli, and G. Giacinto, "Reject Option with Multiple Thresholds," *Pattern Recognition*, vol. 33, pp. 2099-2101, 2000.
- [78] R. H. Nagel, R. M. Nishikawa, J. Papaioannou, and K. Doi, "Analysis of methods for reducing false positives in the automated detection of clustered microcalcifications in mammograms," *Medical Physics*, vol. 25, pp. 1502-1506, 1998.
- [79] P. Chakravarty and R. Jarvis, "People Tracking from a Moving Panoramic Camera," in *Australasia Conference on Robotics and Automation* Canberra, 2008.
- [80] O. Cuisenaire, "Distance transformations: fast algorithms and applications to medical image processing," PhD thesis, Université catholique de Louvain, Louvain-la-Neuve, Belgium, 1999.
- [81] D. Fox, W. Burgard, S. Thrun, and A. B. Cremers, "Position estimation for mobile robots in dynamic environments," in *Proceedings of the Fifteenth National Conference on Artificial Intelligence (AAAI-98)*, Madison, Wisconsin, 1998.
- [82] S. Thrun, M. Bennewitz, W. Burgard, A. B. Cremers, F. Dellaert, D. Fox, D. Hähnel, C. Rosenberg, J. Schulte, and D. Schulz., "MINERVA: A second-generation museum tourguide robot.," in *Proceedings of the International Conference on Robotics and Automation (ICRA '99)*, 1999, pp. 1999 - 2005.
- [83] T. Fawcett, "ROC Graphs: Notes and Practical Considerations for Researchers," Technical Report, HP Laboratories, Palo Alto, USA, 2004.
- [84] V. J. Lumelsky and A. A. Stepanov, "Dynamic path planning for a mobile automaton with limited information on the environment.," *IEEE Trans. Automat. Contr*, vol. 31, pp. 1058-1063, 1986.
- [85] A. Sankaranarayanan and M. Vidyasagar, "A new path planning algorithm for moving a point object amidst unknown obstacles in a plane," in *Proc. of the IEEE Int. Conf. Robot. Autom.* 3, 1990, pp. 1930-1936.
- [86] A. Sankaranarayanan and M. Vidyasagar, "Path planning for moving a point object amidst unknown obstacles in a plane: a new algorithm and a general
-

-
- theory for algorithm development.," in *Proc. of the IEEE Int. Conf. on Decision and Control* 2, 1990, pp. 1111-1119.
- [87] I. Kamon and E. Rivlin, "Sensory-based motion planning with global proofs," *IEEE Trans. Robot. Autom.*, vol. 13, pp. 814-822, 1997.
 - [88] H. Noborio, "A path-planning algorithm for generation of an intuitively reasonable path in an uncertain 2-D workspace," in *Proc. of the Japan-USA Symposium on Flex. Autom.* 2, 1990, pp. 477-480.
 - [89] H. Noborio, Y. Maeda, and K. Urakawa, "A comparative study of sensor-based path-planning algorithms in an unknown maze," in *Proc. of the IEEE/RSI Int. Conf. on Intelligent Robots and Systems* 2, 2000, pp. 909-916.
 - [90] I. Kamon, E. Rivlin, and E. Rimon, "TangentBug: a range-sensor based navigation algorithm," *J. Robot. Res.*, vol. 17, pp. 934-953, 1998.
 - [91] W. S. Ko, L. D. Seneviate, and S. W. E. Earles, "Space representation and map building-A triangulation model to pathplanning with obstacle avoidance," in *Proceedings of the 1993 IEEE/RSJ International Conference on Intelligent Robots and Systems*, 1993, pp. 2222 - 2227.
 - [92] G. Foux, M. Heymann, and A. Bruckstein, "Two-dimensional robot navigation among unknown stationary polygonal obstacles," *IEEE Transactions on Robotics and Automation*, vol. 9, pp. 96 - 102, Feb 1993.
 - [93] R. A. Jarvis, "Collision-Free Trajectory Planning Using the Distance Transforms," *Mechanical Engineering Trans. of the Institution of Engineers, Australia*, vol. 10, September, 1985.
 - [94] T. Bräunl, *Embedded Robotics*. Berlin: Springer-Verlag, 2003.
 - [95] J. Ng and T. Braunl, "Performance Comparison of Bug Navigation Algorithms," *Journal of Intelligent and Robotic Systems*, vol. 50, pp. 73-84, 2007.
 - [96] H. Choset, "Coverage for robotics – A survey of recent results," *Annals of Mathematics and Artificial Intelligence*, vol. 31, pp. 113-126, 2001.
 - [97] Y. Y. Huang, Z. L. Cao, and E. L. Hall, "Region filling operations for mobile robot using computer graphics," in *Proceedings of the IEEE Conference on Robotics and Automation*, 1986, pp. 1607-1614.
 - [98] M. Ollis and A. Stentz, "First results in vision-based crop line tracking," in *IEEE International Conference on Robotics and Automation*, 1996.
 - [99] S. Land and H. Choset, "Coverage path planning for landmine location," in *Third International Symposium on Technology and the Mine Problem*, Monterey, CA, 1998.
-

-
- [100] J. Colegrave and A. Branch, "A case study of autonomous household vacuum cleaner," *AIAA/NASA CIRFFSS*, 1994.
 - [101] A. Zelinsky, R. A. Jarvis, J. C. Byrne, and S. Yuta, "Planning paths of complete coverage of an unstructured environment by a mobile robot," in *Proceedings of International Conference on Advanced Robotics*, Tokyo, Japan, November 1993, pp. 533-538.
 - [102] V. Lumelsky, S. Mukhopadhyay, and K. Sun, "Dynamic path planning in sensor-based terrain acquisition," *IEEE Trans. Robotics Automation*, vol. 6, pp. 462-472, 1990.
 - [103] H. Ishida, T. Ushiku, S. Toyama, H. Taniguchi, and T. Moriizumi, "Mobile robot path planning using vision and olfaction to search for a gas source," in *Proceedings of the 4th IEEE Conference on Sensors*, 2005, pp. 1112–1115.
 - [104] R. Jarvis, "Robotic Inspection and Safe Removal of Suspicious/Abandoned Luggage," in *IEEE Conference on Robotics, Automation and Mechatronics*, 2008, pp. 146-149.
 - [105] S. B. Cole, "Magnetic field-based navigation of a mobile robot," Master thesis, Oklahoma State university, 2005.
 - [106] E. A. Prigge and J. P. How, "Signal architecture for a distributed magnetic local positioning system," *IEEE Sensors Journal*, vol. 4, pp. 864-873, 2004.
 - [107] M. Kim, T. Takeuchi, and N. Y. Chong, "A 3-axis orthogonal antenna for indoor localization," in *First International Workshop on Network Sensing System*, Tokyo, Japan., 2004.
 - [108] F. Amigoni, S. Cadonici, V. Caglioti, and G. Fontana, "Experimenting with a robotic system for localizing magnetic field sources," in *Proceedings of the IEEE International Conference on Human-Computer Interfaces and Measurement Systems*, Giardani Naxos, Italy, 2005, pp. 44-50.
 - [109] T. Tsujimura, S. Shirogane, and N. Yoshizawa, "Electromagnetic system determining the position of tunnelling robots," in *IEE Proceedings on Radar, Sonar and Navigation*, 2000, pp. 331-336.
 - [110] L. Pedersen, "Deployment of electromagnetic sensors for meteorite search," in *Proceedings of the International Conference on Robotics and Automation*, Leuven, Belgium, 1998, pp. 618-623.
 - [111] S. A. Macintyre, "Magnetic Field Measurement," in *The Measurement, Instrumentation and Sensors Handbook*, J. G. Webster, Ed. Boca Raton, Fla: CRC Press published in cooperation with IEEE Press, 1999.
 - [112] A. Brandolini, G. D'Antona, M. Faifer, M. Lazzaroni, and R. Ottoboni, "Low frequency magnetic flux density measurements based on navigation agents,"
-

- in *Proceedings the ISA/IEEE Sensors for Industry Conference*, New Orleans, Louisiana, USA, 2004, pp. 86-90.
- [113] J.L Munoz, J. Tan, C. Adriano, E. Roldan, and J. Sadie, "Detecting ESD events using a loop antenna," in *Electrical Overstress/Electrostatic Discharge Symposium Proceedings*, 2000, pp. 60-64.